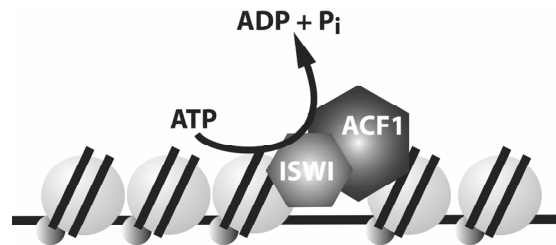


Dissertation zur Erlangung des Doktorgrades
der Fakultät für Biologie
der Ludwig-Maximilians-Universität München

ATP-dependent Remodelling of Linker Histone-Containing Nucleosomal Fibres



Verena K. Maier

München
22. Januar 2009

Eingereicht am 22. Januar 2009

Mündliche Prüfung am 5. März 2009

- | | |
|---------------|--------------------------|
| 1. Gutachter: | Prof. Peter Becker |
| 2. Gutachter: | Prof. Charles David |
| 3. Gutachter: | Prof. Dirk Eick |
| 4. Gutachter: | Prof. Kirsten Jung |
| 5. Gutachter: | Prof. Heinrich Leonhardt |
| 6. Gutachter: | Dr. Angelika Böttger |

Ehrenwörtliche Versicherung

Ich versichere hiermit ehrenwörtlich, dass die vorgelegte Dissertation von mir selbständig und ohne unerlaubte Hilfe angefertigt ist.

München, den

.....

(Unterschrift)

Acknowledgements

First of all, I would like to thank Prof. Peter Becker for giving me the opportunity to join his group, for encouraging and supporting me, for always finding time for discussions even in busy times and for providing a stimulating scientific environment and an exceptionally nice lab atmosphere.

I am especially grateful to Cristina Chioda for constant support, valuable advice, useful discussions, teaching me her technical expertise, careful reading of this manuscript and for being a great friend both inside and outside of the lab.

I also want to express my gratitude to the other members of my thesis advisory committee, Prof. Gernot Längst, Andreas Hochheimer and Prof. Ulrich Hartl for their time and helpful comments.

Moreover, I want to thank Daniela Rhodes for sharing her expertise on chromatin reconstitution.

Additional thanks go to Anton Eberharter for fruitful discussions, to Ragnhild Eskeland, Natascha Kunert and Angie Mitterweger for technical advice and to Catherine Regnard, Andreas Hochheimer, Cristina Chioda and Andrew Routh for providing reagents.

I also would like to thank all the people working at the molecular biology department creating a great working atmosphere, especially my bench neighbours Charlotte, Roxane and Raffaella, the 'lunch group' Torsten, Christian, Sara, Clemens, Ana and Henrike and the members of the 'ABI orchestra', Sandra, Antonia, Florian, Sonja, Franziska and Alexandra. You made it fun to work here!

Philipp, thank you for being who you are and for being there for me.

Last but not least, I want to thank my parents Anton and Anna Maria Maier for supporting me throughout my education.

Table of contents

Summary	1
Zusammenfassung	2
1. Introduction	4
1.1 Levels of chromatin condensation	4
1.2 Linker histones.....	7
1.2.1 The somatic linker histone H1	7
1.2.2 Linker histone variants.....	9
1.3 Principles of regulating chromatin structure.....	10
1.4 ATP-dependent chromatin remodelling factors.....	12
1.4.1 Subfamilies of ATPases.....	12
1.4.2 ISWI-containing chromatin remodelling complexes.....	16
1.4.3 Mechanism of ISWI-dependent nucleosome repositioning.....	16
1.4.4 Regulation of ISWI and its complexes	18
1.5 Interplay between linker histones and ATP-dependent chromatin remodelling... 20	
1.5.1 ATP-dependent remodelling in the presence of linker histones <i>in vitro</i>	20
1.5.2 Role of ISWI complexes in linker histone incorporation	21
1.6 Goals	22
2. Materials and Methods	24
2.1 Material sources.....	24
2.1.1 Laboratory chemicals and biochemicals.....	24
2.1.2 Enzymes.....	25
2.1.3 Antibodies.....	25
2.1.4 Organisms, cells and bacteria	26
2.1.5 Oligonucleotides, plasmids, and baculoviruses	26
2.1.6 Other materials.....	27
2.2 Buffers and solutions	28
2.3 Methods for the preparation and analysis of DNA.....	32
2.3.1 General methods for working with DNA	32
2.3.2 Cloning of 4x601 in pUC19 vector.....	33
2.3.3 Preparation of DNA fragments for the assembly of nucleosomal arrays	34
2.3.4 Radioactive DNA end-labelling.....	35
2.4 Methods for protein analysis and purification of proteins.....	36
2.4.1 Protein quantification.....	36

2.4.2	SDS polyacrylamide gel electrophoresis (SDS-PAGE)	36
2.4.3	Western blotting.....	36
2.4.4	Purification of endogenous histone octamers from <i>Drosophila</i> embryos	37
2.4.5	Expression and purification of recombinant core histones in <i>E. coli</i> and reconstitution of histone octamers	38
2.4.6	Purification of linker histone H1 from <i>Drosophila</i> embryos.....	40
2.4.7	Purification of HMG-D from <i>Drosophila</i> embryos.....	41
2.4.8	Expression and purification of recombinant HMG-D in <i>E. coli</i>	42
2.4.9	Expression and purification of ACF, ISWI, CHD1 and BRG1 in Sf9 cells	43
2.4.10	Sources of other proteins/extracts.....	44
2.4.11	Small scale preparation of nuclei from <i>Drosophila</i> embryos.....	44
2.5	Methods for the reconstitution and analysis of nucleosomal arrays.....	45
2.5.1	Chromatin salt assembly.....	45
2.5.2	Electrophoretic mobility shift assays (EMSA).....	46
2.5.3	MgCl ₂ -precipitation of nucleosomal arrays.....	47
2.5.4	Determination of histone stoichiometry	47
2.5.5	ATPase assays.....	47
2.5.6	Chromatin remodelling reactions.....	48
2.6	Maintenance and analysis of <i>Drosophila</i> stocks.....	49
2.6.1	Fly strains.....	49
2.6.2	Embryo collection and staining	49
3.	Results.....	51
3.1	Reconstitution of chromatin with stoichiometric amounts of linker histones	51
3.1.1	Reconstitution and purification of 12mer nucleosome arrays and chromatosome arrays containing H1 or H5	51
3.1.2	Quality controls of reconstituted chromatin	53
3.2	Linker histone-containing chromatin can be rendered accessible by ACF	54
3.2.1	ACF-mediated chromatin remodelling of nucleosome and chromatosome arrays.....	54
3.2.2	Comparison with the related chromatin remodelling ATPases CHD1 and BRG1	57
3.3	ACF repositions nucleosomes in the presence of linker histones.....	60
3.3.1	ACF-mediated repositioning of nucleosomal particles within nucleosome and chromatosome arrays	60
3.3.2	Repositioning of nucleosomal particles by CHD1 and BRG1	62
3.4	ACF catalyses the movement of chromatosomes.....	65
3.5	H1 may influence the directionality of ACF-mediated nucleosome movements.....	68
3.5.1	Reconstitution of palindromic 8mer 601 arrays	68
3.5.2	Nucleosome and chromatosome repositioning within palindromic arrays.....	71

3.6	The early linker histone substitute HMG-D does not affect the remodelling activity of ACF	73
3.6.1	Reconstitution of 12mer nucleosomal arrays containing HMG-D	73
3.6.2	Remodelling assays with HMG-D-containing chromatin	75
3.7	H1 and HMG-D levels are elevated in <i>acfl</i> null flies.....	76
3.7.1	Generation of polyclonal antibodies directed against H1 and HMG-D.....	76
3.7.2	Immunofluorescence of whole mount <i>Drosophila</i> wild-type and <i>acfl</i> embryos with α -H1 and α -HMG-D antibodies	78
3.7.3	Quantification of H1 and HMG-D levels in nuclei of wild-type versus <i>acfl</i> embryos.....	79
3.8	H1 replaces HMG-D from chromatin in the absence of cofactors	81
3.8.1	H1 associates with preassembled nucleosome arrays.....	81
3.8.2	H1 replaces HMG-D in a purified system without accessory factors.....	82
4.	Discussion	85
4.1	ATP-dependent chromatosome remodelling	85
4.1.1	Remodelling of H1-containing chromatin by specific remodelling factors	85
4.1.2	Limitations of chromatosome remodelling.....	86
4.1.3	Potential mechanisms of chromatosome remodelling	87
4.2	Global linker histone dynamics and chromatin remodelling.....	89
4.2.1	Chromatin remodelling in the presence of early linker histone substitutes.....	89
4.2.2	Global changes of linker histone association with chromatin upon depletion of ISWI-complexes	90
4.3	Effectors of linker histone dynamics	92
4.3.1	Intrinsic properties of linker histones that affect their affinity towards nucleosomes.....	92
4.3.2	Posttranslational modification of linker and core histones.....	93
4.3.3	Linker histone chaperones	94
4.4	Outlook	97
5.	References.....	98
6.	Abbreviations	111
	Curriculum Vitae.....	114

Summary

Eukaryotic genomes are condensed into a multilevel structure called chromatin which serves to organize and package the DNA, but at the same time needs to be flexible to permit regulated access to the stored information. ATP-dependent chromatin remodelling factors largely contribute to this dynamic nature of chromatin by catalysing processes such as the disruption of histone-DNA contacts, nucleosome repositioning and histone exchange. ATP-dependent remodelling has been well documented on a mononucleosomal level, but little is known about its regulation in a more physiological chromatin environment, where neighbouring nucleosomes and linker histones might interfere with the remodelling reaction. If and to what extent remodelling can work on chromatin bound by linker histones remains controversial, in spite of their high abundance and their strong influence on chromatin folding.

We therefore investigated chromatin remodelling in the presence of linker histones H1 or H5 using regularly spaced, oligonucleosomal substrates reconstituted from purified components. Surprisingly, we found that both the remodelling complex ACF – consisting of the ATPase ISWI and the regulatory subunit ACF1 – and ISWI alone were able to catalyse the repositioning of entire chromatosomes (nucleosomes + H1). Linker histones inhibited their remodelling activity by only about 50%. In contrast, the related ATPase CHD1 remodelled chromatin only in the absence of linker histones, suggesting that linker histones allow remodelling by selected factors only. In addition, our data indicate that repositioning in the presence of H1 might be unidirectional.

ACF1 is abundant during early *Drosophila* development, when H1 gradually replaces its early placeholder HMG-D. HMG-D binds to chromatin less tightly than H1 and unlike the latter, did not affect the remodelling activity of ACF in our assay. H1 was able to displace HMG-D from and bind to our reconstituted arrays without the help of cofactors. Strikingly, both H1 and HMG-D are more abundant in embryonic nuclei of *acfl* null flies compared to the wild-type, raising the possibility that an ACF1-containing complex controls linker histone incorporation.

Zusammenfassung

Eukaryotische Genome sind in einer komplexen Struktur namens Chromatin organisiert, durch die die DNA dicht gepackt wird, welche aber auch flexibel genug sein muss, um den Zugriff auf die gespeicherte Information zu ermöglichen. ATP-abhängige *Remodelling* Faktoren tragen zum dynamischen Charakter des Chromatins bei, indem sie beispielsweise DNA-Histon-Kontakte verändern, Nukleosomen verschieben oder Histone austauschen. ATP-abhängiges *Remodelling* ist auf mononukleosomaler Ebene gut untersucht, aber seine Regulation innerhalb einer physiologischen Chromatinumgebung, in der benachbarte Nukleosomen und Linker Histone das *Remodelling* stören könnten, ist nicht gut verstanden. Trotz großer Mengen an Linker Histonen im Zellkern, welche die Chromatinfaltung stark beeinflussen, ist es umstritten, ob und in welchem Ausmaß *Remodelling* auch in Chromatin stattfinden kann, das Linker Histone enthält.

Wir untersuchten den Einfluss der Linker Histone H1 und H5 auf ATP-abhängiges Chromatin *Remodelling*. Dazu benutzten wir Substrate, die aus mehreren Nukleosomen gleichen Abstands bestanden und aus gereinigten Komponenten hergestellt wurden. Erstaunlicherweise verschoben sowohl der *Remodelling* Komplex ACF, der aus der ATPase ISWI und der regulierenden Untereinheit ACF1 besteht, als auch ISWI alleine ganze Chromatosomen (Nukleosom + Linker Histon). Linker Histone verminderten die *Remodelling*-Aktivität dieser Faktoren nur um etwa 50%. Im Gegensatz dazu formte die verwandte ATPase CHD1 nur Chromatin um, das keine Linker Histone enthielt. Es ist daher möglich, dass nur bestimmte *Remodelling* Faktoren Chromatin in Gegenwart von Linker Histonen umformen können. Ausserdem fanden wir Hinweise darauf, dass Nukleosomen, an die H1 gebunden ist, bevorzugt in eine Richtung verschoben werden.

In *Drosophila* wird ACF1 vor allem während der frühen Embryonalentwicklung exprimiert. Zu diesem Zeitpunkt ersetzt H1 seinen Platzhalter HMG-D. HMG-D bindet weniger stark an Chromatin als H1 und hatte in unserem Versuchsaufbau keinen Einfluss auf die *Remodelling*aktivität von ACF. Interessanterweise enthielten die Zellkerne von *acfl* *Knock-out* Fliegen sowohl mehr H1 als auch mehr HMG-D als

Wildtyp Fliegen. Es ist daher möglich, dass ein Komplex, der ACF1 enthält, den Einbau von Linker Histonen in Chromatin kontrolliert.

1. Introduction

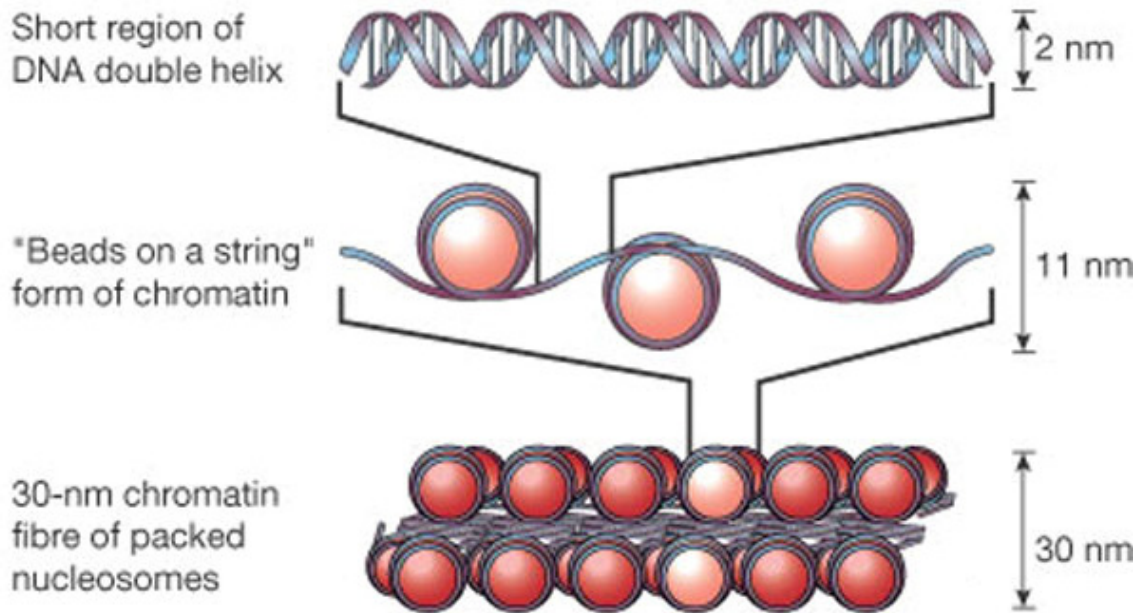
1.1 Levels of chromatin condensation

Eukaryotic genomes are organized into several levels of chromatin condensation achieving a high degree of compaction (Figure 1.1). This complex structure serves to package DNA, but also to regulate its accessibility by fine-tuning its properties via a variety of mechanisms.

The first level of compaction is achieved by the nucleosome: 147 bp of DNA wrapped around the histone octamer in 1.67 left-handed superhelical turns (Luger et al., 1997). The histone octamer is formed by two of each of the core histone proteins H2A, H2B, H3 and H4. Core histones are among the best conserved eukaryotic proteins and comprise a folded globular domain and an unstructured N-terminal tail domain; H2A possesses an additional short C-terminal tail (Thatcher and Gorovsky, 1994). The globular domain consists of a characteristic histone fold motif formed by three α -helices connected by two loops. Histone folds interact with each other in a handshake-like manner resulting in H2A/H2B and H3/H4 dimers (Davey et al., 2002; Luger et al., 1997). In the presence of DNA or at high salt concentrations such as 2 M NaCl, two H2A/H2B and two H3/H4 dimers combine to form the disc shaped histone octamer from which the unstructured tails protrude (Lusser and Kadonaga, 2004). *In vivo*, the majority of nucleosomes are bound by a fifth histone, the linker histone H1. It binds to an additional 20 bp of DNA at the entry/exit site of the nucleosome (Wolffe, 1998).

Nucleosomes are connected by usually 10 to 80 bp stretches of linker DNA, depending on the species and tissue. The linker DNA enters and exits the nucleosome at sites close to each other referred to as the entry/exit site. At low salt concentrations, chromatin appears as a “beads-on-a-string”-like structure called 10 nm fibre where the nucleosomes represent the beads and the DNA the string (van Holde, 1988).

At physiological salt concentrations (approximately 100 mM monovalent or 2.5 mM divalent cations) chromatin folds into the next level of compaction, the 30 nm fibre. The presence of linker histones facilitates formation of these fibres at lower salt

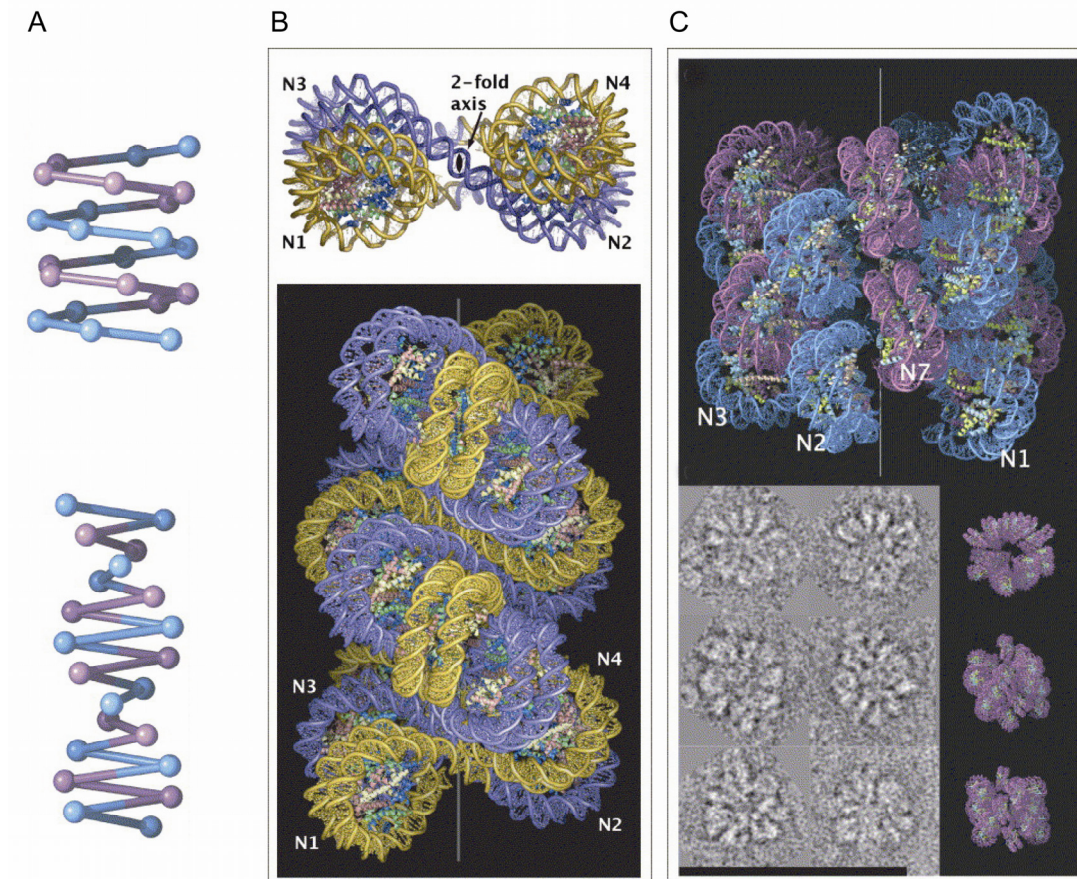


1.1 Basic levels of DNA compaction

The first level of DNA compaction is the nucleosome, in which the DNA (blue) is wrapped around the histone octamer (red) in 1.67 superhelical turns. Short stretches of linker DNA connect adjacent nucleosomes. This 'beads-on-a-string'-like structure is folded into a fibre of about 30 nm in diameter (adapted from Felsenfeld and Groudine, 2003).

concentrations (Clark and Kimura, 1990). A basic patch on the H4 tail, residues 16-20, is critical for full fibre compaction, most likely because it interacts with an acidic patch of the H2A/H2B dimer of the neighbouring nucleosomes (Davey et al., 2002; Dorigo et al., 2003; Luger et al., 1997).

The exact structure of the 30 nm fibre is still a matter of debate. Two competing, but not necessarily exclusive models have emerged as likely candidates: the solenoid and the crossed-linker model (Dorigo et al., 2004) (Figure 1.2). According to the first model, neighbouring nucleosomes follow each other along the same helical path forming a one-start helical structure. In this scenario, linker DNA has to be bent to allow fibre formation. In the second model, nucleosomes are connected by straight linkers and nucleosomes alternate between two helical stacks in a zig-zag arrangement, resulting in a two-start helix. The crystal structure of a tetranucleosome strongly supported the crossed-linker model, because it showed nucleosomes alternating between two stacks of



1.2 Proposed models for the structure of the 30 nm fibre

(A) Schematic representation of two different topologies for the 30 nm fibre. The upper graphic shows a one-start helical structure. In this model, neighbouring nucleosomes follow each other along the same helical path. Alternating helical turns are depicted in blue and magenta. The lower graphic represents a two-start helix with neighbouring nucleosomes crossing between two helical stacks. Adjacent nucleosome pairs are coloured blue and magenta. (B) The crossed-linker model (two-start helix) according to Richmond and colleagues. Nucleosomal positions 1 – 4 are indicated (N1 – N4). Upper picture: Crystal structure of a tetranucleosome. Below: Chromatin fibre model derived by stacking of tetranucleosomal structures and elimination of steric overlap. (C) The interdigitated solenoid model (one-start helix) according to Rhodes and colleagues. Nucleosomal positions 1 – 7 (N1 – N7) are indicated. Upper picture: 30 nm chromatin fibre modelled according to EM measurements. Below: Comparison of the model (right) to EM images of folded chromatin fibres (left) (adapted from Robinson and Rhodes, 2006).

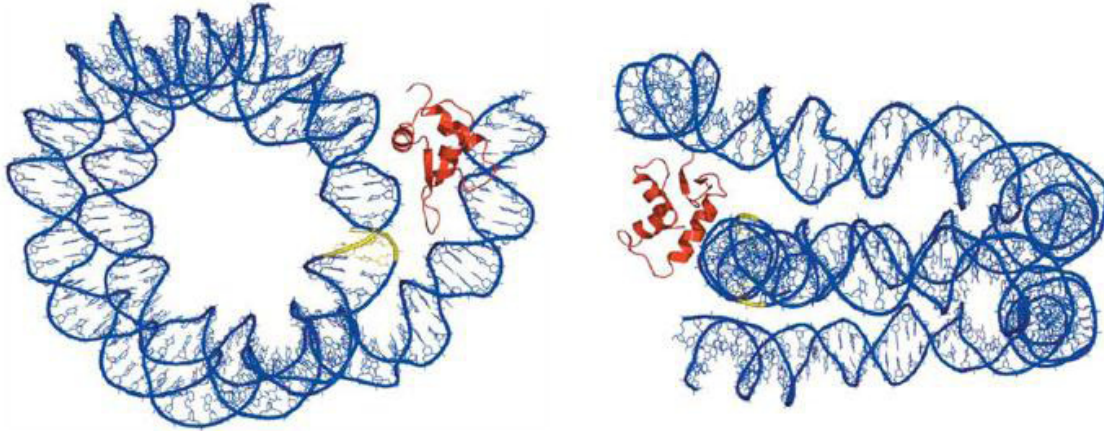
two nucleosomes (Schalch et al., 2005) (Figure 1.2B). However, the tetranucleosomes exhibited an uncommon nucleosomal repeat length of only 167 bp and did not contain linker histones. It is therefore not clear whether they represent a physiological chromatin conformation. Careful electron-microscopy (EM) measurements of long fibres consisting of up to about 70 nucleosomes containing stoichiometric amounts of linker histones yielded an unexpectedly high nucleosome density inconsistent with a two-start helix, but in line with a solenoid model where nucleosomes from successive turns interdigitate (Figure 1.2C). Moreover, the diameter of the fibres remained constant over a range of linker DNA lengths from 177 to 207 bp, which cannot be explained with the crossed-linker model (Robinson et al., 2006). In contrast, fibres with a nucleosomal repeat length of 167 bp bound only about one linker histone for every nucleosome, were less compacted and smaller in diameter (Routh et al., 2008). It is therefore possible that alternative structures of the 30 nm fibre exist *in vivo*, depending on linker DNA length and the presence of linker histones (Robinson and Rhodes, 2006).

Compaction beyond the 30 nm fibre is poorly understood (Felsenfeld and Groudine, 2003). Chromatin fibres are further organized, possibly by attaching to an underlying supporting structure called nuclear scaffold consisting of RNA and proteins. Scaffold or matrix attachment regions (S/MARs) are found every 5-200 kb in eukaryotic genomes. These DNA elements are believed to organize chromatin into distinct domains by dynamic binding to the nuclear matrix. However, the existence of a rigid nuclear scaffold is still controversial (Bode et al., 2003).

1.2 Linker histones

1.2.1 The somatic linker histone H1

As already mentioned, the linker histone H1 facilitates chromatin compaction and stabilizes the 30 nm fibre. Linker histones are structurally unrelated to the core histones and much less evolutionary conserved. A typical H1 consists of a globular winged-helix domain and unstructured N- and C-terminal tail domains. With their globular domains,



1.3 Binding of the linker histone to the nucleosome

Model of H1 bound to a nucleosome viewed from two sides perpendicular to each other. Only the DNA (blue) and the globular domain of H1 (red) are shown. The nucleosome dyad is coloured in yellow (adapted from Brown et al., 2006).

linker histones bind to DNA at the nucleosomal dyad and where it enters the nucleosome protecting additional 20 bp from nuclease digestion. A nucleosome with a short stretch of linker DNA bound by a linker histone is called ‘chromatosome’. (Brown et al., 2006; Sheng et al., 2006) (Figure 1.3). The long and highly basic C-terminus of linker histones presumably interacts with linker DNA and contributes to the stability of binding (Hendzel et al., 2004). Electron microscopy revealed that H1 organizes the two DNA segments entering and exiting the nucleosome core into a ‘stem’ structure (Bednar et al., 1998). Since H1 is an asymmetric molecule and interacts predominantly with DNA on one side of the entry/exit site, the nucleosome is no longer symmetric when it is bound by H1 (Brown et al., 2006).

The presence of linker histones is essential in mice (see 1.2.2) (Fan et al., 2005), but not in unicellular organisms such as budding yeast, the filamentous fungus *Aspergillus nidulans* and the ciliate *Tetrahymena thermophila* (Patterton et al., 1998; Ramon et al., 2000; Shen et al., 1995). Unexpectedly, these knock-out studies concluded that H1 regulates specific genes rather than acting as a global repressor.

Fluorescence recovery after photobleaching (FRAP) studies revealed that H1 is surprisingly dynamic *in vivo*. In these experiments, the residence time on chromatin of

proteins carrying a fluorescent tag is determined by monitoring recovery of fluorescence signal in a small bleached area. For H1, the average residence time on one binding site was estimated to be about 3 min. Although this means that H1 is less mobile than most chromatin-associated proteins, it is considerably faster exchanged than the core histones, which on average stay bound to one site for several hours (Bustin et al., 2005).

1.2.2 Linker histone variants

Many organisms express different variants of H1. For example, 11 linker histone variants have been found in mammals, which differ in their binding affinities, genomic localization and effects on gene expression. These variants can be grouped either according to their spatial expression into somatic and tissue-specific ones or according to their temporal expression into replication dependent variants, mainly expressed during S-phase, and replication-independent replacement variants (Izzo et al., 2008). Single or double knock-outs of several H1 variants in mice did not affect their viability, but resulted in the upregulation of other variants, showing that they can compensate for each other to some extent (Fan et al., 2001). The triple knock-out of the three somatic variants H1c, H1e and H1d, however, led to a 50% reduction of overall H1 levels, embryonic lethality and global changes in nucleosome spacing (Fan et al., 2003b; Fan et al., 2005).

A very specialized linker histone variant named H5 is found in avian erythrocytes where it contributes to the transcriptionally inactive state characteristic of these cells (Sun et al., 1990; Zhou et al., 1998). Because H5 binds to chromatin with a higher affinity than somatic H1, possibly resulting from the presence of a third DNA binding surface (Fan and Roberts, 2006; Ramakrishnan et al., 1993), it has been the preferred variant for structural studies involving linker histones. Modelling the structure of the globular domain of H5 onto the nucleosome has revealed the fact that unlike H1, H5 might be able to form dimers when bound to chromatin, which might contribute to the observed enhanced condensation (Fan and Roberts, 2006).

Conversely, H1 variants can also account for the very open chromatin structure present in early development. *Xenopus* contains an oocyte-specific linker histone B4, which is gradually replaced by somatic H1 variants as the embryo matures (Saeki et al.,

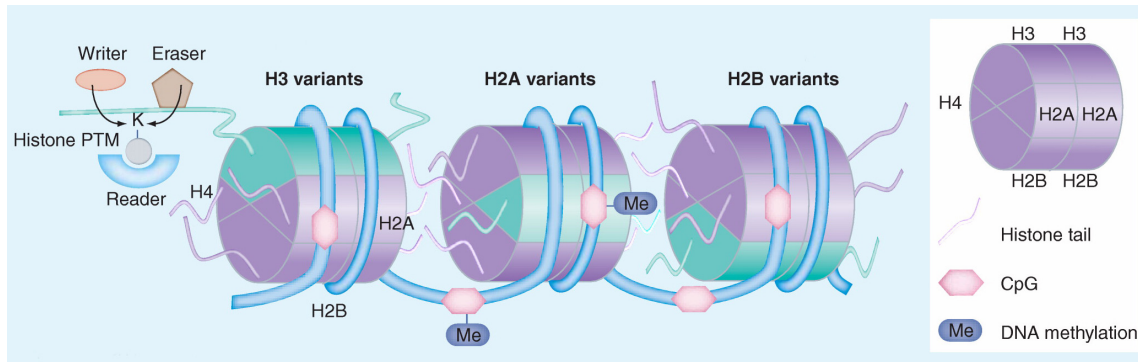
2005). *Drosophila melanogaster* expresses only one linker variant, but early embryonic chromatin is bound by the high mobility group protein HMG-D instead of H1 (Ner et al., 2001; Ner and Travers, 1994). Both B4 and HMG-D bind to the nucleosome with a considerably lower affinity than H1.

1.3 Principles of regulating chromatin structure

The various levels of chromatin condensation not only serve to package DNA, but represent also an important way to regulate the accessibility of DNA and hence of the genetic information. The chromatin state may be altered transiently, e.g. to temporarily alter transcription and during repair after DNA damage, or permanently. The latter case, which includes the propagation of the chromatin state to daughter cells, is commonly referred to as epigenetic memory (Allis et al., 2007).

Several principles, frequently acting in concert with each other, are known to regulate chromatin structure: DNA methylation, posttranslational modifications of histones, histone variants and ATP-dependent chromatin remodelling (Bönisch et al., 2008) (Figures 1.4 and 1.5).

Methylation of cytosine residues on N⁵ represents the most stably inherited epigenetic mark. It is found in vertebrates, many invertebrates and plants (Bird, 2002). Low levels of DNA methylation have even been detected in *Drosophila*, which has long been thought to be devoid of DNA methylation. However, it is present only in early development and found mostly on CpT dinucleotides, whereas most methylation in animals occurs on CpG dinucleotides (Gowher et al., 2000; Lyko et al., 2000). DNA methylation generally leads to long term silencing of the underlying sequence by inhibiting binding of activating factors and by recruiting enzymes that generate a repressive chromatin state (Fuks, 2005; Hendrich and Bird, 1998). DNA methyltransferases (DNMTs) are the enzymes that set and maintain DNA methylation. Through their function they regulate transcription by altering chromatin organization. This is crucial to many complex processes such as differentiation, inactivation of the



1.4 Variability of chromatin components

DNA (blue) can be methylated on selected CpG dinucleotides as indicated. Posttranslational modifications (PTM) of histones are written, erased and recognized by specific factors. Variants of core histones H2A, H2B and H3 are represented in green (adapted from Bönisch et al., 2008).

female mammalian X chromosome and imprinting (monoallelic gene expression) (Bernstein et al., 2007; Bird, 2002).

Histones may carry numerous posttranslational modifications (PTMs), mostly located on, but not limited to, the flexible N-terminal tail domains. Among them are methylation of lysines (mono-, di-, and trimethylation) and arginines (mono-, asymmetrical and symmetrical dimethylation), acetylation and ubiquitinylation of lysines, phosphorylation of serines, threonines and tyrosines, SUMOylation and ADP-ribosylation (Bönisch et al., 2008; Cosgrove et al., 2004). Histone modifications are established and erased by dedicated enzymes such as histone acetyltransferases (HATs), histone deacetylases (HDACs), histone methyltransferases (HMTs) and histone demethylases (HDMs) (Bönisch et al., 2008). PTMs can influence chromatin structure directly by affecting histone-DNA interactions within the same or neighbouring nucleosomes. For example, acetylation of H4 on lysine 16 (H4K16Ac) prevents full chromatin compaction even in the presence of linker histones (Robinson et al., 2008; Shogren-Knaak et al., 2006). Alternatively, PTMs can act indirectly through the recruitment of specific readers. These effector proteins can be attracted either by single histone modifications or combinations thereof on the same tail or on proximal tails as suggested by the 'histone code hypothesis' (Strahl and Allis, 2000).

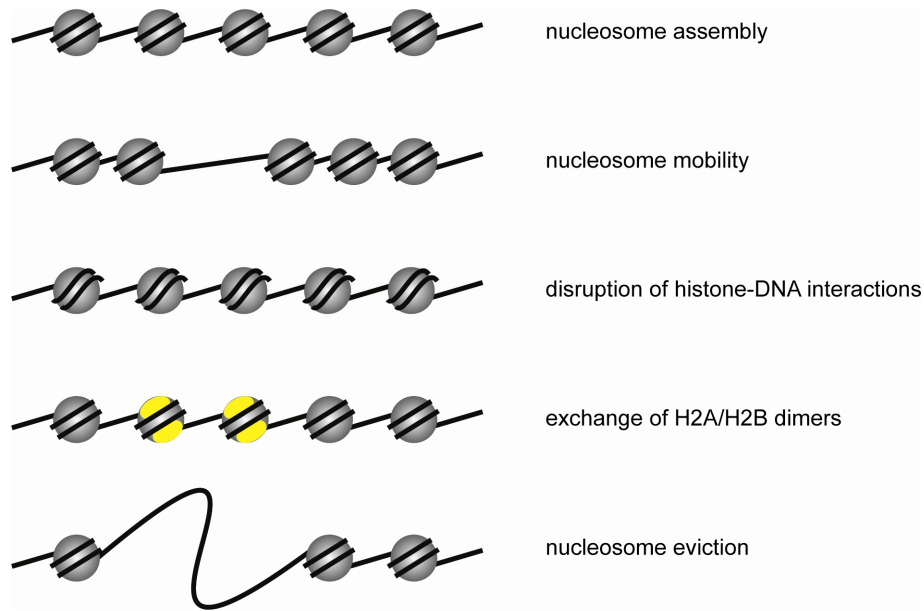
In addition to carrying different modification patterns, nucleosomes can contain variants of histones H2A, H2B, H3 and H1. The number of variants increases with the complexity of the organism (Hake and Allis, 2006). H2A variants are generally the best characterized ones to date. Prominent examples are the H2A variants *Drosophila* H2Av, which is required for heterochromatin formation, mammalian H2A.X, which is involved in DNA double-strand break repair and mammalian H2A.Z, which is essential for survival (Redon et al., 2002; Swaminathan et al., 2005). Histone variants can affect the structure of the nucleosome. For example, nucleosomes containing the centromere-specific H3 variant CENP-A seem to be smaller and less stable than canonical ones (Dalal et al., 2007). Nucleosomes containing H2A.Z are structurally different from canonical ones and appear to be more mobile. They have been implicated both in transcriptional activation and silencing, possibly via interaction with heterochromatin binding protein 1 (HP1) (Ausio, 2006).

Finally, changes in chromatin structure can also be introduced by ATP-dependent chromatin remodelling enzymes, which will be described in the following.

1.4 ATP-dependent chromatin remodelling factors

1.4.1 Subfamilies of ATPases

ATP-dependent nucleosome remodelling factors largely contribute to the dynamic nature of chromatin. Members of this enzyme family couple the hydrolysis of ATP to the disruption of DNA-histone contacts. All remodelling factors contain an ATPase of the SNF2-family, which is typically associated with additional subunits to form large multiprotein complexes (Bao and Shen, 2007; Eberharter and Becker, 2004). The outcome of the remodelling reaction depends on the features of both the ATPase and the regulatory or targeting subunits it associates with. Remodelling factors have been described to introduce conformational changes to the nucleosome, to reposition nucleosomes along DNA (referred to as ‘sliding’), to exchange H2A/H2B dimers, to



1.5 Schematic representation of enzymatic properties assigned to ATP-dependent chromatin remodelling factors

assist nucleosome assembly and to evict entire nucleosomes (Becker and Horz, 2002; Li et al., 2007; Lusser and Kadonaga, 2003) (Figure 1.5).

In vivo, they have been implicated in complex processes such as chromatin assembly, transcription and DNA repair. Impaired nucleosome remodelling may lead to transcriptional deregulation and disease (Wang et al., 2007). They are conserved from yeast to man, which underlines their importance for chromatin regulation (Eberharter and Becker, 2004).

ATP-dependent nucleosome remodelling factors have been divided into subfamilies based on the features of their central ATPase subunits (Figure 1.6).

The SWI/SNF subfamily was the first one to be discovered through a genetic screen in yeast for mutations interfering with mating type switching (SWI) and sucrose fermentation (SNF – sucrose nonfermenting). This screening identified the 11 subunits of the SWI/SNF complex including its ATPase Swi2 or Snf2 (Peterson and Herskowitz, 1992; Sudarsanam and Winston, 2000). SWI/SNF type ATPases harbour a bromodomain, which might target them to acetylated chromatin (Marmorstein an

SWI/SNF Subfamily -

<i>S.cerevisiae</i>	<i>D.melanogaster</i>	<i>H.sapiens</i>
SWI/SNF	BAP PBAP	BAF PBAF
Swi2/Snf2	Sth1*	Brahma+ Brahma+ Brg1 or hBrm+ BRG1*
Swi1/Adr6	Rsc 1,2&4	OSA BAF250 Polybromo Polybromo/BAF 180
	Rsc9	BAP170
Swi3	Rsc8	Moira Moira BAF170&155 BAF170&155
Snf5	Sfh1	Snr1 Snr1 hSNF5/INI1 hSNF5/INI1
Swp82/Yfl049w	Rsc7/ Npl6p	
Swp3/Snf12	Rsc6	BAP60 BAP60 BAF60a BAF60aorb
Arp7/Swp61	Arp7/Rsc11	BAP55 BAP55 BAF53 BAF53
Arp9/Swp59	Arp9/Rsc12	
	Actin	Actin Actin Actin Actin
Snf6		
Swp29/Tfg3/Taf14/Ark		
Rtt102	Rtt102	
Snf11	Rsc 5,10,13-15	

INO80 Subfamily -

<i>S.cerevisiae</i>	<i>H.sapiens</i>
yINO80	ySWR1
Ino80*	Swr1*
Arp8	hIno80*
Arp5	Arp8
Arp4	Arp5
Rvb1	BAF53a/Arp4
Rvb2	Tip49a
les2	Tip49b
les6	hles2/PAPA-1
Act1	hles6/C18orf37
Taf14	Amida
Nhp10	FLJ90652
les1	Aor1/Swc5
les3	Vps71/Swc6
les4	Vps72/Swc2
les5	MCRS1
	FJL20309
	Yaf9
	Bdf1
	Swc1/Swc3
	Swc4/God1

ISWI Subfamily -

<i>S.cerevisiae</i>		<i>D.melanogaster</i>		<i>H.sapiens</i>				<i>M.musculus</i>				
ISW1a	ISW1b	ISW2	ACF	CHRAC	NURF	WCRF/hACF	WICH	hCHRAC	RSF	SNF2h/Cohesin	NoRC	mWICH
Isw1*	Isw1*	Isw2*	ISW1*	ISW1*	ISW1*	hSNF2h*	hSNF2h*	hSNF2h*	hSNF2h*	hSNF2h*	mSNF2h*	mSNF2h*
loc3	loc2	loc4	Itc1	Acf1	Acf1	hAcf1	Wstf	hAcf1		Mi2	Tip5/Baz2a	mWstf
			Dpb4	Chr16				hChr15		Mta1 & 2	p50	
			Dfs1	Chr14				hChr17		HDAC1 & 2	p80	
					Nurf301				p325	RbAp46		
					Nurf55					RbAp48		
					Nurf38					MBD2 & 3		
										Rad21		
										SA1 & 2		
										Smc1 & 3		

CHD Subfamily -

<i>S.cerevisiae</i>	<i>D.melanogaster</i>	<i>M.musculus</i>	<i>H.sapiens</i>
CHD1	Mi2 CHD1	CHD1 Mi2	NuRD ATRX
Chd1*	Chd4* Chd1*	Chd1*	Chd4/Chd3* Chd3/Chd4* ATRX*
	Rpd3		HDAC1 & 2 HDAC1 & 2
			RbAp48 RbAp48
			Icaros 1,2 & 7 RbAp46
			Aiolos MBD3
			MTA2

CHD Subfamily is the least characterized and can have uncharacterized proteins

1.6 Subunit composition of ATP-dependent remodelling complexes belonging to the four characterized subfamilies (classified according to their ATPase subunits)

Asterisks mark the ATPase of each complex. Subunits shared between two or more complexes in the same organism are underlined. Orthologous subunits are shadowed in grey (adapted from Gangaraju and Bartholomew, 2007).

Berger, 2001). *In vivo*, SWI/SNF is required both for transcriptional activation and repression of selected genes (Holstege et al., 1998; Sudarsanam and Winston, 2000). RSC represents a second SWI/SNF complex, which is essential for cell growth and comprises the ATPase Sth1 (Du et al., 1998). Two SWI/SNF complexes, BAP and PBAP, have been found in *Drosophila*. Both contain the ATPase Brahma, but different associated subunits (Mohrmann and Verrijzer, 2005). In humans, SWI/SNF complexes are classified into two forms, BAF and PBAF, which contain the ATPases BRG1 or hBRM, respectively. These complexes can further associate with tissue-specific subunits

or additional subcomplexes (Wang, 2003). BRG1 and BRM as well as the core subunit SNF5 have tumour-suppressive functions in both mice and humans (Wang et al., 2007).

The subfamily most closely related to SWI/SNF ATPases is comprised by ISWI (imitation SWItch) ATPases (Gangaraju and Bartholomew, 2007). They are the focus of this study and will be discussed in more detail in a separate section.

The CHD subfamily is characterized by the presence of chromodomains (Tsukiyama and Wu, 1997). Well-studied remodelling factors belonging to this family include the NURD (nucleosome remodelling and deacetylation) complex and the ATPase CHD1 (chromodomain-helicase DNA binding protein 1). NURD has been isolated from various organisms such as *Drosophila*, *Xenopus* and human. Among other subunits, NURD contains the ATPase Mi-2, MBD3 (methyl-binding protein 3) and the histone deacetylases HDAC1 and 2 (RPD3 in *Drosophila* and *Xenopus*), which target the complex to methylated DNA and couple ATP-dependent remodelling to histone deacetylation, resulting in regulated gene silencing (Tyler and Kadonaga, 1999). CHD1 is found as a monomer both in yeast, flies and mammals. *Drosophila* CHD1 assists the formation of regularly spaced nucleosomal arrays *in vitro* and is required for the deposition of histone variant H3.3 *in vivo* (Konev et al., 2007; Lusser et al., 2005).

Unlike the ATPase domains of other subfamilies, those of INO80-type are bipartited by the insertion of a large spacer region. Yeast INO80.com, the founding member of these complexes, consists of 15 subunits and is involved in DNA repair and transcription (Morrison et al., 2004; Shen et al., 2000; van Attikum et al., 2004). Orthologues exist both in *Drosophila* and mammals. The related yeast SWR1 complex, containing around 13 subunits, broadens the enzymatic range of ATP-dependent remodelling, since it exchanges H2A/H2B dimers for dimers containing the variant H2A.Z both *in vitro* and *in vivo* (Mizuguchi et al., 2004).

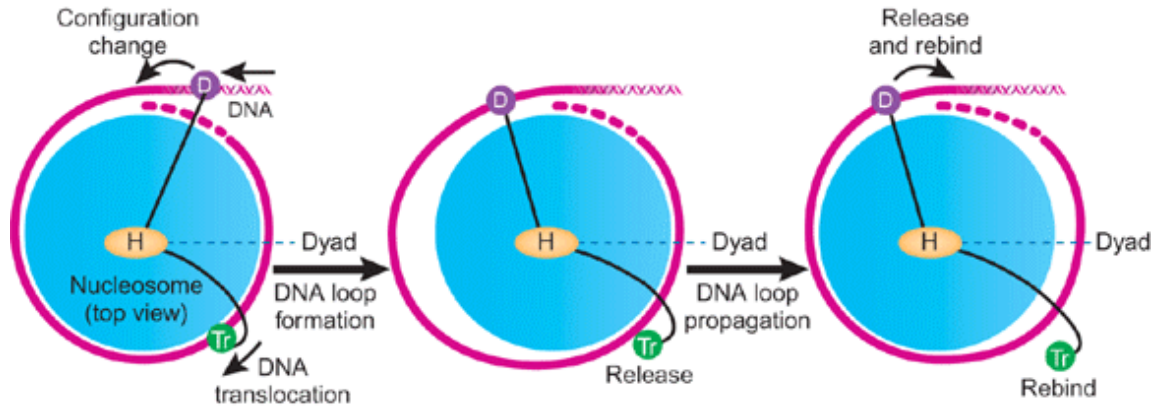
An additional subfamily may be represented by Rad54A, which is most closely related to the INO80 family. It has been shown to perturb DNA and to increase the accessibility of nucleosomal DNA in an ATP-dependent manner (Jaskelioff et al., 2003).

1.4.2 ISWI-containing chromatin remodelling complexes

The ISWI ATPase is characterized by a SANT domain, which may bind to histones and a SLIDE (SANT-like ISWI domain) required for DNA binding and full ATPase activity (Grune et al., 2003). ISWI complexes generally catalyse nucleosome translocations. The first ISWI complexes, NURF, CHRAC and ACF were purified from *Drosophila* by fractionation of embryonic extracts that showed activities in nucleosome spacing and chromatin assembly assays (Eberharter et al., 2001; Ito et al., 1997; Ito et al., 1999; Tsukiyama and Wu, 1995; Varga-Weisz et al., 1997). NURF consists of ISWI, the large regulatory subunit NURF301, the pyrophosphatase NURF38 and the WD40 protein NURF55. CHRAC and ACF contain ISWI and ACF1; in addition CHRAC hosts two small histone fold subunits CHRAC14 and CHRAC16. Furthermore, *Drosophila* ISWI has been shown to interact physically and genetically with Toutatis and physically with RSF1 (Hanai et al., 2008; Vanolst et al., 2005). Homologous complexes of NURF, ACF, CHRAC, and RSF were identified in mammals. Moreover, additional complexes such as NoRC (Nucleolar remodelling complex) and WICH (WSTF-ISWI chromatin remodelling complex) have been described (Eberharter and Becker, 2004). All contain one of the two mammalian ISWI ATPases, SNF2H and SNF2L. Also in yeast, two proteins, ISW1 and ISW2, were found to be highly homologous to *Drosophila* ISWI. ISW1 resides in two distinct complexes, ISW1a and ISW1b (Mellor and Morillon, 2004). ISW2 forms a complex often considered to be the yeast CHRAC homolog, because it not only exhibits nucleosome spacing activity, but also contains Itc1, a subunit related to ACF1, and two small histone fold subunits (Dpb4 and Dls1), which are homologous to CHRAC14 and CHRAC16 (Gelbart et al., 2001). These findings highlight the remarkable conservation of ATP-dependent remodelling factors throughout evolution.

1.4.3 Mechanism of ISWI-dependent nucleosome repositioning

In spite of more than a decade of research on ISWI remodelling complexes, the mechanism of nucleosome translocation is not completely understood. Nevertheless,



1.7 Loop-recapture mechanism for nucleosome sliding catalysed by ISWI

The DNA translocase domain (Tr) binding to nucleosomal DNA at superhelical location 2 and a DNA-binding domain (D) binding to the linker DNA, near the nucleosome entry/exit site, act in concert to create a DNA loop on the nucleosome surface. Tr and D were connected by a hinge region (H). A conformational change in Tr during the ATPase cycle allows DNA release and loop propagation resulting in nucleosome repositioning. The DNA-binding domain then rebinds a new stretch of DNA and the complex returns to its original conformation (adapted from Cairns, 2006).

considerable progress towards understanding the structural details of nucleosome repositioning has been made. ISWI ATPases are DNA translocases (Whitehouse et al., 2003; Zofall et al., 2004). They have been mapped to contact the nucleosome at two sites: a DNA-binding domain contacts the linker DNA close to the entry/exit site and the translocation domain binds a region two helical turns away from the dyad axis (superhelical location 2 – SHL2) (Kagalwala et al., 2004). Both NURF and ISW2 have been suggested to move nucleosomes in steps of approximately 10 bp. These and other findings are accommodated in the currently favoured model for nucleosome sliding, which is a refinement of the earlier proposed loop recapture model (Cairns, 2007; Gangaraju and Bartholomew, 2007; Langst and Becker, 2004) (Figure 1.7). According to this model, the ATPase pumps DNA into the nucleosome by a concerted action of its DNA-binding domain and its translocase domain. This ATP-dependent transformational change results in disruption of histone-DNA contacts and the formation of a small loop. Subsequently, the translocation domain at SHL2 is believed to detach and allow loop propagation around the histone octamer, leading to a new translational position of the nucleosome, approximately 10 bp away from the initial one.

1.4.4 Regulation of ISWI and its complexes

Several mechanisms are known to affect the enzymatic properties of ISWI ATPases. The most straightforward way to alter their activities is through the association of regulatory subunits. For example, ACF1, which is found in both ACF and CHRAC, affects both the quality and efficiency of ISWI functions. Although the DNA- and nucleosome-stimulated ATPase activity of ISWI remains constant upon association with ACF1, the efficiency of mononucleosome sliding is increased approximately by a factor of 10 (Eberharter et al., 2001). Binding of the two histone fold proteins CHRAC14 and CHRAC16 results in an additional fivefold increase in the same assay (Hartlepp et al., 2005). Apart from affecting the remodelling efficiency, subunits can also change the outcome of the remodelling reaction. Whereas ISWI alone catalyses repositioning of mononucleosomes from the centre of short DNA fragments to their end, ACF and CHRAC catalyse sliding to the opposite direction, from the end to the centre of DNA fragments. However, the *in vivo* implications of these observations are not clear. Functional differences are also observed between distinct ISWI-containing complexes. For example ACF and CHRAC promote the formation of regularly spaced nucleosomal arrays (Ito et al., 1997; Varga-Weisz et al., 1997) while NURF disrupts the regularity of preassembled regular chromatin arrays (Tsukiyama and Wu, 1995). Concomitantly, ACF is required for proper chromatin assembly and heterochromatin formation *in vivo*, whereas NURF plays a role in transcriptional regulation (Fyodorov et al., 2004; Tsukiyama and Wu, 1995; Chioda et al., manuscript in preparation).

A second principle affecting ISWI activity is provided by posttranslational modifications of histones. The ATPase activity is stimulated by DNA, but full activation requires the presence of nucleosomes. A short basic stretch of the H4 tail, residues 16 to 20, is essential for this additional stimulation (Clapier et al., 2002). Also H4 peptides alone increase the ATPase activity in the presence of DNA, but acetylation of lysines 12 or 16, both located in the proximity of the critical epitope, reduce the ability of the peptides to stimulate the ISWI ATPase by half (Corona et al., 2002). In agreement, the mononucleosome sliding activity of ACF is reduced by about 50% if mononucleosome containing H4K16Ac are used as substrate (Shogren-Knaak et al., 2006).

Regulatory subunits of ISWI complexes regulate the ATPase not only by changing its enzymatic properties, but also by recruiting it to its sites of action. Both NURF301, the largest subunit of NURF, and ACF1 contain two plant homeodomain (PHD) fingers followed by a bromodomain, which could target the complexes to specifically modified histone tails. Bromodomains interact with acetylated histones, PHD fingers have repeatedly been reported to recognize the methylation status of lysine residues (Baker et al., 2008; Zeng and Zhou, 2002). The second, bromodomain-proximal PHD finger of NURF301 and its human homologue BPTF specifically recognize the H3K4 trimethylation mark and it is believed that NURF is recruited to or stabilized at promoters via this interaction (Wysocka et al., 2006). The PHD fingers of ACF1 have not been identified as targeting domains, so far, but are required for enhancing the remodelling efficiency of ISWI, presumably by anchoring it to the histone octamer (Eberharter et al., 2004b).

Regulation could also be exerted through covalent modification of remodelling complexes themselves. The well-known histone H3-specific acetyltransferase Gcn5 has been shown to acetylate *Drosophila* ISWI both *in vivo* and *in vitro* at a site with sequence similarity to the H3 tail. Antibody staining against the acetylated form in tissue culture cells was reduced upon knock-down of NURF301, but not ACF1. Moreover, acetylated ISWI co-immunoprecipitated with NURF301, but not ACF1 suggesting that acetylated ISWI may reside in NURF, but not in ACF and CHRAC (Ferreira et al., 2007). In addition, PHD fingers have repeatedly been reported to act as E3 SUMO ligases which sumoylate their adjacent bromodomains (Garcia-Dominguez et al., 2008; Ivanov et al., 2007).

ISWI complexes may also be recruited to their sites of action by specific interactions with other chromatin binding proteins involved in specific nuclear processes requiring events of chromatin remodelling. Examples are provided by the hWICH subunit WSTF, which interacts with PCNA and thereby recruits the complex to sites of active replication (Poot et al., 2004) and NURF, which can act in concert with transcription factors to induce transcription *in vitro* (Mizuguchi et al., 1997).

Finally, chromatin remodelling can be controlled by spatial or temporal transcriptional regulation of remodelling complex subunits. ACF1, for instance, is

predominantly expressed during early *Drosophila* development (Chioda et al., manuscript in preparation).

1.5 Interplay between linker histones and ATP-dependent chromatin remodelling

1.5.1 ATP-dependent remodelling in the presence of linker histones *in vitro*

As described above, considerable progress has been made in understanding the substrate requirements of ATP-dependent remodelling factors. However, despite the high abundance of linker histones in the nucleus and their strong effect on chromatin compaction, their effect on remodelling has only been addressed in a handful of studies and remains controversial. In most cells, the majority of nucleosomes are bound by a linker histone, so complete inhibition of remodelling by H1 would limit it to a small fraction of chromatin (Horowitz et al., 1994). It is consequently very important to clarify whether and to what extent ATP-dependent chromatin remodelling factors can act on linker histone-containing chromatin.

Linker histones inhibit the spontaneous sliding of histone octamers on DNA (Pennings et al., 1994; Ura et al., 1995). Similarly, one would expect ATP-dependent nucleosome repositioning to be difficult in the presence of linker histones, since this is likely to involve pulling linker DNA into the nucleosome (Flaus and Owen-Hughes, 2004; Saha et al., 2006). Indeed, incorporation of H1 reduced the ATP-dependent ability of the SWI/SNF complex to increase the accessibility of mononucleosomal DNA (Hill and Imbalzano, 2000). In agreement, addition of H1 inhibited ACF-dependent remodelling of dinucleosomes (Saeki et al., 2005). Conversely, Schnitzler and colleagues concluded that SWI/SNF-dependent repositioning of mononucleosomes was not impaired by H1 (Ramachandran et al., 2003).

Mono- and dinucleosomes are convenient substrates for studying nucleosome remodelling *in vitro*, but they are far from a physiological context of chromatin fibers. *In vitro*, nucleosome movements were also observed within extended arrays of

nucleosomes, which better mimic a chromatin context (Boyer et al., 2000; Corona et al., 1999; Hassan et al., 2001). Considering the strong effect of linker histones on chromatin folding, their impact on chromatin remodelling can only be reliably investigated using nucleosome arrays. Yet, only few studies used oligonucleosomes as substrates to elucidate how linker histones may affect remodelling. Also in this case, the results obtained from these studies are controversial: some indicating an inhibitory effect by linker histones on ATP-dependent chromatin remodelling while other evidences do not support such a view. For example, monitoring the accessibility of nucleosomal DNA in nucleosome arrays, the nucleosome remodelling activities of human SWI/SNF, yeast SWI/SNF, Mi-2 and *Xenopus* ACF were strongly inhibited by the linker histone H5 (Horn et al., 2002). In contrast, when chromatin was assembled by *Drosophila* embryonic extract, repositioning of nucleosomes in an ATP-dependent manner was observed even in the presence of stoichiometric amounts of histone H1 (Varga-Weisz et al., 1995). Subsequently, CHRAC was identified as the remodelling complex harbouring the activity necessary for nucleosome repositioning detected in the embryonic extract (Eberharter et al., 2001; Varga-Weisz et al., 1997). However, to date it remained unclear whether the ability to remodel H1-containing chromatin relied also on cofactors present in the extract.

1.5.2 Role of ISWI complexes in linker histone incorporation

ACF1, the subunit defining ACF and CHRAC, is abundant during early *Drosophila* development, when H1 gradually replaces its early placeholder HMG-D. As already mentioned, ACF not only possesses nucleosome sliding activity, but can also assist the assembly of DNA and histones into regularly spaced nucleosomal arrays (Ito et al., 1997). If H1 is present in such an assembly reaction, it is incorporated into the reconstituted chromatin. This property is not common to all chromatin assembly factors as illustrated by the monomeric remodelling factor CHD1, which assembled only chromatin without H1 (Lusser et al., 2005). Because of its ability of assembling H1 into chromatin it has been proposed that ACF may act as an H1 chaperone.

During later development, a different ISWI complex may be required to deposit H1 onto or maintain it on chromatin as suggested by the *iswi* knock-out phenotype. ISWI depletion is lethal, but mutant flies survive until the third instar larval stage due to maternal ISWI contribution. This allows the analysis of larval polytene chromosomes in salivary glands revealing that ISWI is required for global chromatin organization. The male X chromosome seems to be particularly sensitive to the loss of ISWI, since in homozygous *iswi* null larvae, it is heavily decondensed (Deuring et al., 2000). Expression of a dominant negative form of ISWI results in the decondensation also of the other chromosomes (Corona et al., 2007). The male X chromosome differs from the autosomes and the female X chromosome by chromosome-wide acetylation of H4K16, a modification resulting from the activity of the dosage compensation complex (DCC) (Morales et al., 2004). The DCC, in male flies, regulates the expression of X-linked genes as compensation for the lack of a second X chromosome (Gilfillan et al., 2006). Genetic analysis revealed that global H4K16Ac is both necessary and sufficient for chromosome decondensation upon ISWI depletion (Corona et al., 2002). H4K16Ac counteracts chromatin folding, so it could render chromatin susceptible to defects in chromatin condensation (see 1.3). Strikingly, no H1 is detected on the aberrant chromosome structures observed in *iswi* null flies (Corona et al., 2007), raising the possibility that ISWI might be involved in the loading or maintaining of linker histones on chromatin. Knock-out of the NURF subunit NURF301 resulted in the same decondensation of the male X-chromosome, showing that NURF may account for the *iswi* phenotype (Badenhorst et al., 2002).

1.6 Goals

This work investigates the effect of linker histones on ATP-dependent chromatin remodelling of *Drosophila* ACF making use of a highly homogeneous system comprising oligonucleosomal templates reconstituted from purified components. 12mer nucleosome or chromatosome arrays were subjected to ATP-dependent remodelling by

the complex ACF, its ATPase ISWI and as reference by the ATPases CHD1 and BRG1. The remodelling efficiency of these factors in the absence or presence of linker histones or the early linker histone substitute HMG-D was monitored by changes in accessibility of nucleosomal DNA. Because ACF catalyses nucleosome sliding, movement of nucleosomes was assayed by partial digestion with micrococcal nuclease, which allows to monitor nucleosome positions. Moreover, repositioning of both nucleosomes and chromatosomes was measured directly by mapping the positions of isolated particles after remodelling reactions by primer extension. In addition, we investigated effects of H1 on the directionality of ACF-mediated nucleosome sliding.

Because ACF can assemble H1-containing chromatin *in vitro* (see 1.5.2), we tested whether it has a related function *in vivo*. To monitor H1 and HMG-D dynamics *in vivo*, we raised antibodies against the two proteins and used them in whole mount immunostaining of early *Drosophila* wild-type or *acfl* null embryos. In addition, replacement of HMG-D by H1 was investigated in a purified *in vitro* system.

2. Materials and Methods

2.1 Material sources

2.1.1 Laboratory chemicals and biochemicals

Acrylamide (Rotiphorese Gel [®] 30)	Roth, Karlsruhe
Agarose (ME, LE <i>GP</i> and low melting)	Biozym, Hessisch Oldenburg
Ampicillin	Roth, Karlsruhe
Aprotinin	Sigma, Taufkirchen
ATP	Sigma, Taufkirchen
[γ - ³² P]- ATP	GE Healthcare, Munich
Bacto Agar	BD, France
Bacto Trypton	BD, France
BSA (Bovine serum albumin), 98% pure	Sigma, Taufkirchen
BSA, purified	NEB, Frankfurt/Main
β -Mercaptoethanol	Sigma, Taufkirchen
Chloramphenicol	Roth, Karlsruhe
Coomassie G250	Serva, Heidelberg
[α - ³² P]-dCTP	GE Healthcare, Munich/ Perkin Elmer, Massachusetts
DEAE Sepharose	GE Healthcare, Munich
dNTP-Mix	NEB, Frankfurt/Main
dNTP-Set	Roche, Mannheim
DTT (Dithiothreitol)	Roth, Karlsruhe
EDTA	Sigma, Taufkirchen
EGTA	Sigma, Taufkirchen
Ethidium bromide	Sigma, Taufkirchen
Fetal bovine serum	Sigma, Taufkirchen
3-glycerophosphate	Sigma, Taufkirchen
Glycogen	Roche, Mannheim
Guanidium-Cl	Sigma, Taufkirchen
Hepes (N-(2-Hydroxyethyl)piperazine-H ⁺ - (2-ethanesulfonic acid))	Roth, Karlsruhe
Hydroxyl apatite	Bio-Rad, Munich
Kanamycin	Sigma, Taufkirchen
IPTG	Roth, Karlsruhe
Leupeptin	Sigma, Taufkirchen
NP40 (Igepal CA-630)	Sigma, Taufkirchen
Orange G	Sigma, Taufkirchen
Paraformaldehyde	Sigma, Taufkirchen
Pepstatin	Sigma, Taufkirchen

Phenol	Roth, Karlsruhe
Phenylsepharose	GE Healthcare, Munich
PMSF (Phenylmethanesulfonyl fluoride)	Sigma, Taufkirchen
SDS (Sodium dodecyl sulfate)	Serva, Heidelberg
Sf-900II medium (GibCo)	Invitrogen, Karlsruhe
SYBR gold	MoBiTec, Göttingen
Temed (N,N,N',N'-Tetramethylethylenediamine)	Roth, Karlsruhe
TO-PRO3 (Molecular Probes)	Invitrogen, Karlsruhe
Tris	Invitrogen, Karlsruhe
Triton X-100	Sigma, Taufkirchen
Tween 20	Sigma, Taufkirchen
Vectashield mounting medium	Vector Labs, U.K.
Xylene cyanol	Sigma, Taufkirchen
Yeast extract	Difco, Detroit

All other chemicals were purchased in analytical grade from Merck, Darmstadt.

2.1.2 Enzymes

Antarctic Phosphatase	NEB, Frankfurt/Main
DNA Polymerase I, Large (Klenow) Fragment	NEB, Frankfurt/Main
Klenow Fragment (3' → 5' exo ⁻)	NEB, Frankfurt/Main
Micrococcal nuclease (MNase)	Sigma, Taufkirchen
Polynucleotide Kinase (PNK)	NEB, Frankfurt/Main
Proteinase K	Roche, Mannheim
Restriction endonucleases	NEB, Frankfurt/Main
Taq DNA Polymerase	Roche, Mannheim
	NEB, Frankfurt/Main

2.1.3 Antibodies

Primary antibodies	
chicken α -H1 (raised for this study)	Eurogentech, Netherlands
rabbit α -HMG-D (raised for this study)	Eurogentech, Netherlands
goat α -H4 (commercial)	Santa Cruz Biotechnology, California
rabbit α -H3 (commercial)	Abcam, UK

Secondary antibodies

rabbit α -chicken IgY HRP-conjugated	Promega, Mannheim
α -rabbit HRP-conjugated	Promega, Mannheim
rabbit α -chicken IgY, Hilite Fluor TM 680	AnaSpec, California
donkey α -rabbit IRDye 800	Rockland, Pennsylvania
donkey α -goat IRDye 680	Molecular Probes
α -chicken Alexa 488-conjugated	Jackson Immunoresearch Laboratories, UK
α -rabbit Rhodamine Red X-conjugated	Jackson Immunoresearch Laboratories, UK

2.1.4 Organisms, cells and bacteria

TOP10 <i>E. coli</i> strain	Invitrogen, Karlsruhe
BL21 Codon Plus <i>E. coli</i>	Stratagene,
Sf9 cells (<i>Spodoptera frugiperda</i>)	Novagen

Drosophila yw flies and TM3 and TM6 balancer chromosomes are described in FlyBase (<http://flybase.bio.indiana.edu>)

2.1.5 Oligonucleotides, plasmids, and baculoviruses

2.1.5.1 Primers

All primers were ordered from Biomers, Ulm

13fw	5'-ATCTGACACGTGCCTGGA-3'
13rv	5'-TCCAGGCACGTGTCAGAT-3'
76fw	5'-CGTACGTGCGTTTAAGC-3'
76rv	5'-GCTTAAACGCACGTACG-3'
linker22fw	5'-CTGAGCTCAGATCTATCTAGAGCATGCCCCGAGTC-3'
linker22rv	5'-GACTCGGGCATGCTCTAGATAGATCTGAGCTCAG-3'
linker31fw	5'-CTGAATTCCTGCAGGATCCAGTCTCGGGAC-3'
linker31rv	5'-GTCCCGAGACTGGATCCTGCAGGAATTCAG-3'

2.1.5.2 Plasmids

pBluescript KS	Stratagene, Netherlands
pUC19	Invitrogen, Karlsruhe
pUC18 12x601	Daniela Rhodes, Cambridge
pET3c dH2A	Violette Morales

pET3c dH2B
pET24 HMG-D

Violette Morales
Andrew Travers

2.1.5.3 Baculoviruses

ACF1-flag
ISWI
flag-ISWI
CHD1-flag
flag-BRG1

James Kadonaga
James Kadonaga
Toshi Tsukiyama
Alexandra Lusser
Robert Kingston

2.1.6 Other materials

1 kb DNA marker	NEB, Frankfurt/Main
100 bp DNA marker	NEB, Frankfurt/Main
A-flag M2 agarose	Sigma, Taufkirchen
Bio-Rad Protein Assay (Bradford)	Bio-Rad, Munich
DE81 anion exchanger chromatography paper	Whatman, Rothenburg/Fulda
ECL detection system	GE Healthcare, Munich
Gel Extraction Kit	Qiagen, Hilden
Hiload [®] 16/60 Superdex [®] 200 gel filtration column	GE Healthcare, Munich
Immobilon-P PVDF membrane	Millipore, Massachusetts
Microsep Omega centrifugal devices (10K/30K)	Pall, New York
Miracloth (Calbiochem)	Merck, Darmstadt
MonoS 5/50 GL	GE Healthcare, Munich
peqGOLD Protein Marker	Peqlab Biotechnologie, Erlangen
Plasmid Maxi Kit	Qiagen, Hilden
Plasmid Mini Kit	Qiagen, Hilden
Rotilabo syringe filters	Roth, Karlsruhe
Siliconised reaction tubes, 1.5 ml	Biozym, Hessisch Oldenburg
SpectraPor dialysis membrane	Roth, Karlsruhe
SP-Sepharose column (5 ml)	GE Healthcare, Munich
Super RX Fuji medical X-ray film	Fuji, Düsseldorf
TLC plates	Merck, Darmstadt

2.2 Buffers and solutions

Agar plates for collecting <i>Drosophila</i> embryos	1.8% 2% 0.1%	Bacto agar sucrose acetic acid
Coomassie destaining solution	10% v/v	acetic acid
Coomassie staining solution	10% v/v 0.25% w/v	acetic acid Coomassie Brilliant Blue R-250
DB500/2000	10 mM 500/2000 mM 1 mM 0.01% v/v 1 mM	Tris-Cl pH 7.6 NaCl EDTA pH 8.0 NP40 β -mercaptoethanol (just before use)
DB0/50	10 mM 0/50 mM 1 mM 1 mM	Tris-Cl pH 7.6 NaCl EDTA pH 8.0 β -mercaptoethanol (just before use)
DNA loading buffer (6x)	30% v/v 0.25% w/v	glycerol xylene cyanol, bromophenol blue and/or orange G
EW (embryo wash buffer)	0.7% w/v 0.05% v/v	NaCl Triton X-100
EX40	10 mM 40 mM 1.5 mM 0.5 mM 10% (v/v)	Hepes-KOH pH 7.6 KCl MgCl ₂ EGTA glycerol
Extract buffer	10 mM 10 mM 1.5 mM 0.5 mM 10% (v/v) 10 mM 1 mM	Hepes-KOH pH 7.6 KCl MgCl ₂ EGTA glycerol 3-glycerophosphate (just before use) DTT (just before use) proteinase inhibitors (just before use)

Fixation buffer	50% v/v 10% v/v	methanol acidic acid
Glycine buffer	15 mM 10 mM 5 mM 0.05 mM 0.25 mM 10% v/v 1 mM proteinase inhibitors (just before use)	Hepes-KOH, pH 7.6 KCl MgCl ₂ EDTA EGTA glycerol DDT (just before use)
HEMG for H1 purification	25 mM 12.5 mM 0.1 mM 10% v/v NH ₄ SO ₄ 1 mM 0.2 mM	Hepes-KOH pH 7.6 MgCl ₂ EDTA pH 8.0 glycerol as indicated DDT (just before use) PMSF (just before use)
HEMG200/500 for purification of remodelling enzymes from Sf9 cells	25 mM 200/500 mM 0.5 mM 12.5 mM 10% 0.05% 1 mM proteinase inhibitors (just before use)	Hepes-KOH pH 7.6 KCl EDTA MgCl ₂ glycerol NP40 DTT
HEG100/1000	25 mM 0.1 mM 10% v/v 100/1000 mM 1 mM 0.2 mM	Hepes-NaOH pH 7.6 EDTA pH 8.0 glycerol NaCl DDT (just before use) PMSF (just before use)
HE50/500/1000	50 mM 50/500/1000mM 1mM proteinase inhibitors (just before use)	Hepes-NaOH pH 8.0 NaCl EDTA pH 8.0
K-PO ₄ 100 mM	28 mM 72 mM	KH ₂ PO ₄ K ₂ HPO ₄

Laemmli buffer (3x)	100 mM 3% w/v 45% v/v 0.01% 7.5%	Tris-Cl pH 6.8 SDS glycerol bromophenol blue β -mercaptoethanol
LB-Agar plates	LB-medium 1.5% w/v	Bacto-Agar
LB-Medium	1.0% w/v 0.5% w/v 1.0% w/v pH 7.2	Tryptone Yeast extract NaCl
Loading buffer for primer extension reactions	80% v/v 0.1 M 0.25% w/v	formamid NaCl bromophenol blue
NB (nuclei buffer)	15 mM 60 mM 15 mM 5 mM 0.1 mM proteinase inhibitors (just before use)	Tris-Cl pH 7.4 KCl NaCl MgCl ₂ EGTA pH 8.0
PBS (Phosphate-buffered saline)	1.54 M 15 mM 27 mM	NaCl KH ₂ PO ₄ Na ₂ HPO ₄ *12H ₂ O
PBS-T	PBS containing 0.1% Tween 20	
RB50	10 mM 50 mM 1.5 mM 0.5 mM	Hepes pH 7.6 KCl MgCl ₂ EGTA pH 8.0
Refolding buffer	2 M 10 mM 1mM 5mM	NaCl Tris pH 7.5 EDTA pH 8.0 β -mercaptoethanol (just before use)
Sau200/600	7 M 20 mM 200/600 mM 1 mM 5 mM	Urea (max. 24 h before use) Na-acetate pH 5.2 NaCl EDTA pH 8.0 β -mercaptoethanol (just before use)

Sucrose buffer	15 mM	Hepes-KOH, pH 7.6
	10 mM	KCl
	5 mM	MgCl ₂
	0.05 mM	EDTA
	0.25 mM	EGTA
	30 mM	sucrose
	1 mM	DTT (just before use)
		proteinase inhibitors (just before use)
TAE	40 mM	Tris-acetate
	1 mM	EDTA pH 8.0
TB (0.2x)	9 mM	Tris-borate pH 8.0
TBE	45 mM	Tris-borate
	1 mM	EDTA pH 8.0
TE	10 mM	Tris-Cl
	1 mM	EDTA pH 8.0
Transfer buffer	48 mM	Tris base
	39 mM	glycine
	20% v/v	methanol
	0.0375% w/v	SDS
Tris-buffered phenol pH 8.0	Phenol buffered twice with 0.5 M Tris-Cl pH 8.0 and twice with 0.1 M Tris-Cl pH 8.0	
Tris-glycine buffer	50 mM	Tris base
	384 mM	glycine
Unfolding buffer	7 M	Guanidium-HCl
	20 mM	Tris pH 7.5
	10 mM	DTT (just before use)
Washing buffer for inclusion bodies	50 mM	Tris-Cl pH 7.5
	100 mM	NaCl
	1 mM	EDTA pH 8.0
	5 mM	β-mercaptoethanol (just before use)
		proteinase inhibitors (just before use)

Proteinase inhibitors included 0.2 mM PMSF, 1 mg/l aprotinin, 1 mg/l leupeptin and 0.7 mg/l pepstatin.

2.3 Methods for the preparation and analysis of DNA

2.3.1 General methods for working with DNA

2.3.1.1 Agarose gel electrophoresis

Agarose gel electrophoresis was used to analyse and separate the quality, size and quantity of DNA fragments (Sambrook and Russell, 2001). Depending on the size of the fragments of interest, 0.7-2% w/v agarose solutions in TAE were used. The volume per gel was 50 ml. EtBr was added to a final concentration of 0.5 µg/ml. Electrophoresis was carried out in TAE. After separation, DNA was examined on UV light. If a higher sensitivity was required, instead of including EtBr in the gel, gels were stained after electrophoresis for 30 min with a 1:10000 dilution of SYBRgold[®] in TAE.

Radioactive agarose gels used to analyse chromatin remodelling assays were dried on a gel dryer for 2 h at 50°C on DE81 anion exchange paper and exposed to a phosphoimager screen. Images were acquired with BASReader in a FLA-3000 phosphoimager (Fujifilm) and analysed with AIDA Image Analyzer software.

2.3.1.2 Ethanol precipitation

DNA was precipitated by adding two volumes of ethanol and 1/10 volume of 3 M NaOAc pH 5.2. The mixture was incubated for 1 h on ice or overnight at -20°C and centrifuged for 30 min, at 4°C, 13,000 rpm in a tabletop centrifuge. The pellet was washed with 70% ethanol, dried and resolved in the appropriate buffer.

2.3.1.3 DNA quantification

Plasmid DNA was quantified by measuring the optical density at a wavelength of 260 nm with a NanoDrop[®] (peqlab). One OD unit at 260 nm (OD₂₆₀) corresponds to a concentration of 50 µg DNA/ml. The purity of the DNA can be judged by the ratio OD₂₆₀/OD₂₈₀. Pure DNA preparations have a ratio of 1.8.

2.3.1.4 Transformation of competent bacteria

After thawing on ice, 50 μ l of chemically competent *E. coli* were added to approximately 50 ng plasmid DNA in a precooled 1.5 ml tube. Samples were incubated for 30 min on ice, for 45 s at 42°C and for another 3 min on ice. 200 μ l RT LB were added and the cells were incubated at 37°C for 30 min. Bacteria were streaked out on agar plates containing appropriate antibiotics. Plates were incubated overnight at 37°C.

2.3.1.5 Plasmid preparation

Plasmids were prepared using the Qiagen Plasmid Mini and Maxi kits following the manufacturer's instructions.

2.3.2 Cloning of pUC19 4x601

pUC19 4x601 was generated by partially digesting pUC18 12x601 with *Ava*I (see 2.1.5.2). The fragment comprising four 601 positioning sequences was to linkers 22 and 31 (see 2.1.5.1) with T4 DNA Ligase in the presence of a tenfold excess of linkers. Linkers were prepared by denaturing the appropriate pairs of complementary primers at 95°C followed by renaturation by gradual decrease of the temperature. The short doublestranded DNA fragments were digested by *Ava*I to render their ends compatible with the 4x601 insert and purified from a 6% polyacrylamide gel by the crush and soak method (Sambrook and Russell, 2001).

After the ligation of 4x601 DNA fragments to the linkers, the insert was digested with *Pst*I and *Sac*I which are cutting in linker 22 and linker 31, respectively, and purified from 0.8% agarose gel in TAE using the Qiagen gel extraction kit. Subsequently, the insert was ligated into pUC19 cut with *Sac*I and *Pst*I, which had been purified by the same procedure. Ligations were performed using 30 ng pUC19, a threefold molar excess of the insert and 400 U T4 DNA Ligase in 20 μ l 1x ligation buffer for 1 h at RT. 10 μ l of the ligation reaction was transformed into chemically competent TOP10 *E. coli*. Positive clones were selected on agar plates containing 100 μ g/ml ampicillin. Individual colonies

were picked and grown overnight at 37°C in 5 ml LB medium containing 100 µg/ml ampicillin. Plasmid DNA was purified using the Qiagen Miniprep kit and the presence of the right insert was controlled by analytical SacI/PstI digestion.

2.3.3 Preparation of DNA fragments for the assembly of nucleosomal arrays

2.3.3.1 Preparation of DNA fragments for the assembly of 12mer arrays

50 µg of pUC18-12x601 plasmid were digested with 50 U of EcoRI, HindIII and DraI in a final volume of 100 µl buffer B (Roche, Mannheim). Digestions were carried out for 3 h at 37°C. 1/10 of the reactions were loaded on agarose gel for checking the extent of digestion.

For radioactive chromatin assemblies, 1/5 of 12x601 DNA fragments were labelled by Klenow-exo⁻-Polymerase (see 2.3.4). For this purpose, a fraction of the digested plasmid was purified from agarose gels. 50 µg digested DNA were loaded per 50 ml gel. Electrophoresis was carried out in TAE. A low energy UV handlamp was used to visualize the DNA. When the bands had separated, electrophoresis was stopped and a small rectangle was cut out just below the fragment to be purified. This window was filled with a melted solution of 0.7% w/v low melting agarose in TAE. After the agarose had solidified, electrophoresis was resumed allowing the DNA to migrate into the low melting agarose gel and then it was excised.

To purify the DNA, low melting gel slices were incubated at 65°C until fully melted. DNA was extracted by adding one volume of Tris-buffered phenol (equilibrated with 0.1 M Tris pH 8). After mixing, the tube was centrifuged in a table-top centrifuge at RT for 10 min at 13,000 rpm. The aqueous phase was collected, the organic phase was re-extracted by adding 300 µl of TE pH 8 and spun 5 min, 13,000 rpm. The aqueous phases containing the DNA were extracted with butanol, thereby removing EtBr and reducing the water volume to a final volume of approximately 400 µl.

The DNA was precipitated with ethanol and dissolved in TE. The purity of DNA was checked by agarose gel electrophoresis.

2.3.3.2 Preparation of DNA fragments for the assembly of palindromic 8x601 arrays

Palindromic 8x601 DNA arrays were produced which – if assembled into nucleosomal arrays – contained H1 binding sites facing either outwards or inwards. To obtain arrays with H1 binding sites facing outwards, the pUC18 4x601 plasmid was digested with BglIII (cutting in linker 22) in 100 μ l reactions and subsequently dephosphorylated by Antarctic Phosphatase according to the manufacturer's instructions. After inactivating the Antarctic Phosphatase by heat-denaturation, the DNA was precipitated. After dissolving, DNA fragments were digested by BamHI (cutting in linker 31) and the 4x601 insert was purified from 0.7% agarose by Phenol extraction (see 2.3.3.1). The 4x601 BamHI-BglIII fragments were ligated by T4 DNA Ligase at their BamHI-cut ends and the resulting 8mer arrays were purified from agarose gel by a phenol extraction.

To obtain palindromic arrays with H1 binding sites facing inwards, the same procedure was applied, but plasmids were first digested by BamHI and dephosphorylated. The DNA was then digested with BglIII, 4x601 fragments were purified and ligated with their BglIII-cut ends.

To generate a size of competitor DNA that could be distinct from 8x601 palindromic arrays pUC19 plasmid was digested by EcoRI and HindIII, giving rise to 692 bp, 808 bp and 1167 bp DNA fragments. Enzymes were heat-inactivated and the DNA precipitated.

2.3.4 Radioactive DNA end-labelling

5'-overhangs of DNA fragments resulting from HindIII-digestion, BglIII or BamHI-digestion were filled in with Klenow- exo^- -Polymerase in the presence of [α - 32 P]-dCTP and non-radioactive nucleotides. 2 μ g DNA and 2 U of the polymerase were incubated with dGTP, dATP, dTTP (final concentration 33 μ M each) and 1 μ l of [α - 32 P]-dCTP (10 mCi/ml, 3000 Ci/mmol) in NEB buffer 2 in a final volume of 20 μ l. After 15 min at 37°C, reactions were stopped by addition of 1 μ l 0.5 M EDTA pH 8.0 and inactivation of the enzyme at 75°C for 20 min. The DNA was precipitated and dissolved in TE. The

labelling efficiency was checked by counting the activity of labelled DNA in a Beckmann LS1801 scintillation counter.

2.4 Methods for protein analysis and purification of proteins

2.4.1 Protein quantification

Protein concentrations were determined using the Bio-Rad Protein Assay according to the manufacturer's instructions. BSA (purified) was used as a protein standard. In addition, protein concentrations were estimated by eye by comparing them to a protein standard (BSA) on an SDS polyacrylamide gel.

2.4.2 SDS polyacrylamide gel electrophoresis (SDS-PAGE)

SDS-PAGE was conducted as described (Sambrook and Russell, 2001) in Invitrogen Novex Mini Cell chambers. After separation, proteins were fixed by incubating the gel for 30 min in fixation buffer. The gel was incubated for 30 min - 1 h in Coomassie staining solution, destained in Coomassie destaining solution and dried in a gel dryer for 2 h at 80°C.

2.4.3 Western blotting

Western blotting was carried out as described previously (Sambrook and Russell, 2001) using a Biorad Mini Trans-Blot cell, Immobilon-P PVDF membrane and transfer buffer with the following modifications. Proteins transfer was conducted at 4°C for 12 h at 100 mA, the membrane was rinsed in methanol and let dry at RT. For protein detection, the membrane was activated by soaking it in methanol and then washed twice for 5 min in PBS. Blocking was carried out for 30 min in 3% BSA (98% PURE) in PBS-T. After incubation of the primary antibody in blocking buffer, overnight at 4°C, the

membrane was washed 4 times for 10 min at RT with PBS-T. Secondary antibodies conjugated to HRP (horse radish peroxidase) or IR (infrared) dyes were incubated in blocking buffer for one hour at RT. Subsequently, the membrane was washed 5 times with PBS-T. All secondary antibodies (see 2.1.3) were diluted 1:10,000 with the exception of donkey α -goat IRDye 680, which was diluted 1:15,000.

If secondary antibodies were conjugated to HRP, proteins were detected by chemoluminescence using the GE Healthcare ECL detection system according to the manufacturer's instructions. If secondary antibodies carrying IRDye 680 or IRDye 800 were used, the membrane was dried and proteins were detected by the Odyssey[®] System (Lycor, Bad Homburg).

Primary antibody dilutions

chicken α -H1	1:250
rabbit α -HMG-D	1:300
goat α -H4	1:500
rabbit α -H3	1:5000

2.4.4 Purification of endogenous histone octamers from *Drosophila* embryos

Drosophila embryos 0-12 h AEL were collected on apple-juice-agar plates by rinsing the plates under running water into a sieve. Embryos were dechorionated by adding 25% bleach diluted in EW and stirring them for 3 min on a magnetic stirrer. After putting them back into the sieve, they were washed with 1 l of EW and subsequently with running tap water for 5 min. The sieve was then placed on tissue paper to remove the water as much as possible. All the following steps were conducted at 4°C. 100 g of dechorionated embryos were used as starting material for the purification of histones. Embryos were resuspended in 150 ml glycine buffer, homogenized by passing them 6 times through a Yamato LSC Homogenizer LH-21 at 1000 rpm and filtered through two layers of Miracloth. The flow-through containing the nuclei was centrifuged (10 min, 8000 rpm, SLA-3000 rotor). The nuclei, which formed the upper phase of the biphasic pellet, were solubilized in a final volume of 50 ml sucrose buffer. Nuclei were washed once more in a volume of 50 ml sucrose buffer (10 min,

8000 rpm, SLA-1500 rotor) and dissolved in sucrose buffer to a final volume of 30 ml. In order to digest chromatin to mononucleosomes, 90 μ l 1 M CaCl_2 were added to the nuclei suspension, it was warmed-up for 10 min at 26°C, 74 U MNase were added and the mixture was incubated for another 10 min at 26°C. The reaction was stopped by adding 600 μ l 0.5 M EDTA pH 8.0. The chromatin was pelleted immediately (10 min, 9500 rpm, SS34 rotor) and resuspended in 6 ml TE pH 7.6 containing proteinase inhibitors. The tube was rotated for 45 min at 4°C and centrifuged with 11,000 rpm for 35 min in a SS34 rotor. The salt concentration of the supernatant was adjusted to 0.63 M KCl using a 2 M KCl/100 mM K- PO_4 -buffer. The solution was cleared by centrifugation (15 min, 4000 rpm, Heraeus Megafuge 2.0) and loaded onto a 30 ml hydroxyl apatite column equilibrated with 0.63 M KCl/100 mM K- PO_4 -buffer at 0.5 ml/min. The column was washed with 300 ml 0.63 M KCl/100 mM K- PO_4 -buffer (0.5 ml/min) and the core histones were eluted with 2 M KCl/100 mM K- PO_4 -buffer. 5 ml fractions were collected and samples were analysed by 18% SDS-PAGE for their protein content. Fractions containing equimolar histone amounts were pooled, concentrated in Microsep 10K Omega centrifugal devices and stored at -20°C after addition of glycerol to 50% (Simon and Felsenfeld, 1979).

2.4.5 Expression and purification of recombinant core histones in *E. coli* and reconstitution of histone octamers

Core histones H2A, H2B, H3 and H4 were expressed separately in *E. coli*. Chemically competent BL21 Codon Plus *E. coli* were transformed with 1 μ g of pET histone expression plasmid and grown overnight on Agar plates containing 100 μ g/ml ampicillin. A single colony was picked and inoculated in 400 ml LB medium for 1 h at 37°C. After adding ampicillin to 100 μ g/l and chloramphenicol to 25 μ g/l, the culture was shaken overnight at 37°C. 20 ml of this pre-culture were added to each of 20 500 ml LB (+ 100 μ l/l ampicillin, + 25 μ l/l chloramphenicol) flasks and the bacteria were grown at 37°C until an OD_{595} of 0.6. Histone expression was induced by adding IPTG to 1 mM. After 3 h at 37°C, cells were harvested by centrifugation at 4000 rpm for 20 min in a

Heraeus Cryofuge 6000i and the pellet was frozen. Overexpression of histones was controlled by 18% SDS-PAGE.

The bacterial pellet was resuspended in a volume of 33 ml washing buffer for inclusion bodies. The suspension was first homogenized by 6 runs through a French Pressure Cell Press (ThermoSpectronic) at a pressure of 1000 psi and then sonified by a Branson Digital Sonifier in 50 ml tubes (5 min, 70% amplitude, pulse 5 s on/5 s off). Bacterial extracts were centrifuged (20 min, 18,000 rpm, Sorvall SS34 rotor) and the pellet was washed twice with 40 ml washing buffer containing 1% Triton X-100. To remove traces of Triton, samples were washed twice with 40 ml washing buffer. After the last centrifugation, the pellet containing the inclusion bodies was frozen at 20°C.

1 ml of DMSO was added to the pellet, it was allowed to thaw and homogenized in 5 ml of unfolding buffer. Further unfolding buffer was added to a volume of 40 ml and the mixture was rotated at RT for 1 h to allow unfolding of inclusion bodies. The supernatant of the following centrifugation (20 min, 18,000 rpm, Sorvall SS34 rotor) was dialysed against 3 times for 1 h in 1 l Sau200.

Undissolved material was removed by centrifugation (10 min, 18,000 rpm, Sorvall SS34) and the supernatant was loaded onto a 5 ml SP-Sepharose column, washed with 25 ml Sau200 and eluted with a gradient of Sau600. Fractions containing the expressed histones were pooled and dialysed three times for 1 h in 1 l H₂O. The concentration of the histones was determined with a Nanodrop[®] (peqlab) measuring their OD at 276 nm. Histones were frozen in liquid nitrogen in 1 mg aliquots and stored at -80°C. Histones H2A and H2B were prepared for this thesis, histones H3 and H4 were kindly provided by Dr. Catherine Regnard and Dr. Violette Morales.

8 mg of each histone were lyophilized overnight and dissolved to a concentration of 2 mg/ml in refolding buffer. After incubation for 2.5 h on a rotating wheel, the concentration of each histone was determined with a Nanodrop[®] (peqlab). Each histone concentration was calculated (concentration [mol/l] = OD_{276}/ϵ_{276}) using the coefficient of extinction (ϵ_{276}) given for each histone.

Because it is easier to separate histone octamers from H2A/H2B dimers than from H3/H4 tetramers, H3 and H4 were mixed in an equimolar ratio, whereas H2A and H2B were added with a 20% excess. The protein concentration was adjusted to 2 mg/ml by adding refolding buffer and the solution was dialysed twice against 3 l of refolding

buffer. The solution was cleared by centrifugation (5 min, 4000 rpm, Heraeus Megafuge 2.0) and concentrated to 2 ml using Microsep 30K Omega centrifugal devices.

Histone octamers were loaded onto and eluted from a Hiload[®] 16/60 Superdex[®]200 size exclusion column in refolding buffer at a flow-rate of 1 ml/min. 1 ml fractions were collected and 1 μ l of each fraction was analysed by 18% SDS-PAGE. Fractions containing equimolar amounts of histone octamers were pooled and frozen in 50% glycerol at -20°C (Morales et al., 2004).

	MW [kD]	ϵ_{276} [l/mol]
H2A	11.960	4050
H2B	13.774	6070
H3	15.273	4040
H4	11.236	5400

2.4.6 Purification of linker histone H1 from *Drosophila* embryos

A fraction that contains large amounts of *Drosophila* linker histone H1 is obtained as a byproduct of *Drosophila* transcription extract production (Heberlein and Tjian, 1988). During this procedure, nuclei are isolated from embryos, lysed, and the lysate is fractionated by (NH₄)₂SO₄-precipitation. Proteins required for *in vitro* transcription are pelleted with 35% (NH₄)₂SO₄, whereas H1 remains in the supernatant. The supernatant from a transcription extract preparation from embryos 0 – 12 h AEL was the starting material for further H1 purification; it was kindly provided by Dr. Andreas Hochheimer.

40 ml supernatant containing 2.7 mg/ml protein was cleared by centrifugation for 20 min at 18,000 rpm in a Sorvall SS-34 rotor and by filtration (pore size 0.45 μ m). It was then loaded onto a 20 ml phenylsepharose (XK16) hydrophobic interaction chromatography column equilibrated with HEMG/2.1M NH₄SO₄. The column was washed with 100 ml HEMG/2.1 M NH₄SO₄. A gradient was run from HEMG/2.1 M NH₄SO₄ (buffer A) to HEMG/0.1 M NH₄SO₄ (buffer B). Since H1 was expected to be among the first proteins to elute, the gradient was divided into two steps, the first one from 0-35% buffer B within 60 ml, the second one from 35-100% buffer B within 80 ml. 5 ml fractions were collected. 5 μ l of each fraction were applied on a 12% SDS

polyacrylamide gel to determine the presence of H1. H1-containing fractions were pooled and dialysed twice for 1 h and once overnight against 2 l HEG100. After dialysis, the solution was centrifuged for 30 min at 10,000 rpm in a Sorvall SS-34 rotor. The supernatant was loaded with 0.5 ml/min onto a fast protein liquid chromatography Mono STM 5/50 GL column equilibrated with HEG100. After washing the column with 10 ml HEG100, a 20 ml gradient from HEG100 to HEG1000 was applied, 330 μ l fractions were collected and 1 μ l of each fraction was analysed by 12% SDS-PAGE. The fractions containing H1 were pooled, shock-frozen in liquid nitrogen and stored at -80°C . Alternatively, glycerol was added to 50% v/v and the mixture was stored at -20°C (Croston et al., 1991).

H1 is easily retained on pipet tips and reaction tubes. To minimize loss of the protein, when handling H1-containing samples, siliconized reaction tubes were used and a 20 mg/ml BSA (98% pure) solution was pipetted up and down five times in each tip before use.

2.4.7 Purification of HMG-D from *Drosophila* embryos

Drosophila embryos 0-90 min AEL were collected on applejuice-agar plates, rinsed with water into sieves and allowed to settle into EW on ice to arrest further development. The harvest of four successive collections was pooled. After the embryos had settled, cold EW was replaced by RT EW and the volume was adjusted to 200 ml. After addition of 60 ml of 13% hypochlorite, the embryos were stirred on a magnetic stirrer for 3 min, poured into a collection sieve and rinsed with running tap water for 5 min. To remove the chorion, 200 ml wash buffer was added, embryos were allowed to settle and the supernatant was removed by vacuum aspiration. The volume of the embryos was estimated after two more washes: the first in cold 0.7% w/v NaCl and the second in extract buffer on ice for 15 min in a 60-ml glass homogenizer. The supernatant was removed, and the embryos were homogenized by one stroke at 3000 rpm and ten strokes at 1500 rpm with a pestle connected to a Schütt Homgen drill press. The MgCl_2 -concentration was adjusted to 5 mM and the nuclei were pelleted by centrifugation for 10 min at 10000 rpm in a Sorvall SS34 rotor. The supernatant was centrifuged for 2 h at

45,000 rpm (190,000 x g) in a Beckman SW 56 rotor. The supernatant of this centrifugation, that we refer to as *Drosophila* embryonic extract (DREX) was collected with a syringe, avoiding the floating layer of lipids and the pellet. The extract was frozen in liquid nitrogen (Becker et al., 1994).

20 ml of DREX were incubated for 10 min at 75°C. Precipitated proteins were removed by centrifugation and the supernatant was fractionated by selective $(\text{NH}_4)_2\text{SO}_4$ precipitation. 40% w/v (without considering the increase in volume due to salt addition) $(\text{NH}_4)_2\text{SO}_4$ was added to the mixture, it was stirred for 15 min followed by centrifugation (15 min, 15,000 rpm, Sorvall SS34). The supernatant was precipitated once more by adding $(\text{NH}_4)_2\text{SO}_4$ to 65% w/v, the resulting pellet was resuspended in 2 ml of 50 mM Hepes-KOH pH 7.6/50 mM KCl containing proteinase inhibitors and dialysed 3 times against 1 l of this buffer. Subsequently, it was loaded onto a 1 ml fast protein liquid chromatography Mono STM 5/50 GL column (0.5 ml/min). The column was washed with 10 ml of 50 mM Hepes-KOH pH 7.6/50 mM KCl and proteins were eluted with a 20 ml gradient of Hepes-KOH pH 7.6/1 M NaCl (+ proteinase inhibitors) at a flow-rate of 1 ml/min. 1 ml fractions were collected. HMG-D elutes at 0.3-0.35 M NaCl. 5 μl of each fraction were analysed by 18% SDS-PAGE, HMG-D-containing fractions were pooled, concentrated in Microsep 10K Omega centrifugal devices, frozen in liquid nitrogen and stored at -80°C (Ner et al., 2001).

2.4.8 Expression and purification of recombinant HMG-D in *E. coli*

pET24 HMG-D plasmid was transformed into chemically competent BL21 Codon Plus *E. coli* and the cells were plated on agar plates containing 30 $\mu\text{g}/\mu\text{l}$ kanamycin and 25 $\mu\text{g}/\mu\text{l}$ chloramphenicol. A single colony was picked and inoculated overnight at 37°C in 200 ml LB (+ 30 $\mu\text{g}/\mu\text{l}$ kanamycin, + 25 $\mu\text{g}/\mu\text{l}$ chloramphenicol). 20 ml of this preculture were added to each 500 ml LB (+ 30 $\mu\text{g}/\mu\text{l}$ kanamycin, + 25 $\mu\text{g}/\mu\text{l}$ chloramphenicol). A total of 5 l culture were used and bacteria grown at 37°C until they reached an OD_{600} of 0.8. Expression of HMG-D was induced for 4 h at 37°C by adding IPTG to 250 $\mu\text{g}/\text{ml}$. After 4 hours, cells were pelleted (20 min, 4000 rpm, Heraeus Cryofuge 6000i) and frozen at -20°C. Bacteria were resuspended in 60 ml HE500 and

split into two 30 ml aliquots. Each aliquot was sonified with a Branson Digital Sonifier (2.5 min, 50% amplitude, pulse 10 s on/20 s off), frozen in liquid nitrogen, sonified once more and centrifuged (15 min, 18,000 rpm, Sorall SS34). The supernatant was dialyzed 3 times against 1 l of HE50 and proteins were precipitated by adding $(\text{NH}_4)_2\text{SO}_4$ as in the purification of endogenous HMG-D (see 2.4.7). The 40-65% $(\text{NH}_4)_2\text{SO}_4$ cut was resuspended in HE50, dialysed 3 times against 1 l of HE50 and loaded onto a 65 ml DEAE Sepharose column with 1 ml/min. Due to the capacity of the column, only half of the solution was loaded per run. The column was washed with 200 ml HE50 and the proteins were eluted by applying a 100 ml gradient to HE1000. 5 ml fractions were collected and 5 μl of each fraction were applied on a 18% polyacrylamide gel. Fractions containing HMG-D were pooled and dialysed 3 times against 1 l of HE50. Aliquots were frozen in liquid nitrogen and stored at -80°C (Jones et al., 1994).

2.4.9 Expression and purification of ACF, ISWI, CHD1 and BRG1 in Sf9 cells

1.2×10^7 Sf9 cells per 15 cm round petri dish, covered by 5 ml of Sf-900II medium (Gibco) complemented with 9% foetal bovine serum (Sigma) were infected with baculovirus. For this purpose, the virus was added, the dishes were rocked gently at RT for 1 h followed by addition of 20 ml fresh medium. Cells were infected with viruses carrying constructs of flag-ISWI, flag-CHD1, flag-BRG1 or coinfecting with ACF1-flag and untagged ISWI to produce ACF. Amounts of virus had to be titrated for optimal yield and the necessary 1:1 stoichiometry of ACF1 and ISWI to obtain functional ACF complexes. Protein expression was allowed for 48 h at 27°C . To purify the recombinant protein, cells were washed once by removing the medium and replacing it with 5 ml of cold PBS. Cells were harvested using a cell scratcher. From now on, all steps were performed on ice or at 4°C in the presence of proteinase inhibitors. Cells were pelleted (10 min, 900 rpm in a Heraeus Megafuge 2.0) and resuspended in 800 μl HEMG500 per plate. Cells were frozen in liquid nitrogen, thawed, sonicated immediately (10 s, 50% amplitude, Branson Digital Sonifier) and centrifuged (30 min, 13,000 rpm, tabletop centrifuge) to clear the whole cell extract from cell debris. The supernatant was transferred into a fresh siliconized tube and α -flag M2 agarose beads (equilibrated 5

times in 1.5 ml HEMG500) were added to the supernatant. The amount of beads added to the whole cell extracts corresponded to 10 μ l per plate. Binding of the tagged proteins to α -flag beads was allowed for 3 h on a rotating wheel. After this incubation, the tubes were centrifuged in a table-top centrifuge (2 min, 13,000 rpm), the supernatant was removed and the beads were washed 5 times with 1.5 ml HEMG500 and twice with HEMG200 for 5 min on a rotating wheel. Proteins were eluted for 2 h in an appropriate volume (ca. 25 μ l/plate) of HEMG200 containing 0.5 mg/ml flag-peptide and frozen in liquid nitrogen (modified after Eberharter et al., 2004b).

2.4.10 Sources of other proteins/extracts

H5 was kindly provided by the lab of Daniela Rhodes, Cambridge, UK. It had been purified as described (Huynh et al., 2005). A part of the recombinant histone octamers used in this study was prepared by Dr. Catherine Regnard. Whole *Drosophila* larval extract (gift of Dr. Mariacristina Chioda) was prepared from 5 female third instar larvae. Whole larvae were frozen in liquid nitrogen and grained while still frozen. The samples were immediately dissolved in 100 μ l 2x Laemmli buffer (preheated at 95°C) and denatured for 10 min at 95°C.

2.4.11 Small scale preparation of nuclei from *Drosophila* embryos

To isolate nuclei from fly embryos, all solutions were prechilled at 4°C and procedures were carried out on ice. 1.5 ml reaction tubes were prepared as follows: The inner part of the lid of the tube was cut out and 400 μ l of NB/1.7 M sucrose were added and overlaid by 400 μ l of NB/0.8 M sucrose. A small piece of Miracloth was pinned in between the tube and the lid to cover the opening.

3-10 days old flies hatched from 6-8 bottles (10 cm height, 9 cm diameter) were transferred into cylindrical collecting chambers (10 cm height, 9 cm diameter) covered by a metal mesh that had a mesh size small enough to keep the flies in. Fly embryos were collected on 9 cm agar plates placed on these chambers. The embryos were rinsed into a small sieve with PBS and washed twice with 3 ml NB/0.3 M sucrose. The volume

of the settled embryos was estimated and 3 times this volume of NB/0.3 M sucrose was added. The embryos were homogenized without prior dechoriation in a 1.5 ml reaction tube with a pestle fitting these tubes (micro pistil, Kontes, New Jersey). 100 μ l of the homogenate were loaded onto the Miracloth mesh clipped by the lid of the 1.5 ml reaction tubes. By spinning these tubes for 5 s, the extract was filtered through the mesh. Up to 400 μ l of homogenate were loaded onto each tube. After centrifugation for 10 min, 13,000 rpm in a table-top centrifuge, lipids, cell debris, and cytosol were retained at different solution interfaces while the nuclei formed a white pellet. Nuclei were taken out of the tube with a pipet tip penetrating the sucrose layers, the pipet tip was wiped with a tissue and the nuclei were pooled in a fresh tube containing 500 μ l NB/0.3 M sucrose. Nuclei were pelleted once more by centrifugation at 5000 rpm for 5 min. The supernatant was removed except for about 20 μ l. One volume of 1x Laemmli buffer was added, nuclei were solubilized and samples were denatured at 95°C for 5 min. Protein samples were cleared from debris by a 10 min at 13,000 rpm centrifugation in a table-top centrifuge (Quivy and Becker, 1997).

2.5 Methods for the reconstitution and analysis of nucleosomal arrays

2.5.1 Chromatin salt assembly

Nucleosome and chromatosome arrays were reconstituted by salt dialysis. Dialysis chambers were prepared by cutting a circular hole in the lid of siliconized 1.5 ml tubes. The bottom of these tubes was removed and used upside down as a lid of such micro dialysis chambers. A SpectraPor dialysis membrane with a molecular weight cut-off of 6-8 kD was pinned between the lid and the tube. The tubes were placed upside down on a floating rack. To prevent unspecific protein binding and therefore loss of material, dialysis tubes were filled with 0.5 ml 2mg/ml BSA (98% pure) in DB500 and incubated for two hours. Before use they were rinsed with DB500.

Core histones, 2.5 μ g 601 repeat DNA and competitor DNA were mixed with or without linker histones or HMG-D in a final volume of 50 μ l in high salt buffer (2 M

NaCl, 10 mM Tris pH 7.6 and 0.12 $\mu\text{g}/\mu\text{l}$ BSA final concentrations). 12mer arrays were assembled on 12x601 DNA fragments derived from pUC18 12x601 plasmid. For this purpose, the plasmid was digested with EcoRI, HindIII and DraI (see 2.3.3.1); the fragmented pUC18 vector served as competitor DNA. When preparing radioactive arrays, 20% of 12x601 arrays were purified from the competitor DNA by phenol extraction and labelled by Klenow exo^- -polymerase (see 2.3.4). For the assembly of palindromic 8x601 arrays, 2.5 μg 8x601 fragments (see 2.3.3.2) and 2.5 μg competitor DNA were mixed. 20% of 8x601 fragments were labelled by Klenow exo^- -polymerase. The mixture was carefully pipetted onto the membrane of a dialysis chamber in a floating rack. The rack was then placed into 200 ml DB2000 with the dialysis membrane in contact with the buffer. DB2000 was diluted 1:10 by continuous addition of DB0 over a 13 h period at 4°C. The floating rack was then placed in DB50 for 1 h allowing samples to equilibrate at a final salt concentration of 50 mM NaCl.

Assembled nucleosomal arrays were stored at 4°C in siliconized 1.5 ml tubes. All further handling of chromatin was done in siliconized tubes using tips preblocked with 20 mg/ml BSA (98% PURE) (modified after Huynh et al., 2005).

2.5.2 Electrophoretic mobility shift assays (EMSA)

For native agarose gels Biozym LE *GP* agarose was dissolved in 0.2xTB. H1- and HMG-D-containing chromatin arrays were analysed on 0.7% agarose gel, H5-containing arrays on 1.4% agarose gel. Linker histone-containing arrays were run on 6 cm gels, HMG-D-containing arrays on 20 cm gels. Arrays were visualized by staining the gel after electrophoresis in a solution of 0.2xTB and 0.5 $\mu\text{g}/\text{ml}$ EtBr for 1 h. To monitor which fraction of positioning sequences was bound by histone octamers and H1, 6 pmol arrays were digested by 15 U AvaI in RB50 for 1 h at 26°C, run on 1.1% agarose gels and stained by SYBR[®] gold (Invitrogen, 1:10,000) or 5 $\mu\text{g}/\text{ml}$ EtBr in 0.2xTB for 1 h (modified after Huynh et al., 2005). After staining, gels were destained in 0.2xTB for 30 min.

2.5.3 MgCl₂-precipitation of nucleosomal arrays

Properly folded nucleosomal arrays were purified by precipitation with 5 mM MgCl₂ unless indicated otherwise. After addition of MgCl₂, samples were incubated on ice for 15 min and then centrifuged in a table centrifuge (15 min, 4°C, 13,000 rpm). The chromatin pellet was dissolved in TE pH 7.6 to a DNA concentration of 50 ng/μl. (Schwarz et al., 1996).

2.5.4 Determination of histone stoichiometry

60 pmol arrays were analysed on 15% polyacrylamide gels. Proteins were stained with Coomassie. Intensities of H1, core histone and HMG-D bands were measured using the Odyssey[®] Infra Red Imaging System (LI-COR).

2.5.5 ATPase assays

Approximately 10 pmol of remodelling enzyme were mixed with 200 ng DNA (free or chromatinized) in a final volume of 14 μl EX40. Reactions were started by adding 1 μl of 0.3 μM unlabelled ATP spiked 1:200 with γ-³²P-ATP (5.55 GBq/ml, 150 mCi/mol) in EX40 and incubated at 26°C. Different time points were taken by spotting 1 μl of the reaction onto the longer edge of 10 cm x 20 cm TLC plates. The plate was dried for 5 min and the edge near the samples was placed about 1 cm into a solution of 0.5 M LiCl, 1 M formic acid avoiding that the liquid would touch directly the sample-spots. The buffer was allowed to migrate upwards and until it almost reached the top of the plate. Plates were dried for 5 min at 68°C and exposed to a phosphoimager screen for 10 min. The radioactive signals corresponding to hydrolysed phosphate and to not hydrolysed ATP were quantified with a Phosphoimager using AIDA Image Analyzer software. The two species could be distinguished by their different mobility, which is higher for the phosphate. The percentage of hydrolysed ATP was calculated (Eberharter et al., 2004a).

2.5.6 Chromatin remodelling reactions

All remodelling reactions were carried out for 1 h at 26°C unless indicated otherwise. For monitoring nucleosomal DNA accessibility, 0.6 pmol 12mer nucleosome or chromatosome arrays were incubated in 10 µl RB50 with or without 20 µM ATP. Reactions were started by adding 5 U AluI along with 2.4 pmol ACF (0.3 ACF molecules per nucleosome/chromatosome) or corresponding amounts of CHD1, ISWI or BRG1. Enzyme amounts were normalized on their nucleosome-stimulated ATPase or remodelling activity as indicated). Reactions were stopped by adding 200 ng free DNA. Proteins were removed by Proteinase K (1 h, 37°C), the DNA was precipitated with ethanol and analysed on 1.3% agarose gel in Tris-glycine buffer. After electrophoresis gels were dried and exposed to phosphoimager screens. The percentage of uncut DNA was determined with AIDA Image Analyzer software.

If remodelling reactions were followed by MNase digestion, 1.8 pmol arrays were incubated in 30 µl RB50, 20 µM ATP. Reactions were started by the addition of 7.2 pmol ACF or CHD1, ISWI or BRG1 with equivalent activity (see above). Reactions were stopped by adding 600 ng free DNA. Subsequently samples were incubated with 4×10^{-3} U of MNase (Sigma) for 1, 3, 5, min if reactions contained ACF or ISWI. Different incubation times points (0.5, 1 and 3 min) were required when reactions contained CHD1, BRG1 or no remodeler. As a molecular weight marker, 0.6 pmol nucleosome arrays were digested for 1 h at 26°C with 5 U AluI. Free 12mer 601 repeats (0.6 pmol labelled repeats + 200 ng unlabelled DNA) were digested for 1 min at 26°C with 10^{-4} U of MNase. DNA was processed and visualized as above. 1D-evaluation of selected lanes was performed using AIDA Image Analyzer software.

If primer extension was performed after the remodelling reactions, remodelling was carried out using 3 pmol arrays in 15 µl RB50, 20 µM ATP and 12 pmol ACF. After 1 h, arrays were treated with 10^{-3} U MNase, 1 mM CaCl₂ for 20 min at 26°C. Nucleosomes and chromatosomes were separated on 1.1% native agarose gels and visualized by staining with SYBR[®] gold. Gel slices containing the specific particles were excised. The corresponding DNA was purified using the Qiagen Gel Extraction Kit. 10% of the recovered DNA served as template for primer extension reactions in the presence of 5 µM primers, 0.2 mM dNTPs and 3 U Taq polymerase. Each primer (13fw, 13rv, 76fw or

76rv) was labelled using [γ - 32 P]-ATP and polynucleotide kinase according to the manufacturer's instructions. 12 cycles of amplification were performed: 30 s at 94°C, 30 s at 60°C and 60 s at 68°C. The products of the primer extension reactions were analysed on 7% polyacrylamide gels containing 20% urea in TBE using a Bio-Rad Sequi-Gen[®] sequencing cell.

2.6 Maintenance and analysis of *Drosophila* stocks

2.6.1 Fly strains

Acf1[2]/acf1[2] flies were provided by D. Fyodorov and J.T. Kadonaga. To avoid analysing a population of ACF1-depleted flies accumulating secondary effects due to ACF1 depletion, *acf1[2]* alleles were kept balanced and immunostaining and nuclei purification was performed with homozygote *acf1[2]/acf1[2]* flies between generations III-VI.

2.6.2 Embryo collection and staining

Embryos 0-3 h AEL were collected on 9 cm agar plates from cages containing 3-10 days old adult flies. Embryos were collected in small sieves, rinsed twice with PBS-T and once with milli-Q water and dechorionated by immersion in 25% bleach for 3 min. After washing them intensively with PBS-T and milli-Q water, embryos were transferred into glass jars containing 1.5 ml each of heptane and freshly thawed 3.7% para-formaldehyde (PAF). The two solutions were vigorously shaken for 30 s. The embryos were fixed at the interphase between heptane and PAF for 20 min at RT. Following fixation, PAF (lower phase) was carefully removed and replaced by 3 ml of methanol. Embryos were vortexed for 15 s. Once settled on the bottom of the jar, the embryos were transferred to fresh 1.5 ml tubes and rinsed twice in methanol 100%. Embryos were stored in methanol 100% for a minimum of overnight to a maximum of 7

days at 4°C. Before use, they were re-hydrated by successive 5 min incubations in 80%, 50% and 20% methanol diluted with PBS-T (gently rocking), and lastly by two 5 min PBS-T washes. Primary antibodies (chicken- α -H1 and rabbit α -HMG-D diluted 1:30 each in PBS-T) were incubated for 72 h at 4°C. Samples were washed 3 times, 10 min with PBS-T. Secondary antibodies diluted 1:250 in PBS-T were incubated 3 h at RT. A-chicken antibodies conjugated with Alexa 488 were used for detection of the α -H1, Rhodamine Red X-conjugated α -rabbit antibodies were used for detection of HMG-D. Samples were washed 10 min in PBS-T 0.3% Triton and 2 x 10 min in PBS-T and DNA stained with 1 μ M TO-PRO3 in PBS for 10 min at RT. After two washes with PBS-T, samples were mounted on slides with Vectashield mounting medium. Images were acquired with a Zeiss LSM 510 META confocal microscope equipped with one Argon- and two Helium-ion lasers and processed with Zeiss LSM 510 META Software.

3. Results

3.1 Reconstitution of chromatin with stoichiometric amounts of linker histones

3.1.1 Reconstitution and purification of 12mer nucleosome arrays and chromosome arrays containing H1 or H5

To investigate the effect of linker histones on chromatin remodelling, it was crucial to work with nucleosomal arrays containing one linker histone per histone octamer. Only then we could be certain that any remodelling on these arrays occurred on chromosomes (nucleosomes + linker histone) and not on a fraction of nucleosomes devoid of linker histones. Following a protocol for the reconstitution of homogeneous, uninterrupted, linker histone-containing nucleosomal arrays (Huynh et al., 2005) we assembled 12mer nucleosome and chromosome arrays on 12x200 bp repeats of the 601 nucleosome positioning sequence (Lowary and Widom, 1998). This sequence was selected from competition experiments screening random DNA sequences for their affinity to histone octamers (Lowary and Widom, 1998; Thastrom et al., 1999). The histone octamer binds 150 times stronger to the 601 sequence than to the 5S rDNA sequence, which has also frequently been used to assemble positioned nucleosomes although this sequence allows multiple nucleosome positions (Dong et al., 1990). To assure full occupancy of all 601 sequences, core and linker histones had to be added in slight excess during the reconstitution. To prevent binding of excess histones to positions other than those dictated by the 601 sequence, competitor DNA (crDNA) was included in the assemblies. This allowed controlling the loading of both core and linker histones onto the 601 repeats since excess histones bound to the competitor DNA instead of resulting in oversaturated arrays. Competitor DNA consists of small DNA fragments with an average affinity to histone octamers. In the published protocol, 147 bp fragments derived from the pUC18 vector were used as crDNA (Huynh et al., 2005). We slightly modified this procedure by digesting the pUC18 vector with *Dra*I and using the resulting

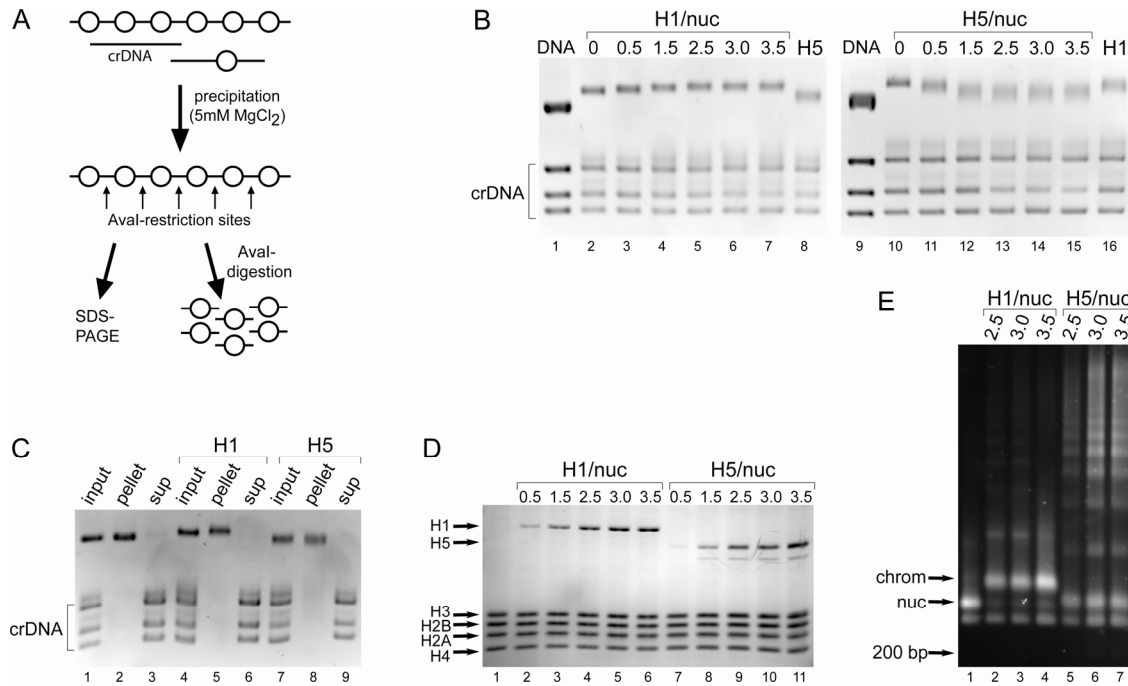


Figure 3.1: Reconstitution of chromatin arrays with stoichiometric amounts of linker histone H1 or H5.

(A) Overview of chromatin reconstitution and quality controls. 12mer nucleosome arrays and chromosome arrays containing linker histone H1 or H5 were assembled on tandem repeats of the 601 nucleosome positioning sequence. To bind excess histones, competitor DNA (crDNA) with lower affinity for histones was added to the assembly. (B) 6 pmol arrays assembled with increasing molar ratios of H1 or H5 (H1/nuc or H5/nuc) were applied on 0.7% or 1.4% native agarose gels, respectively, and stained with EtBr. (C) Arrays were purified from unbound histones and competitor DNA by MgCl₂-precipitation. Corresponding amounts of input, pellet and supernatant (sup) were analysed on 1.4% native agarose gel stained with EtBr. (D) The protein content of 60 pmol nucleosomal arrays after MgCl₂-precipitation was separated on 15% polyacrylamide gel and visualized by Coomassie blue staining to control the relative amounts of core and linker histones. (E) 6 pmol arrays were digested with Aval at 26°C for 1 h, resulting fragments were resolved on 1.1% native agarose gel and stained by SYBRgold[®] to observe positioning sequences unbound by histone octamers (200 bp), nucleosomes (nuc) and chromosomes (chrom).

DNA fragments (between 692 and 1113 bp) as competitor DNA. Since also the 12mer 601 was subcloned into the pUC18 vector, purification of 601 repeats and the production of crDNA could be easily done in one step of enzymatic digestion. Only a fraction of 601 repeats had to be purified to allow specific radioactive labelling.

12mer arrays were assembled using histone octamers and histone H1 purified from *Drosophila* embryos or histone H5 from chicken erythrocytes. H5 binds to nucleosomes with a higher affinity than H1 and leads to a more compact chromatin structure (Thomas and Rees, 1983). It has therefore emerged as the preferred linker histone for structural studies (Fan and Roberts, 2006).

Core histones were added in amounts that resulted in the assembly of uninterrupted 12mer nucleosome arrays. The appropriate amount was determined in pilot experiments where the relative amount of core histones was titrated to obtain uninterrupted nucleosome arrays (not shown). Titrations of linker histones are presented in Figure 1B. Addition of increasing amounts of H1 resulted in a slower migration of the arrays on native agarose gel (best resolved on 0.7% agarose), whereas incorporation of H5 led to faster migrating arrays (best resolved on 1.4% agarose), in agreement with earlier studies (Huynh et al., 2005). The different migration behaviour of H5- versus H1-containing chromosome arrays may reflect an increased compaction of the arrays induced by H5. Addition of more linker histones did not lead to a further change in mobility of the reconstituted chromatin. Instead, excess linker histones bound to the crDNA, as seen in mobility shifts (Figure 3.1B, lanes 6, 7, 14, 15). For further analysis, all arrays were purified by MgCl₂-precipitation to remove excess proteins and free or nucleosomal crDNA (Figure 3.1C). In the presence of 5 mM MgCl₂, nucleosomal arrays self-associate and precipitate, whereas unbound proteins, free DNA and DNA with few bound histone octamers remain soluble (Schwarz et al., 1996).

3.1.2 Quality controls of reconstituted chromatin

The stoichiometric incorporation of linker histones was monitored by controlling the relative amounts of core and linker histones. For this purpose, samples of purified reconstituted chromatin were loaded on a 15% polyacrylamide gel and proteins were stained with Coomassie (Figure 3.1D). The amount of each histone was determined by densitometry on a LI-COR Odyssey machine. Stoichiometric, saturating levels of linker histones were reached at a molar ratio of 2.5 molecules of linker histones per 601

sequence. Excess histones bound to the crDNA and were removed during the purification step.

To further control the complete occupancy of 601 sequences by histone octamers, arrays were digested by *Ava*I, which cuts between those sequences (Figure 3.1A). Digestion of the nucleosome arrays yielded mononucleosomes, but no free 200 bp DNA fragments, which can be distinguished by native agarose gel electrophoresis (Figure 3.1E, lane 1). Evidently, the vast majority of 601 sequences was bound by a histone octamer. A small fraction of subnucleosomal particles was visible as a band migrating slightly faster than mononucleosomes. This assay showed furthermore that nucleosomes did not occupy alternative positions to the ones dictated by the 601 sequence, since they did not occlude the *Ava*I site.

*Ava*I-digestion of H1-containing chromatin yielded mostly chromatosomes and only a minor fraction of nucleosomes (Figure 3.1E, lanes 2-4). The nucleosomal fraction did not decrease upon increase of H1, showing that saturation was already reached. H5-containing arrays were more resistant to digestion by *Ava*I, again hinting that H5 and H1 bind to and compact chromatin in a different manner.

We conclude that the reconstituted chromatin consists of regular nucleosomal arrays with stoichiometric levels of linker histones. All arrays used for remodelling reactions were quality-controlled by the methods described.

3.2 Linker histone-containing chromatin can be rendered accessible by ACF

3.2.1 ACF-mediated chromatin remodelling of nucleosome and chromatosome arrays

As a quantitative measure for chromatin remodelling, we monitored changes in the accessibility of nucleosomal DNA. For this purpose, we reconstituted nucleosome or chromatosome arrays on DNA labelled radioactively on one end and incubated them with an excess of the restriction endonuclease *Alu*I, whose recognition site is located

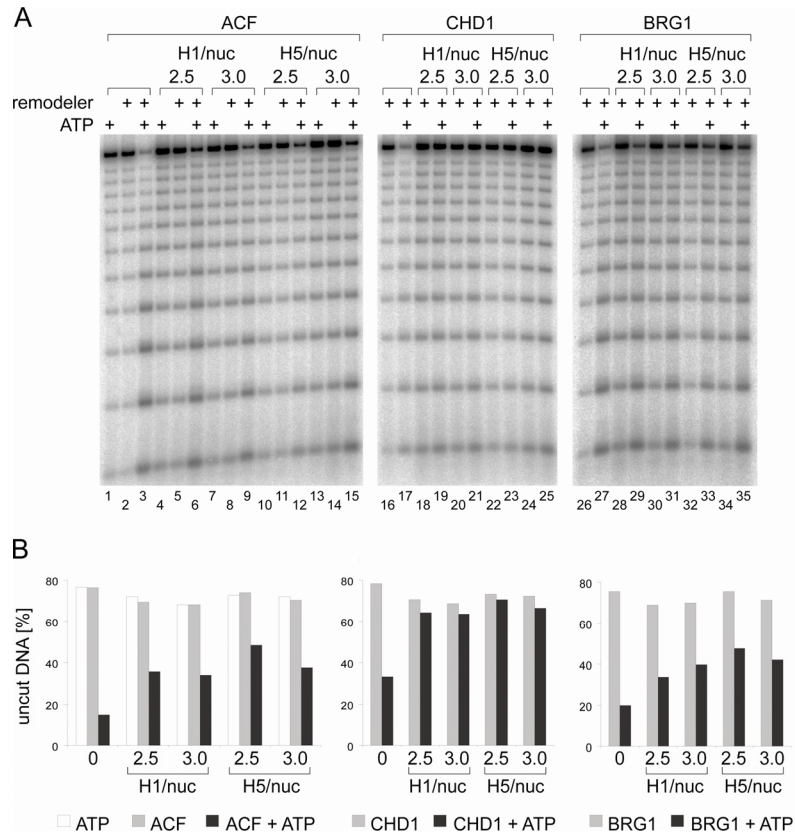


Figure 3.2: Remodelling by ACF or BRG1 increases the accessibility of nucleosomal DNA within linker histone-containing chromatin

(A) Nucleosome and chromosome arrays were assembled on end-labelled DNA using different molar ratios of linker histone H1 or H5 per positioning sequence (H1/nuc or H5/nuc). 0.6 pmol arrays were used as substrate in remodelling assays for ACF, CHD1 or BRG1. To monitor the accessibility of nucleosomal DNA, the enzyme AluI was added together with 2.4 pmol ACF or an amount of CHD1 or BRG1 with equal ATPase activity. After 1 h proteins were removed by Proteinase K and the DNA was analysed on 1.3% agarose gel. (B) Quantification of relative amounts of uncut DNA in (A).

within the nucleosome positioning sequence, 45 bp into the nucleosome. Without remodelling activity, about 70% of arrays were resistant to cleavage (Figure 3.2B), demonstrating that seven out of 10 arrays did not contain a single accessible positioning sequence. On these uninterrupted arrays the development of restriction site accessibility was now monitored in the presence of ATP and *Drosophila* ACF expressed from baculovirus vectors in insect cells. Arrays were incubated with AluI and with or without ACF and ATP at 26°C. After 1 h, the reactions were quenched by adding an excess of

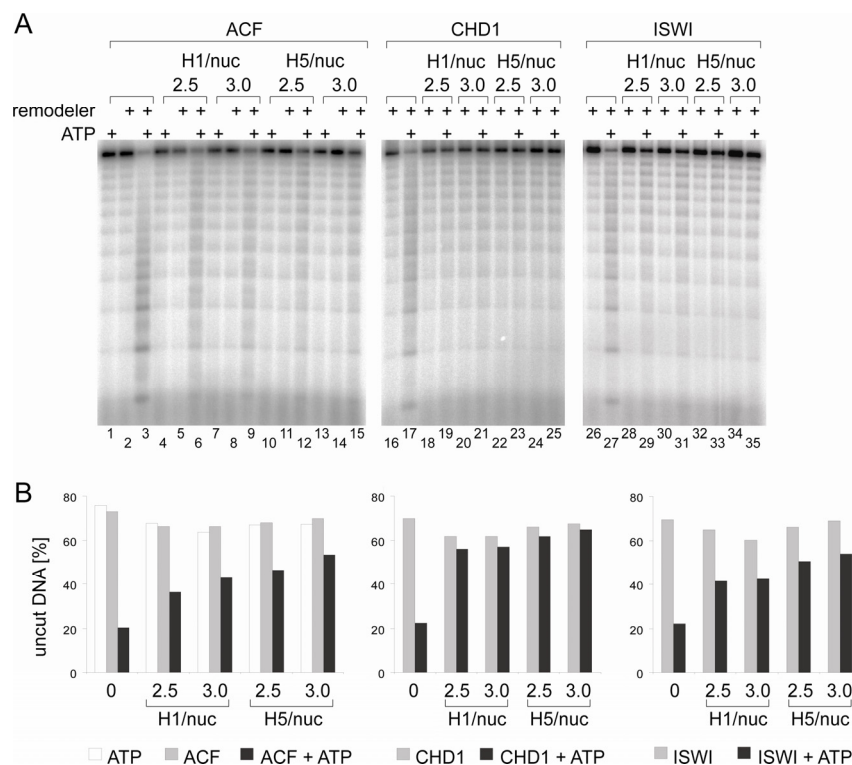


Figure 3.3: Comparison of the effect of linker histones on the remodelling activities of ACF, CHD1 and ISWI

(A) Nucleosome arrays and H1- or H5-containing chromatosome arrays were remodelled by ACF, CHD1 or ISWI and analysed as described in figure 3.3. Amounts of remodellers were standardized on their remodelling activities in the absence of linker histones. (B) Quantification of relative amounts of uncut DNA in (A).

unlabelled DNA, the total DNA was purified and analysed on agarose gel. Comparing the percentages of uncut DNA after remodelling confirmed that ACF increased the accessibility of nucleosomal DNA in an ATP-dependent manner. Upon addition of both ACF and ATP, 80% of otherwise resistant arrays were cleaved (Figure 3.2A, lane 3). Strikingly, also in the presence of H1, 48% of otherwise resistant arrays were cleaved if ACF and ATP were added (Figure 3.2A, lanes 6 and 9). This shows that a significant gain of ATP-dependent accessibility could be generated even in the presence of H1, although the extent of chromatin opening was reduced. When probing arrays assembled with a higher molar ratio of H1 per 601 sequence, the degree of inhibition remained the same, showing that the ability of ACF to remodel was not due to sub-saturating H1

levels. Remarkably, ACF was able to promote access of the endonuclease even to the highly compacted H5-containing chromatin. 35-45% of resistant H5 chromatosome arrays were cleaved in the presence of both ACF and ATP (Figure 3.2A, lanes 12 and 15). These observations are in line with an earlier study from the Peterson lab (Horn et al., 2002) who concluded that in the presence of H5, *Xenopus* ACF was able to decrease the fraction of nuclease resistant arrays from 85% to 60% in an ATP-dependent manner.

In order to find out whether the ability of ACF to remodel chromatosomes resides in its ATPase ISWI or requires its associated subunit ACF1, we repeated the assay with ISWI alone. The remodelling activity of ISWI in the presence of linker histones H1 or H5 was similar to that of ACF (Figure 3.3A, lanes 26-35). Consequently, it is possible that all ISWI-containing complexes are capable of remodelling linker histone-containing chromatin. Along this line, Tamkun and colleagues suggest that ISWI, possibly in the context of the NURF complex, may affect H1 association with chromosomes *in vivo* (Corona et al., 2007), although to date, no direct biochemical evidence has been provided.

3.2.2 Comparison with the related chromatin remodelling ATPases CHD1 and BRG1

We wondered whether the ability to remodel chromatosomes is a characteristic of all chromatin remodelling factors or whether ACF is an exception in this respect. ACF is able to assist in the formation of H1-containing chromatin, whereas the nucleosome remodelling ATPase CHD1 can only promote nucleosome assembly, but is unable to incorporate also the linker histone (Lusser et al., 2005). To test whether these differences in chromatin assembly were reflected in remodelling, we compared CHD1 to ACF in our assay. To assure that the parallel reactions contained equivalent nucleosome remodelling activity we first standardized the enzyme inputs according to their nucleosome-stimulated ATPase activity. Similar to ACF, CHD1 enhanced the accessibility towards AluI in an ATP-dependent manner (Figure 3.2A lanes 16 and 17).

However, in the presence of linker histones H1 or H5, no remodelling activity could be observed (Figure 3.2A, lanes 18-25). We also compared enzyme amounts that were

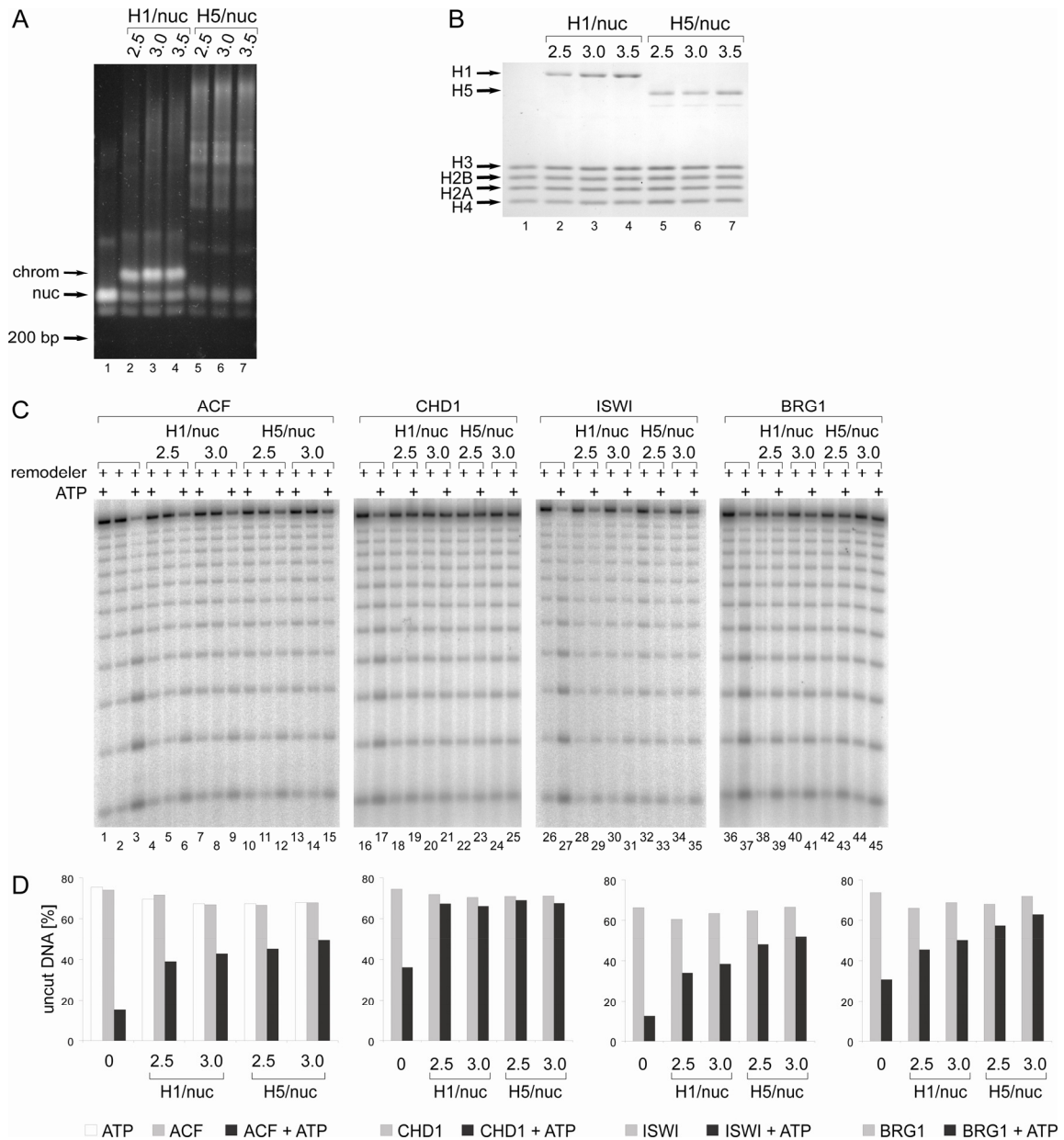


Figure 3.4: The absence of histone modifications does not significantly affect the remodelling activities of ACF, CHD1, ISWI or BRG1 on nucleosome or chromatosome arrays

Nucleosome and chromatosome arrays were assembled on 12mer repeats of the 601 nucleosome positioning sequence using recombinant histone octamers and different molar ratios of linker histone H1 or H5 per positioning sequence (H1/nuc or H5/nuc). Arrays were purified by $MgCl_2$ -precipitation. (A) To monitor the occupancy of positioning sequences by histone octamers and linker histones, 6 pmol arrays were digested to nucleosomes and chromatosomes by the endonuclease *Ava*I. Unbound positioning sequences (200 bp), nucleosomes (nuc) and chromatosomes (chrom) were separated on 1.1% agarose gel and stained by SYBRgold[®]. (B) 15% polyacrylamide gel of 60 pmol arrays purified by $MgCl_2$ -precipitation to examine the stoichiometry of core and linker histones. (C) Remodelling assays with ACF, CHD1, ISWI or BRG1 were performed and analysed as described in figure 3.2. (D) Quantification of relative amounts of uncut DNA in (C).

equally active on nucleosome arrays for their activity on chromosome arrays, with similar results (Figure 3.3A, lanes 16-25). This indicates that remodelling of chromosome arrays by ACF does not result from incomplete reconstitution of the arrays. Moreover, we showed that ISWI and ACF are better suited than CHD1 to remodel linker histone-containing chromatin.

As an additional control we included human BRG1 in our analysis. BRG1 is one of two SWI/SNF-type ATPases, which are associated to seven or more subunits *in vivo* to form SWI/SNF complexes (Nagl et al., 2007). The isolated ATPase subunit also functions as a remodelling factor *in vitro* (Fan et al., 2003a). Using our system, we found that BRG1 remodels nucleosome and chromosome arrays with an efficiency similar to that ACF (Figure 3.2A, lanes 26-35). Hence, the ability to remodel chromosome arrays may be a more widespread, albeit not universal feature of chromatin remodelling factors.

To elucidate whether the presence of histone modifications influenced the outcome of these experiments, arrays were also assembled using recombinant *Drosophila* histones expressed in *E. coli* (Figure 3.4A, B). These, in contrast to those purified from *Drosophila* embryos, did not carry any post-translational modifications. The features of chromatin reconstituted with recombinant histone octamers in the absence or presence of linker histones were essentially the same as with endogenous octamers, at least according to our quality control assays. Monitoring DNA accessibility, ACF, ISWI, CHD1 and BRG1 were able to remodel arrays assembled with recombinant histones and with or without H1 or H5 to the same extent as those assembled with endogenous histones (Figure 3.4C, D).

3.3 ACF repositions nucleosomes in the presence of linker histones

3.3.1 ACF-mediated repositioning of nucleosomal particles within nucleosome and chromosome arrays

Accessibility of nucleosomal DNA provides a quantitative measure of chromatin remodelling. It does not, however, give information about the nature of such remodelling, since an increase in DNA accessibility may result from nucleosome repositioning as well as from disruption of histone-DNA contacts without nucleosome movements (Fan et al., 2003a). Since ACF repositions mononucleosomes on short DNA fragments (Eberharter et al., 2001), we wanted to test whether it could also do so in our system and whether this activity was affected by the presence of linker histones. To visualize potential nucleosome movements within the chromosome arrays we subjected reconstituted, end-labelled chromatin to remodelling by ACF and then probed nucleosome positions by partial digestion with micrococcal nuclease (MNase). MNase digestion in the absence of remodelling yielded a highly regular ladder of DNA fragments (Figure 3.5A, lanes 2-7). This pattern was dramatically altered when arrays had been incubated with both ACF and ATP (Figure 3.5A, lanes 8-10). The cleavage profile resembled the one obtained from digesting free DNA (Figure 3.5A, lane 1) suggesting that nucleosome positions had been randomized by ATP-dependent remodelling. These ATP-dependent changes were clearly visualized by comparing densitometry profiles of corresponding lanes (Figure 3.5E).

Digestion of chromosome arrays also yielded a regular cleavage pattern, but an additional band was visible below each of the bands obtained from nucleosome arrays (Figure 3.5A, lanes 12-17 and 22-27). These bands were particularly strong if arrays contained H5 and most likely reflect structural alterations of the linker DNA upon linker histone binding. After remodelling by ACF, the pattern obtained from H1 chromosome arrays changed, again becoming similar to the one obtained from free DNA. Notably, this change was also apparent in the case of the highly compact H5 chromosome arrays (Figure 3.5A, lanes 28-30).

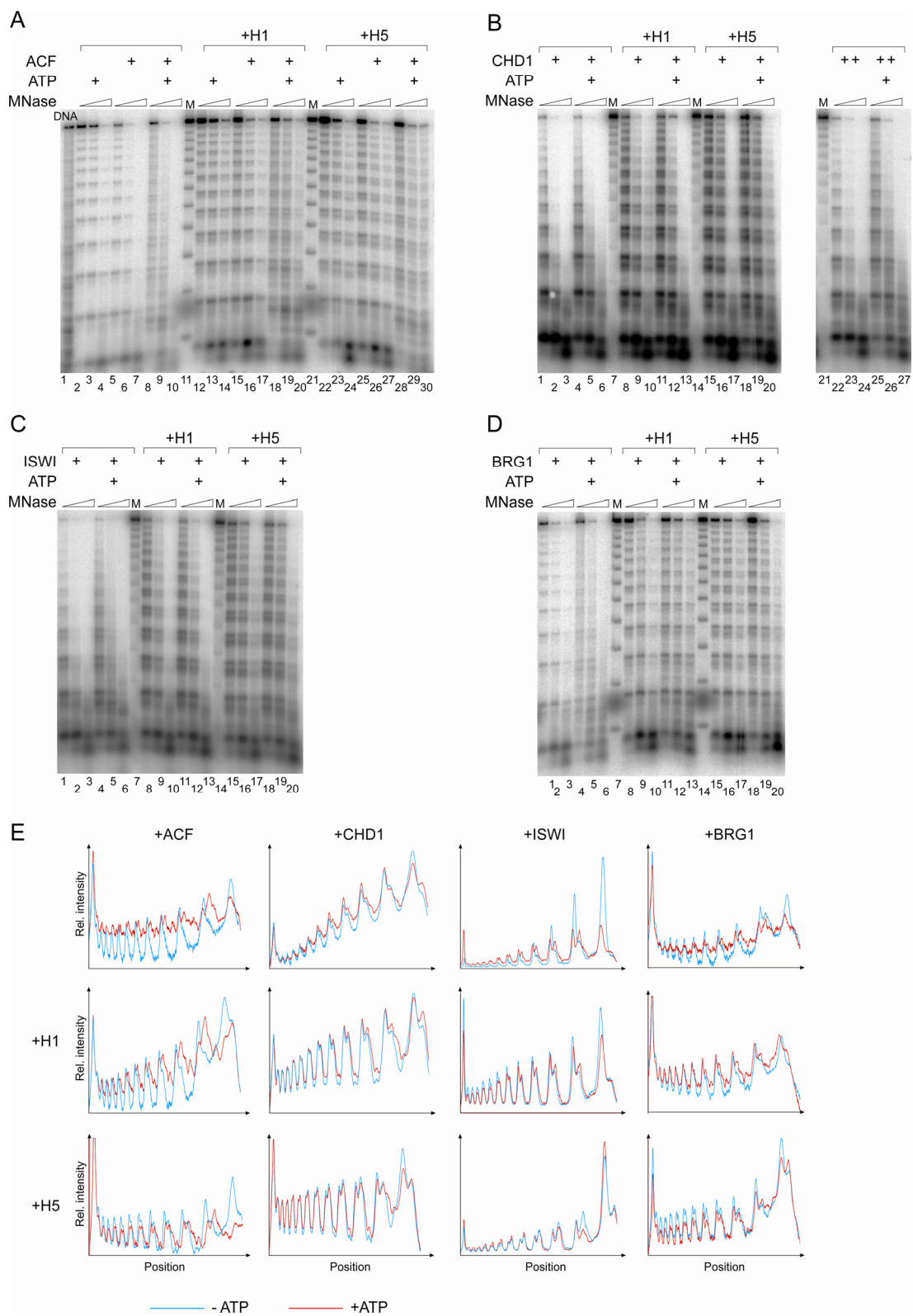


Figure 3.5 (previous page): ACF and BRG1 reposition nucleosomes also in the presence of linker histones

1.8 pmol end-labelled nucleosome or chromatosome arrays (containing either H1 or H5) were incubated with ATP and 7.2 pmol ACF (A), CHD1 (B), ISWI (C) or BRG1 (D). For (B)-(D), lanes 1-20, amounts of CHD1, ISWI or BRG1 were chosen that exhibited equal remodelling activities to that of ACF on nucleosome arrays (judged by AluI digestion, see figures 3.2 and 3.3). The fivefold amount of CHD1 was used in (B), lanes 21-27. After 1 h, DNA was partially digested by MNase (3 time points), purified and separated by agarose gel electrophoresis. Lane 1 in (A) shows the MNase digestion pattern obtained from free 12mer 601 repeats. As a molecular weight marker (M), nucleosome arrays were digested by AluI. (C) Densitometry profiles of selected lanes (A, lanes 5, 8, 16, 26 and 29; B, lanes 1, 4, 8, 11, 16 and 19; C, lanes 1, 4, 8, 11, 15 and 18; D, lanes 1, 4, 8, 11, 16 and 19). MNase digests of remodelling reactions performed with (red) or without ATP (blue) were compared; ACF, CHD1 ISWI, BRG1, H1 and H5 were present during the reaction as indicated.

We repeated the assay with ISWI alone to test whether it is also able to catalyse nucleosome movements within nucleosome and chromatosome arrays. ISWI alone changed the digestion pattern of both nucleosome and chromatosome arrays, but to a lesser extent than ACF (Figure 3.5C). This is consistent with previous experiments using mononucleosomal substrates, where ACF1 increased the sliding efficiency of ISWI (Eberharter et al., 2001).

3.3.2 Repositioning of nucleosomal particles by CHD1 and BRG1

To investigate whether remodelling factors other than ACF are able to reposition nucleosomes within nucleosome and chromatosome arrays, we also performed partial MNase digestions after remodelling by CHD1 and BRG1. Protein amounts were normalized based on their remodelling activities on nucleosome arrays (see 3.2).

CHD1 did not catalyse significant ATP-dependent changes of the MNase digestion pattern in presence or absence of linker histones. Densitometry profiles of digests after incubation with CHD1 with or without ATP were largely overlapping (Figure 3.5B, E) showing that CHD1 slides nucleosomes much less efficiently than ACF. This conclusion was confirmed by the observation that even the fivefold amount of CHD1 did not induce any significant ATP-dependent changes in the MNase digestion pattern (Figure 3.5B,

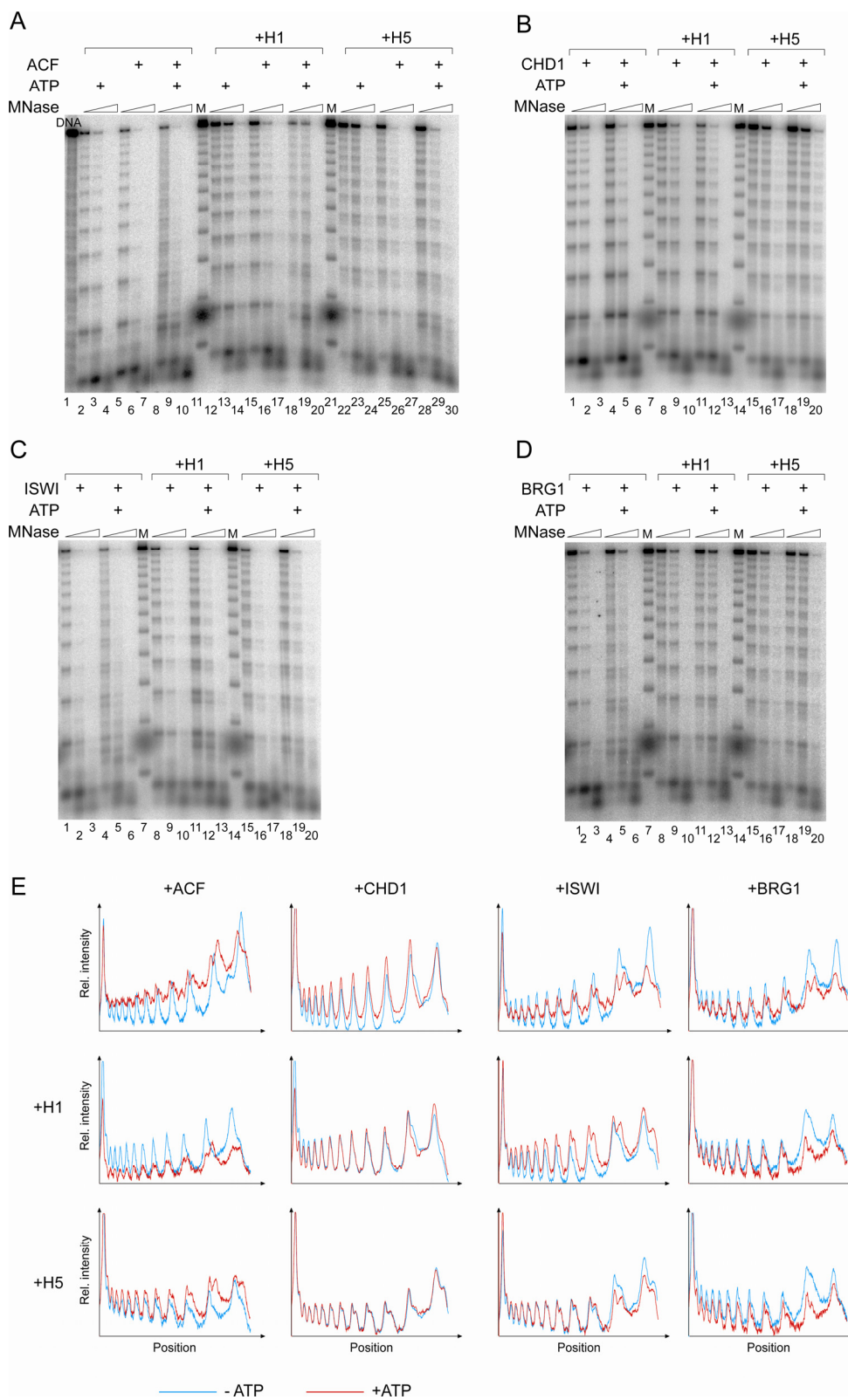


Figure 3.6 (previous page): Nucleosome repositioning by ACF, CHD1, ISWI and BRG1 in the absence or presence of linker histones is not significantly influenced by histone modifications.

Nucleosome mobilization assays with ACF (A), CHD1 (B), ISWI (C) and BRG1 (D) were performed as in figure 3.5 using nucleosome and chromatosome arrays assembled with recombinant histone octamers. Nucleosome arrays digested by AluI served as a molecular weight marker (M). As a control, free 12mer 601 repeats were digested by limiting amounts of MNase (A, lane 1). (C) Densitometry profiles of selected lanes (A, lanes 5, 8, 15, 18, 25, and 28; B, lanes 1, 4, 8, 11, 16 and 19; C and D, lanes 1, 4, 8, 10, 15 and 18).

lanes 21-27). This result, taken together with the one from the AluI-accessibility assay, shows that access to oligonucleosomal DNA can be generated by two distinct strategies: nucleosome sliding (by ACF) and nucleosome remodelling without overt changes in histone octamer positions (by CHD1).

The ATPase BRG1 catalysed ATP-dependent alterations of the nucleosome array cleavage pattern similar to ACF (Figure 3.5D, lanes 1-6). Changes were also detected when remodelling H1 or H5 chromatosome arrays with BRG1, but they were less pronounced than the ACF-dependent ones (Figure 3.5D, lanes 8-20).

In summary, repositioning of nucleosomal particles within linker histone-containing chromatin can be achieved by some, but not all remodelling factors.

As before, the experiments were repeated with recombinant histone octamers generated in *E. coli* to test whether the results were affected by the presence of post-translational histone modifications. Changes of the MNase cleavage patterns in absence or presence of linker histones caused by ACF, ISWI and CHD1 were comparable to those within arrays assembled with endogenous core histones (Figure 3.6A-C). Repositioning by BRG1, however, seemed to be more inhibited by H1 or H5 than when assays were performed with histones carrying PTMs (Figure 3.6D). These subtle differences raise the possibility that BRG1 might be regulated by histone modifications.

3.4 ACF catalyses the movement of chromatosomes

Since ACF can assist the assembly of H1-containing chromatin (Lusser et al., 2005), it might also be able to catalyze the opposite reaction, the eviction of H1. Hence, it is possible that nucleosome repositioning by ACF is a result of transient or permanent disassembly of the linker histone.

We therefore wanted to explore whether linker histones were still associated to nucleosomes after their repositioning by ACF. For this purpose, we subjected our arrays to remodelling reactions as described above and subsequently digested them with MNase to mononucleosomes or -chromatosomes, respectively. Histones protect bound DNA from the exonuclease activity of MNase, so the DNA fragments resistant to MNase digestion correspond to the positions of the nucleosomes and chromatosomes. The two species were separated on a native agarose gel (Figure 3.7A). In agreement with the literature (Nightingale et al., 1996) MNase treatment led to displacement of a fraction of H1 from the chromatosomes, so that a mixture of nucleosomes and chromatosomes was obtained from the digestion of chromatosome arrays independent of whether they had been remodelled. We did not observe the so-called ‘chromatosome stop’ when H5 chromatosome arrays were digested, so we did not include them in this experiment. Nucleosomes (from nucleosome arrays) and chromatosomes (from chromatosome arrays) were excised and the DNA was purified. The nucleosomal positions were then mapped by primer extension using radiolabelled primers. The positions of nucleosomal particles can be deduced from the length of the resulting single-stranded DNA and the position of the primer. Forward and reverse primers complementary to two different positions, 13 and 76 bp into the nucleosome (13fw, 13rv, 76fw and 76rv, see Figure 3.7B) were added in four separate reactions of primer extension.

Nucleosomal DNA purified from unremodelled arrays gave rise to several bands for all four primers, most likely due to single-stranded nicks generated by MNase (Cockell et al., 1983). The most prominent band in each reaction, however, confirmed the nucleosome position defined by the 601 sequence (asterisks in figure 3.7C, D). For example, annealing and extension of the 13rv primer resulted in the expected 33 bp band

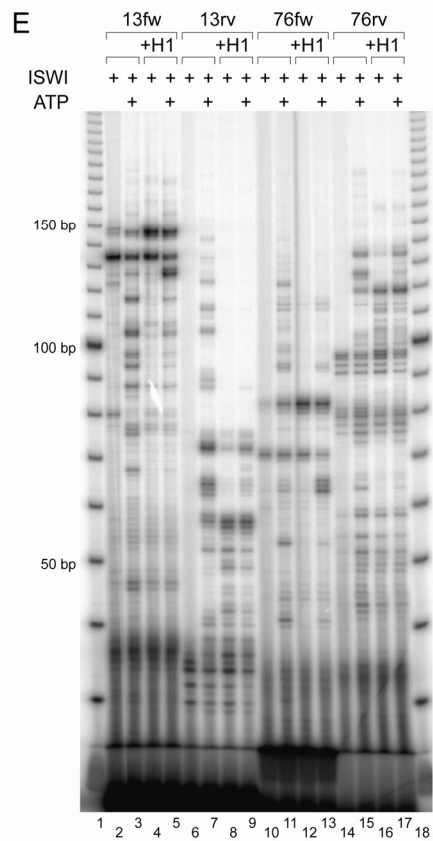
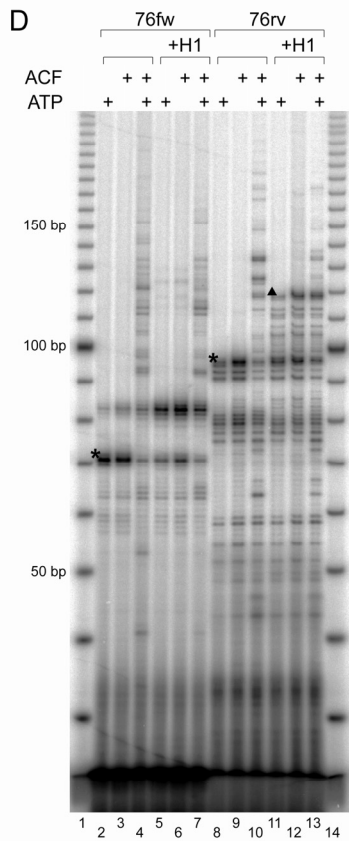
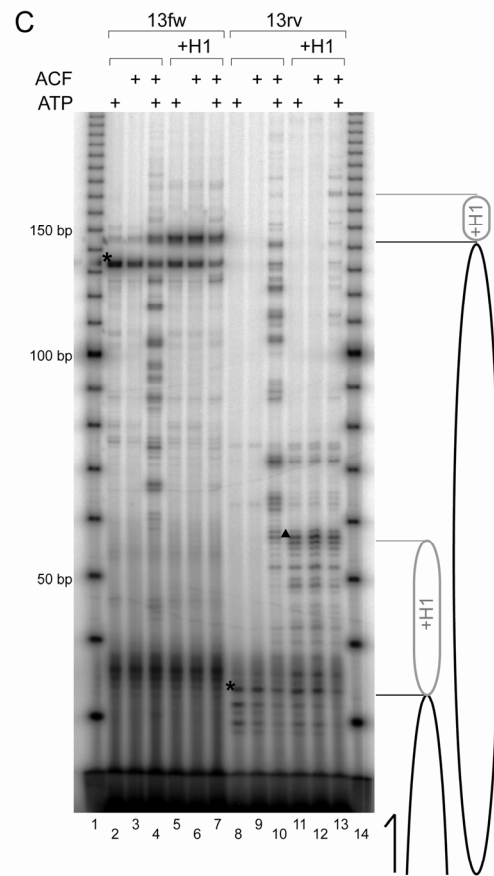
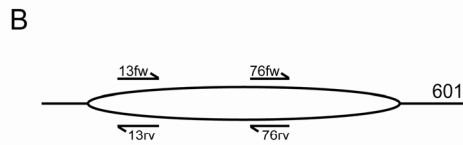
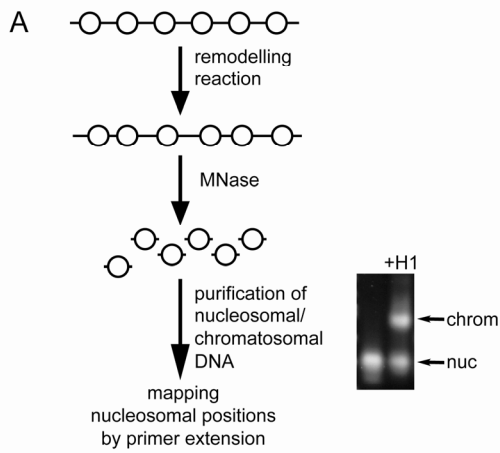


Figure 3.7 (previous page): ACF and ISWI catalyse the movement of chromatosomes

(A) Scheme of experimental steps to map nucleosome positions after remodelling reactions. Nucleosome arrays or H1 chromatosome arrays were incubated with or without ACF or ISWI and ATP. After 1 h arrays were digested to nucleosomes or chromatosomes by MNase. Nucleosomes and chromatosomes were then separated by preparative agarose gel electrophoresis. Nucleosomes (from nucleosome arrays) and chromatosomes (from chromatosome arrays) were excised from 1.1% native agarose gel and the DNA was extracted. To map positions of nucleosomes/chromatosomes, primer extension was performed with the primers depicted in (B). (B) Annealing positions of the primers used for primer extension reactions (13fw, 13rv, 76fw and 76rv). Arrows indicate the primers, the black line the DNA and the oval the position of the nucleosome before the remodelling reaction. (C) Primer extension reactions after ACF-mediated remodelling with primers 13fw and 13rv performed on isolated nucleosomal/chromatosomal DNA were analysed on 7% polyacrylamide 20% urea gels. For reactions conducted with 13rv, nucleosome positions corresponding to the indicated bands are represented by drawings at the right side of the gel. (D) Same as (C), but with primers 76fw and 76rv. (E) Primer extension reactions after remodelling by ISWI with primers 13fw, 13rv, 76fw and 76rv analysed as in (C) and (D).

(Figure 3.7C, lane 8). Primer extensions with the reverse primer 13rv and 76rv revealed that the DNA fragments derived from chromatosomes were 20 bp longer at the 5' end than nucleosomal ones (triangles in figure 3.7C, D). This is in accordance with the fact that H1 protects 20 bp of linker DNA from nuclease digestion (Simpson, 1978) and hints at an asymmetric interaction of the linker histone with the nucleosome.

Upon remodelling by ACF, besides the band corresponding to the position defined by the 601 sequence, we could detect several additional bands with all four primers, demonstrating repositioning of nucleosomes. The most striking effect was observed with the 13rv primer. Without remodelling, the 33 bp fragment indicative of 601-directed positioning was most prominent. When both ACF and ATP had been added to the remodelling reaction, bands of different sizes up to approximately 150 bp were obtained, showing that nucleosomes had been repositioned along the entire length of the DNA repeat (Figure 3.7C, lane 10). Prominent bands considerably longer than 150 bp are not expected, because the nucleosome protects only 147 bp from nuclease digestion. Intriguingly, fragments of various sizes were also obtained from DNA which was purified from chromatosomes after remodelling, revealing movements of chromatosomes throughout the length of the 601 repeat (Figure 3.7C, lane 13). Not surprisingly, the largest bands observed were slightly longer (up to approximately 180

bp) due to H1 binding. Since in this assay, the DNA was obtained from gel-purified chromatosomes after a remodelling reaction, we conclude that ACF is able to reposition entire chromatosomes on DNA in an ATP-dependent manner without permanently evicting H1.

Also when conducting the experiment with ISWI alone, repositioning was detected both in absence and presence of H1 (Figure 3.7E). Unlike in the partial MNase digestion experiment, no major differences in the extent of repositioning could be observed. This might result from the increased sensitivity of the primer extension experiment, which detects much less frequent repositioning events, but is not a good measure for the overall incidence of repositioning. However, the predominant positions obtained upon ISWI remodelling deviated from those detected after incubation with ACF, these differences being even stronger in the presence of H1 (Fig. 3.7, compare e. g. C, lane 7 and E, lane 5, C, lane 13 and E, lane 9 or D, lane 7 and E, lane 13). This indicates different positions favoured by ISWI and ACF as shown previously for mononucleosomes (Eberharter et al., 2001) demonstrating that the presence of ACF1 can affect the outcome of ISWI-dependent remodelling reactions.

The experiments presented were controlled in a highly purified system and contribute to our understanding of remodelling of nucleosomal fibres. The data presented so far have mostly been published (Maier et al., 2007). The following sections include preliminary data which represent both *in vivo* and *in vitro* attempts to follow up our results described in this first part.

3.5 H1 may influence the directionality of ACF-mediated nucleosome movements

3.5.1 Reconstitution of palindromic 8mer 601 arrays

Primer extension on nucleosomal and chromatosomal DNA after remodelling demonstrated that ACF can reposition nucleosomes as well as chromatosomes along DNA. However, the data revealed differences in the positions of the particles after

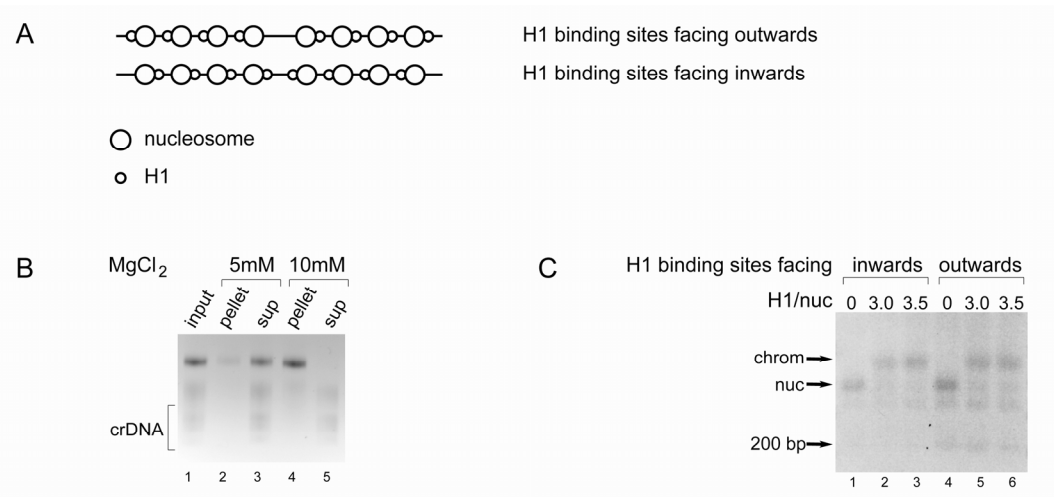


Figure 3.8: Reconstitution of 8mer nucleosome and chromosome arrays assembled on DNA consisting of a palindromic arrangement of 601 sequences

(A) Schematic representation of palindromic chromosome arrays: 4mer tandem 601 arrays were ligated either with their H1 binding sites (°) facing inwards or facing outwards. Nucleosome or chromosome arrays were reconstituted on these DNA fragments by salt dialysis in the presence of competitor DNA (crDNA). (B) MgCl₂-precipitation of nucleosome arrays assembled on DNA described in (A). Corresponding amounts of input, pellet and supernatant (sup) were analysed on 0.7% native agarose gel and stained with EtBr. Complete precipitation required addition of 10 mM MgCl₂. (C) To monitor the occupancy of positioning sequences by histone octamers and linker histones, 6 pmol arrays were digested to nucleosomes and chromosomes by *Ava*I. Unbound positioning sequences (200 bp), nucleosomes (nuc) and chromosomes (chrom) were separated on native 1.1% agarose gel. Arrays assembled with a ratio of 3 H1 per 601 sequence (H1/nuc) were used for further experiments.

remodelling. As stated above, we observed an additional protection of 20 bp upon H1 binding only when reverse primers were used, suggesting that H1 interacted predominantly with one side of the nucleosome. For simplicity, from now on, this side will be referred to as the H1-bound side of the nucleosome. In reactions with reverse primers, fragments detected after remodelling which are smaller than the one prior remodelling indicate movement away from the H1-bound side of the nucleosome and bigger fragments result from sliding towards the opposite direction. The reverse concept applies to the forward primers. Upon remodelling nucleosome arrays, we observed bands smaller than the one corresponding to the unremodelled state. This was true for any of the primers except 13rv, which cannot detect such fragments as it anneals very

close to the border of the position of the unremodelled nucleosome (Figure 3.7C, lane 4 and D, lanes 4, 10). In contrast, only 76rv, not the forward primers, elongates prominent smaller fragments after remodelling of chromosome arrays (Figure 3.7D, lanes 7, 13), suggesting that movements are only catalysed away from H1, not towards H1. This conclusion is reinforced by looking at the appearance of bands running higher than those obtained without remodelling. When forward primers were elongated, such bands appeared after remodelling both of nucleosome and chromosome arrays (Figure 3.7C, lanes 4, 7 and D, lanes 4, 7). Using 76rv, higher bands appearing after remodelling of chromosome arrays are much weaker than those obtained from nucleosome arrays (Figure 3.7D, lanes 10, 13). Prominent very large fragments after chromosome remodelling are detected with 13rv (Figure 3.7C, lane 13), but these could result from neighbouring chromosomes moving to that position. These observations suggest that ACF moves chromosomes preferentially away from the H1 bound side. To further test this hypothesis, we assembled nucleosome and chromosome arrays on linear palindromic 8x601 arrays consisting of four 601 sequences orientated head-to-tail in one direction followed by four 601 sequences orientated in the opposite direction. Two kinds of such arrays were produced, with their H1 binding sides either ‘facing outwards’ or facing each other in the middle (‘facing inwards’, figure 3.8A). If ACF moved chromosomes only away from H1, chromosome movements into the central linker DNA would be favourable in the ‘facing outwards’ arrays, whereas such movements would be hindered in the ‘facing inwards’ arrays.

Nucleosome and chromosome arrays were assembled by salt dialysis in the presence of competitor DNA as described above (see 3.1). Again, excess histones and competitor DNA were removed by MgCl₂-precipitation. However, 10 mM instead of 5 mM MgCl₂ were necessary to fully precipitate the palindromic arrays, pointing to a lower level of compaction (Figure 3.8B). Occupancy of 601 sequences with core and linker histones was controlled by AvaI-digestion as before (Figure 3.8C). Saturation with both histone octamers and H1 was achieved.

3.5.2 Nucleosome and chromosome repositioning within palindromic arrays

We attempted to monitor nucleosome and chromosome positions within palindromic arrays by partial MNase digestions after remodelling as described for 12x601 arrays. 8mer arrays carried radioactive labels on both ends instead of only on one end, because both ends were cut by the same restriction enzyme (BamHI or BglII) so both overhangs were filled in with labelled dCTP. We aimed for similar degrees of repositioning in nucleosome and chromosome arrays to be able to compare the directionality of sliding in the absence and presence of H1. Therefore, to account for its reduced remodelling activity in the presence of H1, twice as much ACF was added to chromosome arrays as to nucleosome arrays. Arrays incubated with ACF, but no ATP gave rise to a regular MNase pattern with bands reflecting the positions of the accessible linker DNA (Figure 3.9A, lanes 1-3, 7-9, 13-15 and 19-21). However, the digestion pattern was constantly more smeary than the one obtained from 12mer arrays, which we attribute to promiscuous annealing of the palindromic fragments after inadvertent denaturation of DNA during the experiment. Nucleosomes moving into the linker DNA are expected to decrease its accessibility towards MNase. In agreement, bands were less sharp if ATP had been present during the reaction, indicating repositioning of nucleosomes (Figure 3.9A, lanes 4-6, 10-12, 16-18 and 22-24). In the absence of H1, changes in accessibility were similar for all linker DNAs as judged by the intensities of the corresponding bands (Figure 3.9A, lanes 4-6 and 10-12). When H1 was facing outwards, the band representing the central linker DNA decreased slightly more than the other bands, indicating that chromosome movements into this region might be favoured (Figure 3.9A, lanes 16-18). Conversely, the band corresponding to this region became particularly prominent after remodelling when H1 bound to the sides of the nucleosomes facing inwards, therefore flanking the central linker DNA. This suggests that chromosomes are not easily moved there (Figure 3.9A, lanes 22-24). The differences are more visible when comparing densitometry profiles of lanes corresponding to reactions with and without ATP (Figure 3.9B). These data indicate that ACF-mediated chromosome movements in the direction of the H1-bound side may be hindered. Although reproducible, the observed effect of H1 binding was very small,

suggesting that H1 binding might cause preferred repositioning away from rather than complete inhibition of movements towards the H1-bound side.

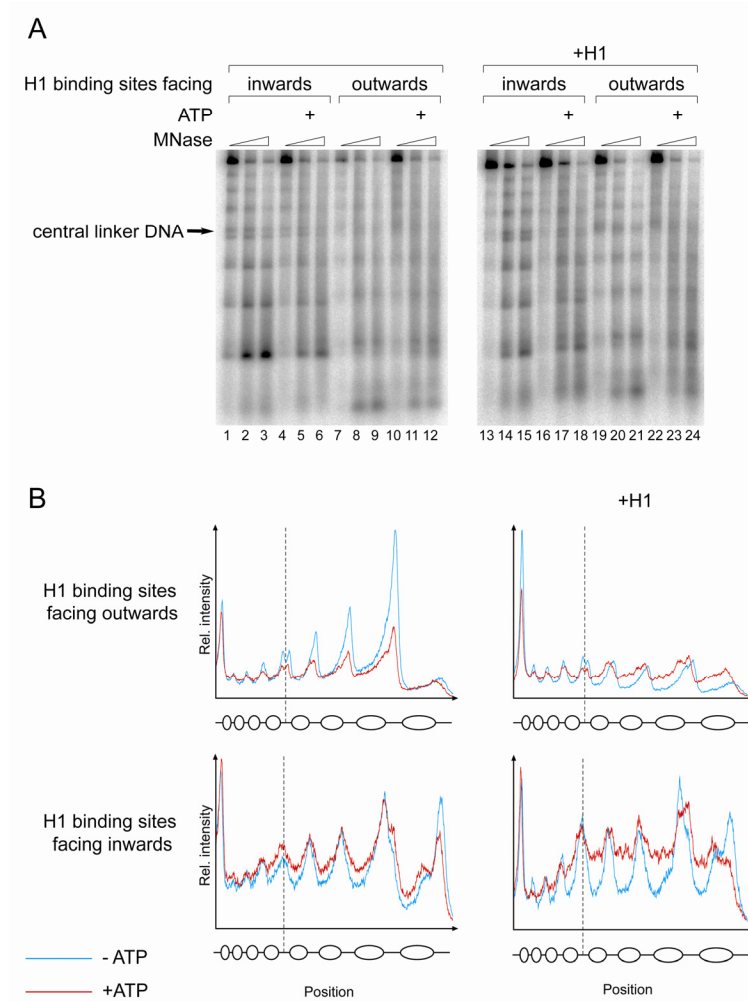


Figure 3.9: H1 may influence the direction of ACF-mediated nucleosomes movements

(A) Palindromic nucleosome and chromosome arrays labelled on both ends were incubated with or without ACF and ATP. After 1 h, reactions were stopped and partially digested by MNase (3 time points). The DNA was purified and analysed on 1.3% agarose gel. (B) Densitometry profiles of selected lanes (A, lanes 2, 5, 8, 11, 14, 17, 20 and 23). In arrays with H1 binding sites facing inwards, the peak corresponding to the central linker DNA (marked by the dotted line) became most prominent after remodelling in the presence, but not in the absence of H1, suggesting that chromosomes might be moved away from this region. In contrast, after remodelling of chromosome arrays with H1 binding sites facing outwards, the central peak sites decreased more than the other peaks, indicating that chromosomes were preferentially moved away from the H1-bound side.

3.6 The early linker histone substitute HMG-D does not affect the remodelling activity of ACF

3.6.1 Reconstitution of 12mer nucleosomal arrays containing HMG-D

Drosophila ACF is very abundant during cleavage and decreases during development (Chioda et al., manuscript in preparation). During cleavage, the first nuclear divisions occur in the absence of H1 and chromatin contains the high mobility group protein HMG-D, instead. Therefore, and because HMG-D binds to nucleosomal arrays but is displaced by H1, it has been postulated that it could behave as a structural component of chromatin in preblastoderm embryos. In this case it would support a structure which is condensed but less compact than H1-containing chromatin and may therefore enable the atypically fast replication events in embryonic chromatin (Ner et al., 2001; Ner and Travers, 1994). A related HMG protein, human HMGB1 was shown to enhance ACF-dependent mononucleosome sliding (Bonaldi et al., 2002). We therefore decided to investigate whether and how HMG-D could affect the remodelling activity of ACF. Would it partially inhibit remodelling similar to H1 or rather facilitate remodelling like HMGB1?

12mer nucleosomal arrays were assembled with histone octamers as described above (see 3.1). Different amounts of HMG-D were added to the assembly reaction. HMG-D binding to the arrays was monitored by EMSA (Figure 3.10A). Both nucleosomal arrays and competitor DNA migrated slower upon addition of increasing HMG-D amounts (Figure 3.10A, lanes 3-14). Unlike H1, HMG-D exhibited no preference for chromatin over free or poorly assembled DNA. Even when large protein amounts were used, no point of saturation was reached at which adding more HMG-D did not further enhance the band shift. Indeed, 12mer 601 arrays and competitor DNA migrated gradually slower upon adding increasing amounts of HMG-D. At a molar ratio of about 20 HMG-D per nucleosome, the bands became smeary, indicating oversaturation (Figure 3.10A, lane 13). At this ratio, arrays migrated already considerably slower than arrays saturated with H1 (Figure 3.10A, lane 15). Consequently, it was not possible to determine at which

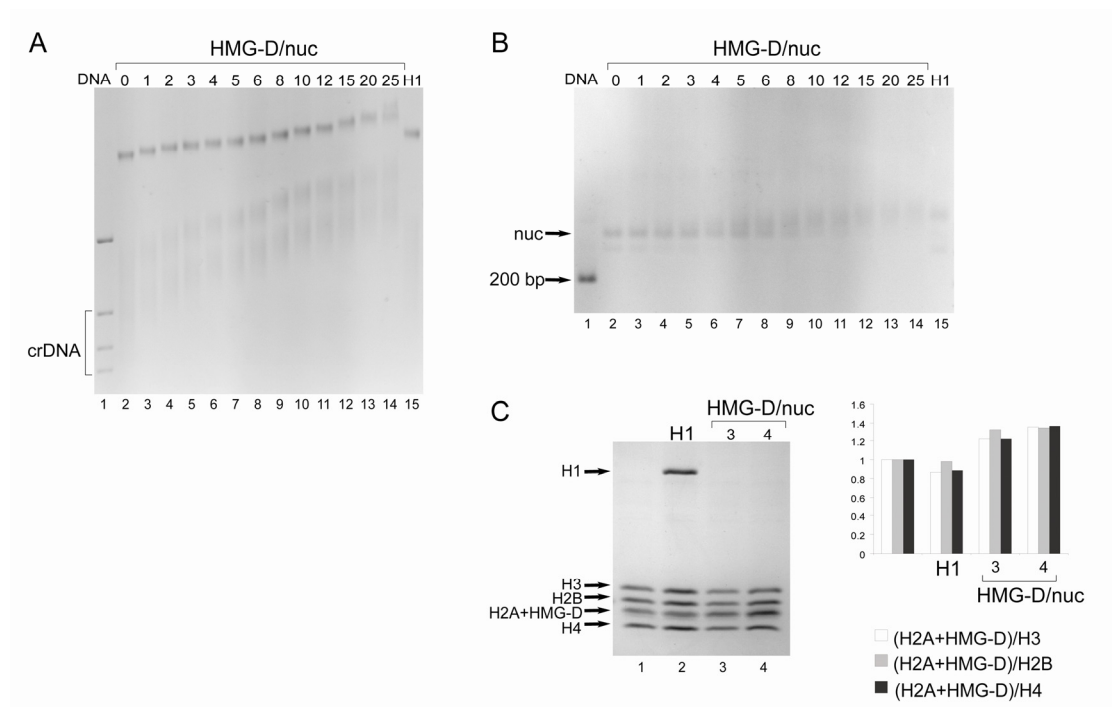


Figure 3.10: Reconstitution of 12mer nucleosomal arrays containing HMG-D

(A) 6 pmol 12mer nucleosomal arrays assembled by salt dialysis with increasing ratios of HMG-D per 601 sequence (HMG-D/nuc) were analysed on a native 0.7% agarose gel. DNA without histones (lane 1) and arrays assembled with saturating amounts of H1 (lane 15) served as references. Competitor DNA (crDNA) was present during all reconstitutions. (B) *Ava*I-digestion of nucleosomal arrays with increasing amounts of HMG-D as described in figure 3.1. (C) 15% polyacrylamide gel of nucleosomal arrays after $MgCl_2$ -precipitation with HMG-D/nuc as indicated. Histones and HMG-D were stained with Coomassie and bands were quantified. The band containing both HMG-D and H2A was normalized on H3, H2B or H4 as indicated. Intensity ratios were compared to arrays assembled without HMG-D.

input ratio each nucleosome was bound by one HMG-D nor did we know whether this would represent a physiologically relevant state.

The *Ava*I-digestion (see 3.1.2) could have been an alternative to determine the HMG-D amount that resulted in the incorporation of one HMG-D per nucleosome, the assumed physiological stoichiometry. However, also this assay failed to reveal this amount since increasing HMG-D yielded a continuous upwards shift of mononucleosomes until they migrated even slower than chromatosomes (Figure 3.10B).

The analysis of HMG-D incorporation into chromatin by SDS-PAGE was complicated by the fact that HMG-D migrates at the same position as H2A. To be able to estimate the degree of HMG-D incorporation, the band corresponding to H2A and HMG-D was quantified and normalized on the intensities of the other three histone bands (Figure 3.10C). Relative band intensities derived from chromatin without any HMG-D were used as a reference. When adding a molar ratio of 4 HMG-D per 601 sequence at the beginning of the assembly, the band corresponding to H2A and HMG-D was about 1.4 times as intense as the one measured for HMG-D free chromatin, meaning that about 80% of all nucleosomes were occupied with one HMG-D. Such chromatin was used for HMG-D experiments presented in the following.

3.6.2 Remodelling assays with HMG-D-containing chromatin

The ability of ACF to remodel nucleosomal arrays with or without HMG-D was determined by monitoring ATP-dependent increases in the accessibility of nucleosomal DNA to endonucleases as described above (see 3.2). As a reference, H1-containing chromatin was included in the experiment. ACF was added at a molar ratio of approximately four complexes per 12mer array and the mixture was incubated for 1 h at 26°C. HMG-D had no effect on the remodelling efficiency of ACF, while H1 partially inhibited ACF-dependent remodelling as shown earlier (Figure 3.11A, lanes 9, 12). However, considering that HMGB1 only moderately enhanced mononucleosome repositioning by ACF and that the strongest effect was observed after shorter remodelling reactions (Bonaldi et al., 2002), we repeated the experiment by incubating the arrays for only 10 min. In addition, reactions with a molar ratio of only 2 ACF per 12mer nucleosome array were included to achieve an even lower degree of remodelling (Figure 3.11C). Even under these conditions, no difference in ACF remodelling efficiency was observed when arrays containing HMG-D were compared to simple nucleosome arrays (Figure 3.11D). Hence, with our system, we could not detect any effects of HMG-D on the efficiency of ACF to remodel nucleosome arrays.

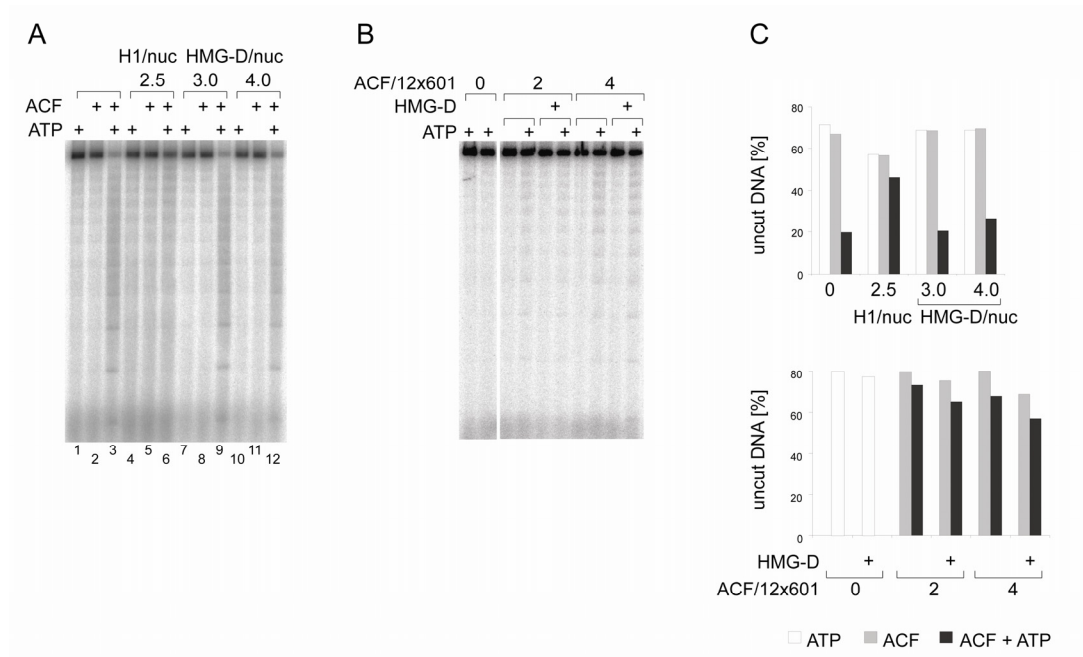


Figure 3.11: HMG-D does not affect the remodelling activity of ACF

(A) ATP and/or 4 ACF per 12mer array were added to 12mer end-labelled nucleosomal arrays assembled with saturating amounts of H1 or with different ratios of HMG-D per 601 sequence (HMG-D/nuc) as indicated. After 1 h at 26°C, the DNA was purified and analysed on 1.3% agarose gel. (B) 12mer nucleosomal arrays assembled with or without 4 HMG-D/nuc were incubated with different molar ratios of ACF (ACF/12x601) and with or without ATP for 10 min at 26°C. The DNA was analysed as in (A). (C) Quantification of relative amounts of uncut DNA in (A) and (B).

3.7 H1 and HMG-D levels are elevated in *acf1* null flies

3.7.1 Generation of polyclonal antibodies directed against H1 and HMG-D

Several observations suggest that ACF could affect the incorporation of H1 into chromatin. First, it has been shown to assist the assembly of H1-containing chromatin arrays *in vitro*, indicating that it might function as an H1 chaperone (Lusser et al., 2005). Second, we could show that, unlike the related remodelling ATPase CHD1, ACF is able to remodel H1-containing chromatin arrays (see 3.2.2). Finally, ACF1 is detected in nuclei during cleavage, when HMG-D is replaced by H1 (Chioda et al.,

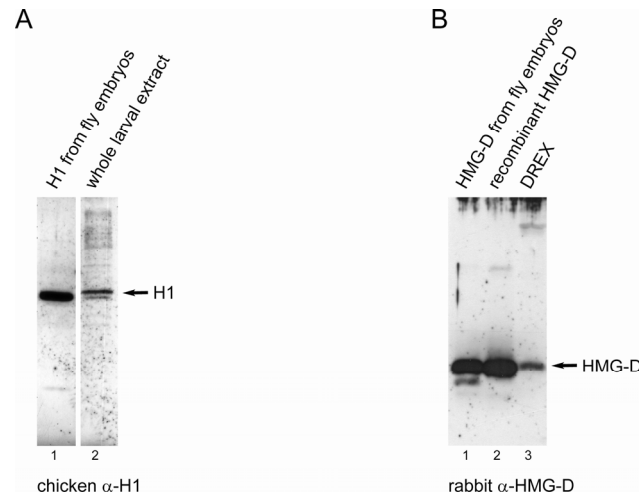


Figure 3.12: Characterization of antibodies against H1 and HMG-D

Antibodies against endogenous *Drosophila* H1 and HMG-D were raised in chicken and rabbit, respectively. (A) The specificity of the α -H1-antibody was assayed by Western blot on H1 purified from embryos 0-12 h AEL and whole larval extract. (B) The α -HMG-D antibody was tested by Western blot on HMG-D purified from embryos 0-90 min AEL, recombinant HMG-D expressed in *E. coli* and *Drosophila* embryonic extract (DREX) from embryos 0-90 min AEL.

manuscript in preparation). We therefore wanted to investigate whether H1 and HMG-D incorporation into chromatin during embryonic development was affected by ACF/CHRAC *in vivo*.

We were not satisfied with the performance of available antibodies against H1 and HMG-D in immunofluorescence experiments. Therefore, we generated polyclonal antibodies in chicken and rabbit directed against H1 and HMG-D, respectively. The α -H1 antibody was purified from egg-yolk and its specificity was assayed by Western blot. It recognized both purified H1 and endogenous H1 from whole larval extract. Only one unspecific band near the signal corresponding to the molecular weight of H1 was detected (Figure 3.12A). The antiserum obtained from rabbit immunized with HMG-D was tested on recombinant HMG-D expressed in *E. coli*, endogenous HMG-D purified from embryos 0-90 min AEL and *Drosophila* embryonic extract (0-90 min AEL) (Becker et al., 1994). The antibody detected a band corresponding to HMG-D, but also a weaker band of approximately 50 kD (Figure 3.12B).

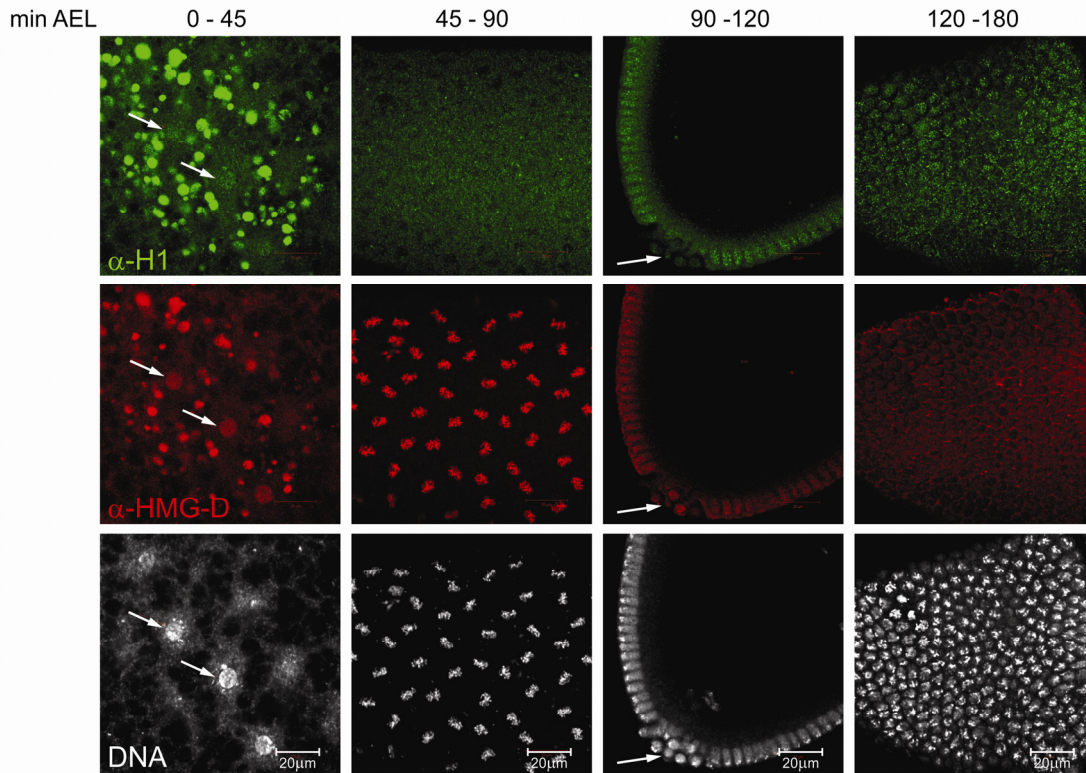


Figure 3.13: Distribution of H1 and HMG-D in early *Drosophila* development

Whole mount immunofluorescence of embryos 0-3 h AEL. H1 (green) and HMG-D (red) were detected with the antibodies raised (see figure 3.12), DNA (white) was stained with TO-PRO3. HMG-D localized to nuclei approximately from nuclear division 4 onwards (arrows, 0-45 min) and was enriched on mitotic chromosomes (45-90 min) and pole cells (arrow, 90-120 min). In gastrulating embryos, some nuclei retained HMG-D staining (120-180 min). H1 was detected in nuclei from nuclear division 10 onwards (90-120 min) and in most nuclei of gastrulating embryos (120-180 min).

3.7.2 Immunofluorescence of whole mount *Drosophila* wild-type and *acfl* embryos with α -H1 and α -HMG-D antibodies

Both antibodies were used for staining of embryos 0-3 h AEL. Nuclear staining by the α -HMG-D antibody was observed from nuclear division 4 onwards (Figure 3.13, 0-45 min). As development proceeded to nuclear division 6-9 during which nuclei migrate to the surface of the embryo, the HMG-D antibody stained mitotic chromosomes in accordance with the literature (Ner and Travers, 1994) (Figure 3.13, 45-90min). During nuclear divisions 10-11, nuclei are stained weaker for HMG-D and it was enriched on

the pole cells which will give rise to the gonads (Figure 3.13, 90-120 min). HMG-D was also detected in few nuclei of gastrulating embryos (Figure 3.13, 120-180 min).

Very different stainings were obtained with the α -H1 antibody. No H1 was detected in early nuclei. A cytosolic granular staining was obtained, most likely resulting from non-specific staining of abundant yolk proteins; embryos do not contain H1 at this stage (Figure 3.13, 0-45 min) (Ner and Travers, 1994). Nuclear H1 staining was only observed from nuclear division 10-11 onwards (Figure 3.13, 90-120 min). Interestingly, at this point, heterochromatin starts to form, which is in line with a role of the linker histone in chromatin compaction. In gastrulating embryos, H1 was detected in most nuclei. These findings, which are in line with earlier studies, support the specificity of our antibodies.

We now compared H1 and HMG-D stainings of wild-type embryos to those of homozygous *acfl* flies (Figure 3.14A). *Acfl* refers to the *acfl[2]* null allele described by Fyodorov et al. (Fyodorov et al., 2004). In *acfl* embryos, nuclei exhibited obvious defects in chromatin organization (Figure 3.14A, 90-120 min), showing that ACF1 is required for chromatin assembly. Strikingly, both the H1 and HMG-D staining were stronger in *acfl* embryos. H1 and HMG-D levels were also elevated in gastrulating embryos (Figure 3.14A, 120-180 min).

3.7.3 Quantification of H1 and HMG-D levels in nuclei of wild-type versus *acfl* embryos

To quantify the differences of H1 and HMG-D amounts observed in immunofluorescence between wild-type and *acfl* embryos, nuclei were purified from embryos 0-2 h AEL and 0-15 h AEL. Relative H1 and HMG-D amounts were determined by Western blot using the LI-COR Odyssey[®] System. H3 was used as a reference and signals for H1 and HMG-D were normalized accordingly.

As observed by immunostainings, both H1 and HMG-D levels were higher in *acfl* embryos than in the wild-type, regardless of the embryonic stage examined (Figure 3.14B, C). To exclude that these differences in protein levels were due to accelerated development, we determined how many embryos were still in cleavage and how many were already gastrulating. No differences between *acfl* and wild-type embryos were

detected, showing that the altered H1 and HMG-D levels in *acfl* embryos were not the result of global changes in development. These observations suggest that an ACF1-containing complex affects H1 and HMG-D incorporation *in vivo*. It may play an active role in controlling the association of these proteins with chromatin or influence linker histone deposition more indirectly through the regulation of other factors.

3.8 H1 replaces HMG-D from chromatin in the absence of cofactors

3.8.1 H1 associates with preassembled nucleosome arrays

As described above, early embryonic chromatin does not contain H1, but HMG-D, which is gradually replaced by H1 as the embryo develops (see 3.7.1). We wondered whether the association of HMG-D or H1 required the assistance of other factors such as ACF. It was shown previously that H1 can replace HMG-D from chromatin. However, the chromatin arrays in this study were assembled by *Drosophila* embryonic extract. The chromatin was purified for the analysis, but most likely still contained an unknown number of chromatin binding factors (Ner et al., 2001). We therefore reinvestigated HMG-D replacement by H1 in our purified system.

Nucleosomal arrays were assembled with and without HMG-D at a molar ratio of 4 HMG-D per 601 sequence as described above (see 3.6.1). H1 was titrated to these arrays either before or after MgCl₂-precipitation, so either in the absence or in the presence of competitor DNA which could bind excess H1. H1 was added at calculated input ratios between two and ten molecules per 601 sequence. These input ratios most likely do not reflect the ratios of available H1 per nucleosome, since H1 readily sticks to tubes and tips, in spite of using siliconized tubes and preblocking tips with BSA (98% PURE). Arrays were incubated with H1 for 5 min at 26°C and applied on 0.7% agarose gel in 0.2xTB. Chromatin assembled in the presence of saturating H1 amounts served as a reference (Figure 3.15).

H1 addition led to a shift on native agarose gel until at a calculated input ratio of four H1 per 601 sequence, the arrays migrated at the same height as those assembled in the

presence of H1 (Figure 3.15A, lanes 3, 5, 8, 10). Addition of more H1 shifted the arrays beyond this point and generated a smeary band (Figure 3.15A, lane 4). This smeariness was less pronounced if competitor DNA was still present, showing that it can buffer excess H1 to some extent (Figure 3.15A, lane 9). In the absence of H1, HMG-D-containing arrays migrated slightly slower than those without HMG-D, but after H1 addition, they also approached the migration behaviour of arrays assembled with H1. This suggests that H1 binds to nucleosome arrays with the same affinity whether or not they contain HMG-D.

3.8.2 H1 replaces HMG-D in a purified system without accessory factors

The EMSA allowed us to directly observe H1 binding to nucleosomal arrays, but did not reveal how much H1 was incorporated. To quantify the amount of bound H1, nucleosome arrays with or without HMG-D containing competitor DNA were incubated with H1 as before and purified from unbound proteins by $MgCl_2$ -precipitation. The H1 and HMG-D contents of the arrays were then quantified by Western blot using a LICOR Odyssey machine and normalized on the amount of H4. As a reference, the H1 content of chromatosome arrays assembled in the presence of H1 and the HMG-D content of HMG-D-containing arrays without H1 addition were also determined (Figure 3.15B, C).

H1 was incorporated into the arrays already at a ratio of two H1 per nucleosome (Figure 3.15B, lane 3). The amount of bound H1 did not increase notably when more H1 was added. At a tenfold excess of H1 over nucleosomes, non-stoichiometric incorporation suggested by the EMSA was not reflected in this experiment, possibly because excess H1 was removed during the precipitation step (Figure 3.15B, lanes 4, 5). Interestingly, when adding low H1 levels, both H1 and HMG-D were bound to the arrays in approximately stoichiometric amounts to the nucleosome (Figure 3.15B, lane 7). Apparently, under these conditions, H1 and HMG-D can be incorporated in nucleosomal arrays at the same time. Upon addition of more H1, HMG-D levels decreased whereas H1 levels remained constant (Figure 3.15B, lanes 8, 9).

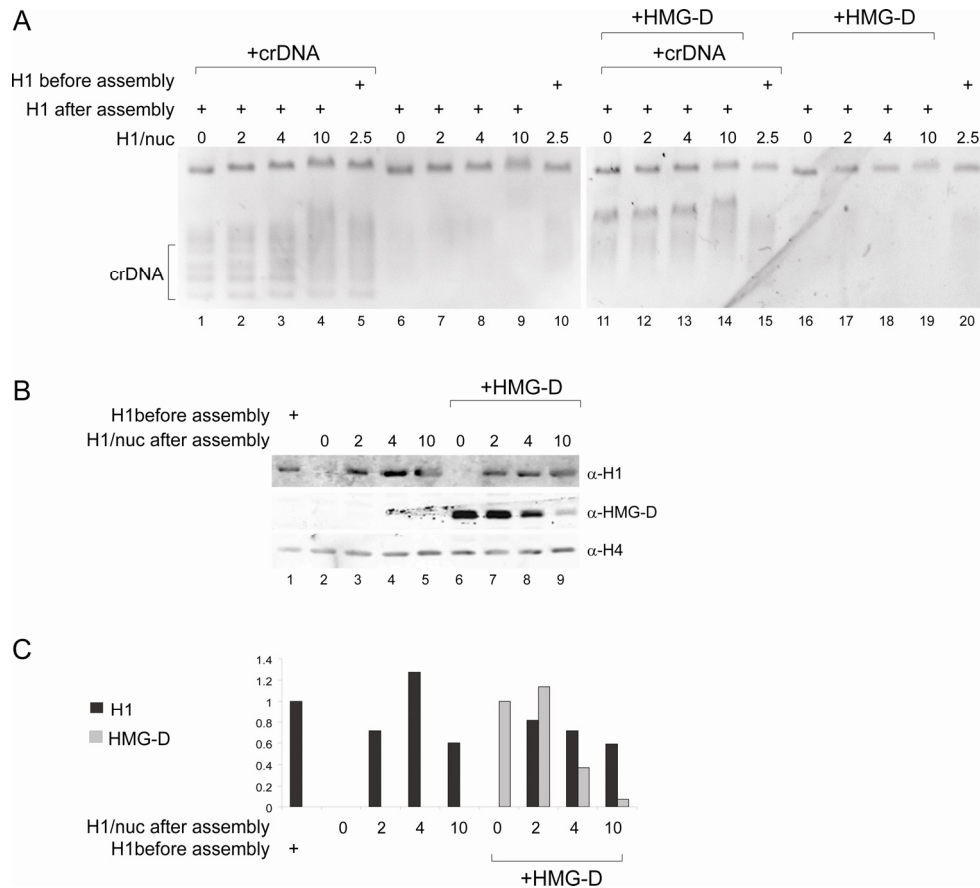


Figure 3.15: H1 binds to nucleosome arrays and replaces HMG-D in the absence of cofactors

(A) 6 pmol 12mer nucleosomal arrays assembled with (lanes 11-14 and 16-19) or without (lanes 1-4 and 6-9) HMG-D were mixed with increasing molar ratios of H1 per 601 sequence (H1/nuc) in the presence (lanes 1-4 and 11-14) or absence (lanes 6-9 and 16-19) of competitor DNA (crDNA). Arrays were incubated for 5 min at 26°C and run on native 0.7% agarose gel. Their migration behaviour was compared to that of arrays with saturating amounts of H1 added at high salt at the beginning of the reconstitution (lanes 5, 10, 15 and 20). (B) Nucleosomal arrays with crDNA were mixed with H1 and incubated for 5 min at 26°C. Arrays were precipitated with 5 mM MgCl₂ and their H1, HMG-D and H4 levels were analysed by Western blot. (C) Quantification of (B). H1 (black) and HMG-D (grey) were normalized on H4; H1 and HMG-D per H4 ratios of arrays assembled in the presence of H1 or HMG-D (without addition of H1), respectively, served as references.

Taken together, we showed that also in a purified system, HMG-D is replaced by H1 by simple competition. *In vivo*, this process may require a tighter control. ACF, which assists assembly of H1-containing chromatin *in vitro* (Lusser and Kadonaga, 2005), may potentially act as an H1 chaperone that regulates H1 loading onto chromatin and prevents premature H1 incorporation *in vivo*, a hypothesis supported by the altered H1 levels in *acfl* flies.

4. Discussion

4.1 ATP-dependent chromosome remodelling

4.1.1 Remodelling of H1-containing chromatin by specific remodelling factors

Since most of the eukaryotic genome is organized in H1-containing chromatin fibres (Horowitz et al., 1994), this folded chromatin presumably presents the most common and abundant substrate for ATP-dependent chromatin remodelling enzymes. In order to understand whether nucleosome remodelling can occur on the bulk of interphase chromatin or whether it is restricted to the chromatin fraction devoid of linker histones, it was important to investigate whether and to what extent remodelling factors can deal with H1-containing chromatin. Yet, to date, such studies yielded contradictory results and were subject to certain limitations of the experimental setups which did not allow clear cut conclusions (summarized in 1.5.1).

We therefore decided to address this issue in a more purified system making use of regular nucleosome and chromosome arrays assembled from purified components. These arrays were subjected to remodelling by the complex ACF, its ATPase ISWI alone and the ATPases CHD1 and BRG1.

To our surprise, we found that ACF, ISWI and BRG1 were able to increase the access to nucleosomal DNA even if the arrays contained stoichiometric amounts of H1 or H5, albeit less efficiently than in linker histone free chromatin. By contrast, the remodelling activity of the related ATPase CHD1 was completely inhibited by the presence of linker histones. Strikingly, we also observed nucleosome movements catalysed by ACF, and to a lesser extent by ISWI and BRG1, within arrays saturated with linker histones. Moreover, we detected considerable movements of entire chromosomes catalysed by ACF and ISWI, showing that ACF-dependent remodelling does not depend on the permanent dissociation of H1 from chromatin. CHD1 on the other hand did not catalyse significant nucleosome repositioning within our arrays, whether or not linker histones were present. This illustrates that access to DNA can be

generated not only by nucleosome repositioning, but also by other means, like the detachment of DNA from the histone surface without movement of the octamer on DNA. In addition, it shows that not all remodelling factors are able to remodel linker histone-containing chromatin equally well. We therefore suggest a distinction between ‘nucleosome remodellers’, which are only able to remodel nucleosomes devoid of H1, and ‘chromatin remodellers’, which can also remodel chromatosomes (Figure 4.1).

Interestingly, ACF can assist the histone chaperone NAP-1 in the assembly of H1-containing chromatin, whereas under the same conditions, CHD1 only promotes the assembly of linker histone-free arrays (Lusser et al., 2005). The ability of remodelling factors to incorporate H1 into chromatin may thus correlate with their remodelling efficiencies in the presence of the linker histone.

4.1.2 Limitations of chromatosome remodelling

We were surprised by the efficiency of chromatosome remodelling considering the potential obstacles brought about by the linker histone. First, H1 binding limits the amount of free linker DNA. The length of linker DNA turned out to be an important parameter for the efficiency of ACF-dependent remodelling (Yang et al., 2006). Second, nuclease protection experiments with H1 or ISWI revealed similar sites of interaction with the nucleosome (Strohner et al., 2005; Zofall et al., 2004), so the two proteins are likely to compete for the same binding site on the nucleosome substrate. In addition, H1 restricts the flexibility of the linker DNA and therefore hinders loosening of histone-DNA contacts at the point of entry into the nucleosome, a step required for all remodelling events (Sheng et al., 2006). Finally, the increased compaction of the nucleosome fibre promoted by linker histones might restrict access of remodelling factors towards chromatin, since according to both currently favoured models for the structure of the 30 nm fibre, the linker DNA and hence all points of access for remodelling enzymes are located inside the chromatin fibre (Dorigo et al., 2004; Robinson and Rhodes, 2006). Considering that according to FRAP experiments each H1 molecule is associated with chromatin most of the time (Misteli et al., 2000), one would therefore expect it to counteract ATP-dependent remodelling.

4.1.3 Potential mechanisms of chromosome remodelling

In line with the concerns listed above, the literature so far mostly suggested that linker histones inhibit chromatin remodelling (Hill and Imbalzano, 2000; Horn et al., 2002; Saeki et al., 2005; Varga-Weisz et al., 1995). However, looking carefully at these studies, residual remodelling activity was still observed also in the presence of linker histones. This has largely been attributed to incomplete loading of the substrate with linker histones. We tried to rule out this possibility by tightly controlling the stoichiometric incorporation of linker histones into reconstituted chromatin arrays. Still, ACF and BRG1 could remodel these arrays to a considerable extent.

We wondered why we observed such strong ATP-dependent repositioning of chromosomes. We considered that the H1 we purified from *Drosophila* embryos may carry covalent modifications which could facilitate its mobilization. H1 is highly phosphorylated during mitosis (Sarg et al., 2006) and its hyperphosphorylation interferes with DNA binding (Hill et al., 1991). Along this line, hyperphosphorylation of H5 abolished its ability to inhibit SWI/SNF dependent chromatin remodelling (Horn et al., 2002). However, no extensive phosphorylation was detected by mass-spectrometrical analysis of H1 purified from *Drosophila* embryos (Villar-Garea and Imhof, 2008). We therefore consider it unlikely that phosphorylation influenced the outcome of our experiments. Moreover, the fact that CHD1 was able to remodel chromatin only in the absence, but not in the presence of linker histones emphasized their repressive nature towards remodelling.

Our findings raise the question about the possible mechanism for ATP-dependent chromosome repositioning. Remodelling factors disrupt the interactions between DNA and also other proteins than core histones (Kikyo et al., 2000; Nagaich et al., 2004; Sprouse et al., 2006), so they might transiently displace H1 from the nucleosome. This may be achieved by transiently displacing linker histones to a secondary site on the nucleosome or to an acceptor site on the remodelling factor. *In vivo*, such H1 eviction events may be assisted by H1 chaperones. A candidate for an H1 chaperone is represented by NAP-1, which cooperates with ACF in the assembly of H1-containing chromatin (Lusser et al., 2005). It is conceivable that these two proteins can also

cooperate to catalyse the opposite reaction, H1 disassembly. However, since we did not include a chaperone in our experiment, alternative mechanisms have to be considered.

Chromatosome movements might already be facilitated if only the linker histone's globular domain was temporarily lifted off the nucleosome, while the C-terminal domain remained associated with the linker DNA. Such a scenario is reminiscent of documented changes on H1 interaction due to transcription, where selective cross-linking in *Drosophila* showed that the globular domain but not the C-terminal tail of linker histones was reversibly displaced from chromatin (Nacheva et al., 1989). In agreement with these considerations, the C-terminal tail contributes to the binding of H1 to the nucleosome and strongly affects the residence time of H1 on chromatin (Catez et al., 2006; Hendzel et al., 2004).

The analysis of chromatosome positions by primer extension revealed that in our arrays, H1 protects DNA from nuclease digestion mainly on one side of the nucleosome, suggesting an asymmetrical binding of H1 in agreement with earlier observations (Brown et al., 2006; Zhou et al., 1998). Site-directed DNA crosslinking experiments indicated that also the yeast ATPase ISW2 contacts linker DNA only on one side of the nucleosome (Dang et al., 2006). Moreover, modelling its electron microscopy structure on the nucleosome, Hainfeld and co-workers concluded that hCHRAC may bind to the nucleosome in a similar manner (Hu et al., 2008). On the other hand, footprinting studies of ACF suggested that ACF interacts symmetrically with the nucleosome (Strohner et al., 2005). It is however possible that in the presence of H1, ACF binds only to one side of the nucleosomal entry/exit site. Hence, we hypothesize that ACF binds to DNA at the entry/exit side of the nucleosome on the side not contacted by the globular domain of H1. Loop formation and propagation would then result in movement of the histone octamer and displacement of the globular H1 domain. Subsequently, H1 would relocate to the new entry/exit site of the nucleosome. According to this model, ACF-mediated nucleosome sliding would be unidirectional in the presence of H1. We began to test this hypothesis by subjecting palindromic 601 arrays to remodelling reactions and monitoring nucleosome and chromatosome movements by partial MNase digestion. Although these experiments indicated a slight preference of nucleosomal movements away from the H1-bound side compared to the opposite direction, we could not prove unambiguously that H1 restricted ACF-mediated sliding to one direction. Further

experiments will be necessary to clarify whether sliding is unidirectional in the presence of H1.

4.2 Global linker histone dynamics and chromatin remodelling

4.2.1 Chromatin remodelling in the presence of early linker histone substitutes

Most eukaryotic cells contain approximately one linker histone per nucleosome, but this ratio varies between organisms and cell types. Interestingly, this ratio is higher in transcriptionally inactive cells – e. g. 1.3 in avian erythrocytes – and considerably lower in embryonic cells where chromatin is less compacted than in differentiated cells (Woodcock et al., 2006). Mammalian stem cells contain only 0.5 H1 per nucleosome (Fan et al., 2005), and in early stages of fly and frog development somatic H1 is entirely replaced by HMG-D or by the specialized linker histone B4, respectively, both binding to the nucleosome with a considerably lower affinity than H1 (Dimitrov and Wolffe, 1996; Ner et al., 2001). It is therefore believed that H1 levels may globally define the degree of chromatin plasticity and that H1 generally counteracts chromatin dynamics. In agreement, our assays showed that H1 and even more so H5 antagonize remodelling.

ACF is abundant during early *Drosophila* embryogenesis when chromatin initially does not contain H1, but HMG-D. Similar to H1, HMG-D increases the nucleosomal repeat length (Ner et al., 2001). It has therefore been proposed to serve as a linker histone substitute in early chromatin. However, monitoring DNA accessibility during remodelling by ACF, we did not see any changes in remodelling efficiency upon HMG-D incorporation. Unlike canonical linker histones, HMG-D was “transparent” in our assay. This could be due to the lower affinity of HMG-D towards chromatin. Also, HMG-D-containing nucleosomal arrays may be less compact than those containing H1.

Our results are in line with earlier experiments in *Xenopus*, where H1 but not the early linker histone B4 inhibited ACF-mediated remodelling in dinucleosomes (Saeki et al., 2005). We did not observe facilitation of nucleosome remodelling upon HMG-D binding as previously reported for the closely related HMGB1, which unlike HMG-D

harbours two HMG box domains (Bonaldi et al., 2002). In this study, HMGB1 binding accelerated ACF-dependent mononucleosome sliding, possibly by increasing DNA flexibility. Conversely, HMGB1 inhibited remodelling when the highly acidic C-terminus of HMGB1 was deleted, which is composed of 20 uninterrupted glutamates and aspartates. The deletion mutant exhibits an affinity towards nucleosomes two orders of magnitude higher than the full-length protein, so it might lock the nucleosome and prevent repositioning. The C-terminus of HMG-D also harbours an acidic patch; however, it consists of only ten acidic amino acids interrupted by two serins. This might result in a less dynamic interaction of HMG-D with the nucleosome than HMGB1 and could therefore explain why HMG-D did not enhance nucleosome remodelling in our assay. Alternatively, mononucleosome sliding might represent a more sensitive assay to measure small differences in efficiency. Yet, we can conclude that chromatin is more permissive towards chromatin remodelling if it contains HMG-D instead of H1. This could facilitate formation of compact chromatin domains by ACF/CHRAC during differentiation.

4.2.2 Global changes of linker histone association with chromatin upon depletion of ISWI-complexes

Kadonaga and co-workers showed that *in vitro* ACF assists the incorporation of both core and linker histones into chromatin (Lusser and Kadonaga, 2003) raising the possibility that ACF might act as a linker histone chaperone. We therefore investigated whether *in vivo* the depletion of ACF/CHRAC affected the association of H1 and its early substitute HMG-D with chromatin. For this reason we monitored H1 and HMGD in flies carrying a null allele for *acfl*, the defining subunit of ACF/ CHRAC.

It has been reported previously that ACF1 depletion in flies leads to reduced viability and a less regular chromatin structure with a shorter nucleosome repeat length and it was suggested that CHRAC and/or ACF promote the formation of repressive chromatin structures (Fyodorov et al., 2004). Unexpectedly, we found that both H1 and HMG-D levels were increased in *acfl* flies. This finding may be interpreted in the context of our biochemical results. ACF may be required to control the correct and stoichiometric

incorporation of linker histones under physiological conditions via its proposed chaperone activity. Previous experiments with chromatin assembled by *Drosophila* embryonic extract showed that H1 replaces HMG-D, but at that time could not exclude the presence of additional factors that could assist this reaction (Ner et al., 2001). We now demonstrated that H1 readily binds to and replaces HMG-D from salt-assembled chromatin in a purified system. We showed furthermore that H1 can bind to preassembled chromatin without the assistance of cofactors *in vitro*. H1 and HMG-D could bind to nucleosomal arrays in stoichiometric amounts at the same time. This observation could mean that there are two distinct binding sites for H1 and/or HMG-D on chromatin. Along this line, Travers and colleagues showed that HMG-D binds to chromatin with two distinct affinities, presumably reflecting two distinct binding sites. H1 preferentially displaced HMG-D from its higher affinity site, implying that this might represent the nucleosomal entry/exit site (Ner et al., 2001). Furthermore, they demonstrated a physical interaction between H1 and HMG-D. Accordingly, in our assay, H1 might first displace HMG-D from the entry/exit site of the nucleosome by competition. Additional H1 may then bind to HMG-D and lead to dissociation.

In agreement with the finding that H1 binds chromatin without the help of a chaperone, linker histones freely exchange between DNA and chromatin binding sites without the help of cofactors (Orrego et al., 2007). ACF/CHRAC may therefore be part of a mechanism that regulates this association in order to prevent uncontrolled H1 incorporation. Alternatively, the increase in H1 and HMG-D levels in *acfl* flies might be an attempt to compensate for the reduction of both nucleosome repeat length and chromatin compaction. After all, most homozygous *acfl* flies are not viable and the analysed individuals are escapers that most likely survived because of compensatory mechanisms. It also has to be considered that H1 and HMG-D expression is increased indirectly through the misregulation of other factors.

A different phenotype results from the knock-out of the ATPase ISWI. H1 was found to be absent in the decondensed chromosome structures characteristic of these flies, raising the possibility that it could be required for loading H1 onto chromatin (Corona et al., 2007) (see 1.5.2). This chromosome decondensation was also observed in NURF301 knock-out flies, but not ACF1 knock-out flies, showing that ACF/CHRAC were not involved in this phenotype (Badenhorst et al., 2002). Also in this case,

compensatory and indirect effects must be considered and further studies will be necessary to elucidate the mechanisms behind. Still, these results point at a potential link between linker histone binding to chromatin and ISWI complexes.

4.3 Effectors of linker histone dynamics

4.3.1 Intrinsic properties of linker histones that affect their affinity towards nucleosomes

The observations described above raise the possibility that ATP-dependent remodelling might play a role in controlling the association of linker histones with chromatin. However, it is not clear how the remodelling of linker histone-containing chromatin can be regulated. Reviewing the principles controlling linker histone dynamics might reveal potential functional interactions with ATP-dependent chromatin remodelling.

Although generally speaking nucleosomes are very stable structures, reversible detachments of DNA segments from the octamer surface are observed (Anderson et al., 2002; Li et al., 2005; Poirier et al., 2008). This dynamic nature of histone DNA interactions may be prerequisite for ATP-dependent remodelling. In analogy, the ability to remodel linker histone-containing chromatin is likely to be influenced by the intrinsic affinity of linker histones, which can differ between H1 variants.

Different subtypes of H1 are found in many organisms (see 1.2.2). The affinities of these variants for chromatin differ considerably. In rat, the somatic variant H1d, exhibits a 19 fold higher affinity than H1a, another somatic variant (Orrego et al., 2007). Accordingly, variants exhibit different degrees of mobility *in vivo*, as revealed by FRAP experiments in human cells (Th'ng et al., 2005). These differences in affinities may account for the observed distinct effects of these variants on gene expression and chromatin structure (Alami et al., 2003; Gunjan et al., 1999) and may also affect ATP-dependent remodelling.

An extreme example for how a linker histone variant controls chromatin condensation is provided by H5 (see 1.2.2). In our assay, H5, which binds to chromatin with higher affinity than somatic H1, inhibited chromatin remodelling to a larger degree than H1, but not entirely. Conversely, the early linker histone substitute in *Drosophila* HMG-D, which binds to chromatin ten times weaker than somatic H1 (Ner et al., 2001), did not decrease remodelling efficiency.

4.3.2 Posttranslational modifications of linker histones

Nucleosome remodelling can be affected by posttranslational modifications of core histones. Histone modifications might influence remodelling directly, e. g. by changing the affinity of the nucleosome to remodelling factors or indirectly by alterations in fibre folding. For instance, as already mentioned (see 1.3 and 1.4.4), acetylation of histone H4 on lysine 16 (H4K16) counteracts both chromatin condensation and ISWI-dependent remodelling (Corona et al., 2002; Shogren-Knaak et al., 2006). Linker histones have been found to be phosphorylated, methylated, acetylated, ubiquitinated and formylated (Wisniewski et al., 2007), the best characterized modification being their C-terminal phosphorylation. Phosphorylated linker histones are associated to mitotic chromosomes and concomitantly, overall phosphorylation increases during mitosis (Zlatanova et al., 2000). In addition, phosphorylation of linker histones regulates transcription and reduces their affinity to chromatin (Catez et al., 2006; Dou et al., 1999). This is reflected by the fact that phosphorylation of linker histone releases their inhibitory effect on chromatin remodelling (Horn et al., 2002). Expression of point mutants mimicking a constitutively phosphorylated state counteracts differentiation of murine erythroleukemia (MEL) cells in spite of representing only one fifth of total H1 amounts. Moreover, in these cells, not only the mutant H1, but also endogenous H1 exhibited an increased mobility. This means that a mutation that disrupts the C-terminal interaction of H1 with the linker DNA affects chromatin structure not only locally by reducing the affinity of the mutant protein to the nucleosome but also influences folding globally and thereby alters the binding properties of wild-type histones (Yellajoshyula and Brown, 2006). The observation that H1 variants exhibit differences in their modification patterns adds another level of

complexity for regulating their binding to chromatin (Wisniewski et al., 2007). In addition, H1 modifications may integrate the linker histone into the network of heterochromatin formation. Along this line, H1K26 methylation is recognized by heterochromatin protein 1 (HP1) whereas phosphorylation on K27 prevents this interaction (Daujat et al., 2005).

Local and global interactions of H1 are not only influenced by modifications of the linker histone itself but also by the modification status of the nucleosomes it associates with. In FRAP experiments, the residence time of H1 on chromatin decreased considerably upon addition of the histone deacetylase inhibitor TSA (Misteli et al., 2000). However, the non-specific effect of this general drug does not exclude the possibility that H1 itself or other factors could be hyperacetylated and contribute to the elevated H1 mobility. Vaquero and colleagues exemplified how chromatin structure can be jointly regulated by core and linker histone modifications (Vaquero et al., 2006). They showed that the human HDAC SirT1 promotes the formation of facultative heterochromatin by binding and recruiting H1 and by deacetylation of H1K27, H3K9 and H4K16. This supports the idea that chromatin fibre folding requires both global histone deacetylation and H1 incorporation. H1 occupancy can also be regulated via histone modifications very locally. This is illustrated by a recent study demonstrating that the stepwise histone acetylation and H2A deubiquitination facilitated H1 dissociation from the promoters of androgen receptor-regulated genes and increased their transcription (Zhu et al., 2007).

4.3.3 Linker histone chaperones

In contrast to nucleosome repositioning, which is catalysed by remodelling enzymes alone, histone deposition and eviction usually depends on the assistance of chaperones acting as histone donors or acceptors (Loyola and Almouzni, 2004; Tyler, 2002; Workman, 2006). For example, as stated above, CHD1 or ACF can assemble chromatin in concert with the well-known histone chaperone NAP-1 *in vitro* (Lusser et al., 2005). NAP-1 can also promote nucleosome disassembly in cooperation with the yeast remodelling factor RSC (Lorch et al., 2006). The histone chaperone nucleoplasmin, on

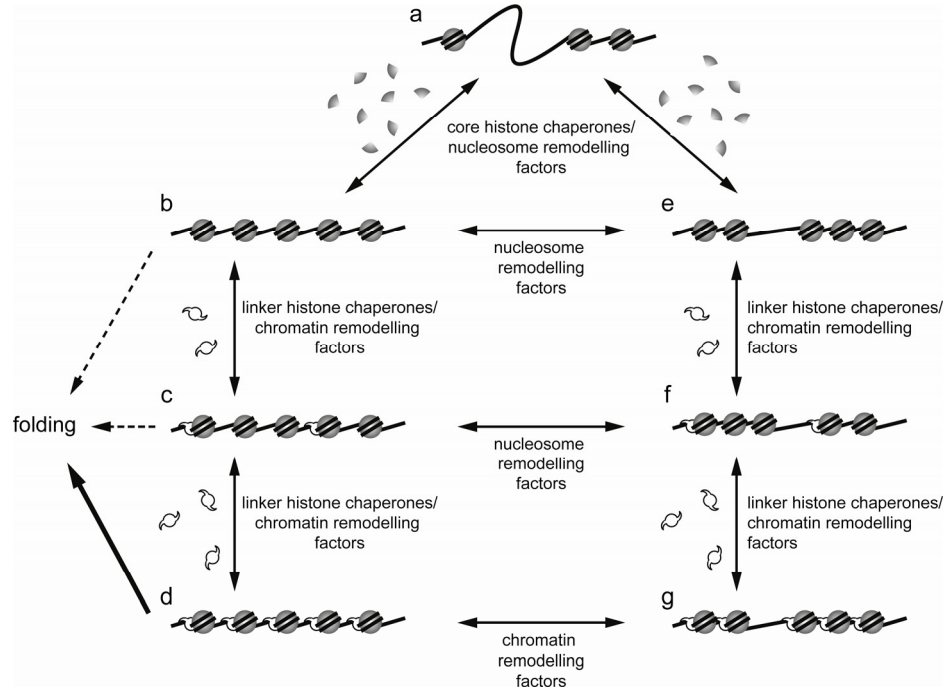


Figure 4.1: Interconversion of chromatin states through the interplay of core and linker histone chaperones and ATP-dependent remodelling factors.

The scenarios describe states of chromatin that differ in the regularity of the chromatin fibre and in core and linker histone stoichiometry. Spheres depict histone octamers around which the DNA (black line) is wound to form nucleosomes. Linker histones are represented in white. (a) Nucleosome fibre containing a nucleosome-free gap; (b) regularly spaced nucleosome array; (c) regularly spaced nucleosome array containing substoichiometric levels of H1; (d) regularly spaced nucleosome array with saturating linker histone levels; (e) irregularly spaced nucleosome array that may arise after nucleosome assembly or if a nucleosome-free region is generated by nucleosome sliding; (f) nucleosome array containing substoichiometric levels of H1, where the nucleosome devoid of H1 have been selectively moved; (g) irregularly spaced nucleosome arrays that may arise when nucleosomes are moved on DNA. Histone chaperones and ATP-dependent remodelling factors can act in concert to assemble core and linker histones onto DNA (a to e). Binding linker histones allows remodelling by chromatin remodelling factors but not nucleosome remodelling factors (b, d, e, g). If present in substoichiometric amounts, linker histones may determine which nucleosomes are repositioned preferentially. Sliding may also be directional in the presence of H1 (c, f).

the other hand, can facilitate nucleosome mobilization by SWI/SNF and ACF *in vitro* (Angelov et al., 2006).

Similarly, linker histone chaperones may contribute to regulate H1 dynamics. To date, the *in vitro* assembly of H1-containing chromatin arrays by ACF and NAP-1 represents the only reported cooperation of a histone chaperone and a remodelling enzyme in the context of H1-chromatin interactions (Figure 4.1a-d) (Lusser et al., 2005). The histone chaperone NAP-1 can both load H1 onto and evict H1 from chromatin fibres *in vitro* (Kepert et al., 2005; Mazurkiewicz et al., 2006). A number of other H1 binding proteins have been found to be involved in H1 deposition or eviction (Figure 4.1b, c, d). Nucleoplasmin, an abundant nuclear protein in *Xenopus* oocytes, removes somatic linker histone variants from chromatin and thereby facilitates transcription *in vitro* (Dimitrov and Wolffe, 1996). The opposite function, H1 assembly, might be fulfilled by the nuclear autoantigenic sperm protein (NASP). Since this protein binds to H1 and deposits it onto free DNA *in vitro*, it might also serve as an H1 assembly factor (Alekseev et al., 2003). NASP is essential for cell proliferation and normal development *in vivo*. It has therefore been suggested that H1 is involved in controlling chromatin assembly after cell division (Richardson et al., 2006). Presumably more subtle functions in controlling H1 interaction with chromatin are accomplished by prothymosin α and parathymosin. Both bind to H1 *in vitro* and *in vivo* and restrict the association of H1 with chromatin *in vitro*. (Karetsou et al., 1998; Martic et al., 2005). However, proper definition of an H1 chaperone may require isolation of a complex.

Taken together, the same principles that govern core histone dynamics – intrinsic affinity, variant properties, modification status and chaperone interactions – may also control the association of linker histones with chromatin and hence increase the regulatory complexity.

4.4 Outlook

In this study, we analysed the influence of linker histones and their early substitute HMG-D on ATP-dependent chromatin remodelling. The results give insight into how chromatin remodelling works in the context of higher order chromatin structures. Moreover, our *in vitro* assays can now be used to elucidate the contribution of individual proteins domains, for instance the PHD fingers and the bromodomain of ACF1, to higher-order chromatin structure remodelling. The assays presents also valuable tools to investigate how further factors like histone modifications, chromatin binding proteins (e. g. HP1) and histone variants affect chromatin remodelling. In contrast to remodelling assays using mononucleosomes, our assays will also reveal effects resulting from differences in chromatin folding.

In addition, our data suggested that ACF-mediated repositioning in the presence of H1 might be unidirectional. This represents an interesting concept, because it would mean that linker histones influence nucleosomal positions.

We also monitored exchange of HMG-D by H1 and showed that H1 and HMG-D incorporation is globally affected by the absence of ACF1. Further experiments will be necessary to reveal by which mechanism ACF1 complexes affect H1 association with chromatin.

5. References

- Alami, R., Fan, Y., Pack, S., Sonbuchner, T.M., Besse, A., Lin, Q., Grealley, J.M., Skoultchi, A.I., and Bouhassira, E.E. (2003). Mammalian linker-histone subtypes differentially affect gene expression in vivo. *Proceedings of the National Academy of Sciences of the United States of America* *100*, 5920-5925.
- Alekseev, O.M., Bencic, D.C., Richardson, R.T., Widgren, E.E., and O'Rand, M.G. (2003). Overexpression of the Linker histone-binding protein tNASP affects progression through the cell cycle. *J Biol Chem* *278*, 8846-8852.
- Allis, C.D., Jenuwein, T., and Reinberg, D. (2007). *Epigenetics* (Cold Spring Harbor, New York, Cold Spring Harbor Laboratory Press).
- Anderson, J.D., Thastrom, A., and Widom, J. (2002). Spontaneous access of proteins to buried nucleosomal DNA target sites occurs via a mechanism that is distinct from nucleosome translocation. *Molecular and cellular biology* *22*, 7147-7157.
- Angelov, D., Bondarenko, V.A., Almagro, S., Menoni, H., Mongelard, F., Hans, F., Mietton, F., Studitsky, V.M., Hamiche, A., Dimitrov, S., *et al.* (2006). Nucleolin is a histone chaperone with FACT-like activity and assists remodeling of nucleosomes. *Embo J* *25*, 1669-1679.
- Ausio, J. (2006). Histone variants--the structure behind the function. *Briefings in functional genomics & proteomics* *5*, 228-243.
- Badenhorst, P., Voas, M., Rebay, I., and Wu, C. (2002). Biological functions of the ISWI chromatin remodeling complex NURF. *Genes Dev* *16*, 3186-3198.
- Baker, L.A., Allis, C.D., and Wang, G.G. (2008). PHD fingers in human diseases: Disorders arising from misinterpreting epigenetic marks. *Mutat Res* *647*, 3-12.
- Bao, Y., and Shen, X. (2007). SnapShot: chromatin remodeling complexes. *Cell* *129*, 632.
- Becker, P.B., and Horz, W. (2002). ATP-dependent nucleosome remodeling. *Annu Rev Biochem* *71*, 247-273.
- Becker, P.B., Tsukiyama, T., and Wu, C. (1994). Chromatin assembly extracts from *Drosophila* embryos. *Methods Cell Biol* *44*, 207-223.
- Bednar, J., Horowitz, R.A., Grigoryev, S.A., Carruthers, L.M., Hansen, J.C., Koster, A.J., and Woodcock, C.L. (1998). Nucleosomes, linker DNA, and linker histone form a unique structural motif that directs the higher-order folding and compaction of chromatin. *Proceedings of the National Academy of Sciences of the United States of America* *95*, 14173-14178.
- Bernstein, B.E., Meissner, A., and Lander, E.S. (2007). The mammalian epigenome. *Cell* *128*, 669-681.
- Bird, A. (2002). DNA methylation patterns and epigenetic memory. *Genes Dev* *16*, 6-21.

- Bode, J., Goetze, S., Heng, H., Krawetz, S.A., and Benham, C. (2003). From DNA structure to gene expression: mediators of nuclear compartmentalization and dynamics. *Chromosome Res* *11*, 435-445.
- Bonaldi, T., Langst, G., Strohner, R., Becker, P.B., and Bianchi, M.E. (2002). The DNA chaperone HMGB1 facilitates ACF/CHRAC-dependent nucleosome sliding. *Embo J* *21*, 6865-6873.
- Bönisch, C., Nieratschker, S.M., Orfanos, N.K., and Hake, S.B. (2008). Chromatin proteomics and epigenetic regulatory circuits. *Expert Rev Proteomics* *5*, 105-119.
- Boyer, L.A., Logie, C., Bonte, E., Becker, P.B., Wade, P.A., Wolffe, A.P., Wu, C., Imbalzano, A.N., and Peterson, C.L. (2000). Functional delineation of three groups of the ATP-dependent family of chromatin remodeling enzymes. *J Biol Chem* *275*, 18864-18870.
- Brown, D.T., Izard, T., and Misteli, T. (2006). Mapping the interaction surface of linker histone H1(0) with the nucleosome of native chromatin in vivo. *Nat Struct Mol Biol* *13*, 250-255.
- Bustin, M., Catez, F., and Lim, J.H. (2005). The dynamics of histone H1 function in chromatin. *Mol Cell* *17*, 617-620.
- Cairns, B.R. (2007). Chromatin remodeling: insights and intrigue from single-molecule studies. *Nat Struct Mol Biol* *14*, 989-996.
- Catez, F., Ueda, T., and Bustin, M. (2006). Determinants of histone H1 mobility and chromatin binding in living cells. *Nat Struct Mol Biol* *13*, 305-310.
- Clapier, C.R., Nightingale, K.P., and Becker, P.B. (2002). A critical epitope for substrate recognition by the nucleosome remodeling ATPase ISWI. *Nucleic Acids Res* *30*, 649-655.
- Clark, D.J., and Kimura, T. (1990). Electrostatic mechanism of chromatin folding. *J Mol Biol* *211*, 883-896.
- Cockell, M., Rhodes, D., and Klug, A. (1983). Location of the primary sites of micrococcal nuclease cleavage on the nucleosome core. *J Mol Biol* *170*, 423-446.
- Corona, D.F., Clapier, C.R., Becker, P.B., and Tamkun, J.W. (2002). Modulation of ISWI function by site-specific histone acetylation. *EMBO Rep* *3*, 242-247.
- Corona, D.F., Langst, G., Clapier, C.R., Bonte, E.J., Ferrari, S., Tamkun, J.W., and Becker, P.B. (1999). ISWI is an ATP-dependent nucleosome remodeling factor. *Mol Cell* *3*, 239-245.
- Corona, D.F., Siriaco, G., Armstrong, J.A., Snarskaya, N., McClymont, S.A., Scott, M.P., and Tamkun, J.W. (2007). ISWI regulates higher-order chromatin structure and histone H1 assembly in vivo. *PLoS Biol* *5*, e232.
- Cosgrove, M.S., Boeke, J.D., and Wolberger, C. (2004). Regulated nucleosome mobility and the histone code. *Nat Struct Mol Biol* *11*, 1037-1043.

- Croston, G.E., Lira, L.M., and Kadonaga, J.T. (1991). A general method for purification of H1 histones that are active for repression of basal RNA polymerase II transcription. *Protein Expr Purif* 2, 162-169.
- Dalal, Y., Furuyama, T., Vermaak, D., and Henikoff, S. (2007). Structure, dynamics, and evolution of centromeric nucleosomes. *Proceedings of the National Academy of Sciences of the United States of America* 104, 15974-15981.
- Dang, W., Kagalwala, M.N., and Bartholomew, B. (2006). Regulation of ISW2 by concerted action of histone H4 tail and extranucleosomal DNA. *Molecular and cellular biology* 26, 7388-7396.
- Daujat, S., Zeissler, U., Waldmann, T., Happel, N., and Schneider, R. (2005). HP1 binds specifically to Lys26-methylated histone H1.4, whereas simultaneous Ser27 phosphorylation blocks HP1 binding. *J Biol Chem* 280, 38090-38095.
- Davey, C.A., Sargent, D.F., Luger, K., Maeder, A.W., and Richmond, T.J. (2002). Solvent mediated interactions in the structure of the nucleosome core particle at 1.9 Å resolution. *J Mol Biol* 319, 1097-1113.
- Deuring, R., Fanti, L., Armstrong, J.A., Sarte, M., Papoulas, O., Prestel, M., Daubresse, G., Verardo, M., Moseley, S.L., Berloco, M., *et al.* (2000). The ISWI chromatin-remodeling protein is required for gene expression and the maintenance of higher order chromatin structure in vivo. *Mol Cell* 5, 355-365.
- Dimitrov, S., and Wolffe, A.P. (1996). Remodeling somatic nuclei in *Xenopus laevis* egg extracts: molecular mechanisms for the selective release of histones H1 and H1(0) from chromatin and the acquisition of transcriptional competence. *Embo J* 15, 5897-5906.
- Dong, F., Hansen, J.C., and van Holde, K.E. (1990). DNA and protein determinants of nucleosome positioning on sea urchin 5S rRNA gene sequences in vitro. *Proceedings of the National Academy of Sciences of the United States of America* 87, 5724-5728.
- Dorigo, B., Schalch, T., Bystricky, K., and Richmond, T.J. (2003). Chromatin fiber folding: requirement for the histone H4 N-terminal tail. *J Mol Biol* 327, 85-96.
- Dorigo, B., Schalch, T., Kulangara, A., Duda, S., Schroeder, R.R., and Richmond, T.J. (2004). Nucleosome arrays reveal the two-start organization of the chromatin fiber. *Science* 306, 1571-1573.
- Dou, Y., Mizzen, C.A., Abrams, M., Allis, C.D., and Gorovskiy, M.A. (1999). Phosphorylation of linker histone H1 regulates gene expression in vivo by mimicking H1 removal. *Mol Cell* 4, 641-647.
- Du, J., Nasir, I., Benton, B.K., Kladdé, M.P., and Laurent, B.C. (1998). Sth1p, a *Saccharomyces cerevisiae* Snf2p/Swi2p homolog, is an essential ATPase in RSC and differs from Snf/Swi in its interactions with histones and chromatin-associated proteins. *Genetics* 150, 987-1005.
- Eberharter, A., and Becker, P.B. (2004). ATP-dependent nucleosome remodelling: factors and functions. *J Cell Sci* 117, 3707-3711.

- Eberharter, A., Ferrari, S., Langst, G., Straub, T., Imhof, A., Varga-Weisz, P., Wilm, M., and Becker, P.B. (2001). Acf1, the largest subunit of CHRAC, regulates ISWI-induced nucleosome remodelling. *Embo J* *20*, 3781-3788.
- Eberharter, A., Langst, G., and Becker, P.B. (2004a). A nucleosome sliding assay for chromatin remodeling factors. *Methods Enzymol* *377*, 344-353.
- Eberharter, A., Vetter, I., Ferreira, R., and Becker, P.B. (2004b). ACF1 improves the effectiveness of nucleosome mobilization by ISWI through PHD-histone contacts. *Embo J* *23*, 4029-4039.
- Fan, H.Y., He, X., Kingston, R.E., and Narlikar, G.J. (2003a). Distinct strategies to make nucleosomal DNA accessible. *Mol Cell* *11*, 1311-1322.
- Fan, L., and Roberts, V.A. (2006). Complex of linker histone H5 with the nucleosome and its implications for chromatin packing. *Proceedings of the National Academy of Sciences of the United States of America* *103*, 8384-8389.
- Fan, Y., Nikitina, T., Morin-Kensicki, E.M., Zhao, J., Magnuson, T.R., Woodcock, C.L., and Skoultschi, A.I. (2003b). H1 linker histones are essential for mouse development and affect nucleosome spacing in vivo. *Molecular and cellular biology* *23*, 4559-4572.
- Fan, Y., Nikitina, T., Zhao, J., Fleury, T.J., Bhattacharyya, R., Bouhassira, E.E., Stein, A., Woodcock, C.L., and Skoultschi, A.I. (2005). Histone H1 depletion in mammals alters global chromatin structure but causes specific changes in gene regulation. *Cell* *123*, 1199-1212.
- Fan, Y., Sirotkin, A., Russell, R.G., Ayala, J., and Skoultschi, A.I. (2001). Individual somatic H1 subtypes are dispensable for mouse development even in mice lacking the H1(0) replacement subtype. *Molecular and cellular biology* *21*, 7933-7943.
- Felsenfeld, G., and Groudine, M. (2003). Controlling the double helix. *Nature* *421*, 448-453.
- Ferreira, R., Eberharter, A., Bonaldi, T., Chioda, M., Imhof, A., and Becker, P.B. (2007). Site-specific acetylation of ISWI by GCN5. *BMC Mol Biol* *8*, 73.
- Flaus, A., and Owen-Hughes, T. (2004). Mechanisms for ATP-dependent chromatin remodelling: farewell to the tuna-can octamer? *Curr Opin Genet Dev* *14*, 165-173.
- Foe, V.E., and Alberts, B.M. (1983). Studies of nuclear and cytoplasmic behaviour during the five mitotic cycles that precede gastrulation in *Drosophila* embryogenesis. *J Cell Sci* *61*, 31-70.
- Fuks, F. (2005). DNA methylation and histone modifications: teaming up to silence genes. *Curr Opin Genet Dev* *15*, 490-495.
- Fyodorov, D.V., Blower, M.D., Karpen, G.H., and Kadonaga, J.T. (2004). Acf1 confers unique activities to ACF/CHRAC and promotes the formation rather than disruption of chromatin in vivo. *Genes Dev* *18*, 170-183.
- Gangaraju, V.K., and Bartholomew, B. (2007). Mechanisms of ATP dependent chromatin remodeling. *Mutat Res* *618*, 3-17.

- Garcia-Dominguez, M., March-Diaz, R., and Reyes, J.C. (2008). The PHD domain of plant PIAS proteins mediates sumoylation of bromodomain GTE proteins. *J Biol Chem* *283*, 21469-21477.
- Gelbart, M.E., Rechsteiner, T., Richmond, T.J., and Tsukiyama, T. (2001). Interactions of Isw2 chromatin remodeling complex with nucleosomal arrays: analyses using recombinant yeast histones and immobilized templates. *Molecular and cellular biology* *21*, 2098-2106.
- Gilfillan, G.D., Straub, T., de Wit, E., Greil, F., Lamm, R., van Steensel, B., and Becker, P.B. (2006). Chromosome-wide gene-specific targeting of the *Drosophila* dosage compensation complex. *Genes Dev* *20*, 858-870.
- Gowher, H., Leismann, O., and Jeltsch, A. (2000). DNA of *Drosophila melanogaster* contains 5-methylcytosine. *Embo J* *19*, 6918-6923.
- Grune, T., Brzeski, J., Eberharter, A., Clapier, C.R., Corona, D.F., Becker, P.B., and Muller, C.W. (2003). Crystal structure and functional analysis of a nucleosome recognition module of the remodeling factor ISWI. *Mol Cell* *12*, 449-460.
- Gunjan, A., Alexander, B.T., Sittman, D.B., and Brown, D.T. (1999). Effects of H1 histone variant overexpression on chromatin structure. *J Biol Chem* *274*, 37950-37956.
- Hake, S.B., and Allis, C.D. (2006). Histone H3 variants and their potential role in indexing mammalian genomes: the "H3 barcode hypothesis". *Proceedings of the National Academy of Sciences of the United States of America* *103*, 6428-6435.
- Hanai, K., Furuhashi, H., Yamamoto, T., Akasaka, K., and Hirose, S. (2008). RSF governs silent chromatin formation via histone H2Av replacement. *PLoS Genet* *4*, e1000011.
- Hartlepp, K.F., Fernandez-Tornero, C., Eberharter, A., Grune, T., Muller, C.W., and Becker, P.B. (2005). The histone fold subunits of *Drosophila* CHRAC facilitate nucleosome sliding through dynamic DNA interactions. *Molecular and cellular biology* *25*, 9886-9896.
- Hassan, A.H., Neely, K.E., and Workman, J.L. (2001). Histone acetyltransferase complexes stabilize swi/snf binding to promoter nucleosomes. *Cell* *104*, 817-827.
- Heberlein, U., and Tjian, R. (1988). Temporal pattern of alcohol dehydrogenase gene transcription reproduced by *Drosophila* stage-specific embryonic extracts. *Nature* *331*, 410-415.
- Hendrich, B., and Bird, A. (1998). Identification and characterization of a family of mammalian methyl-CpG binding proteins. *Molecular and cellular biology* *18*, 6538-6547.
- Hendzel, M.J., Lever, M.A., Crawford, E., and Th'ng, J.P. (2004). The C-terminal domain is the primary determinant of histone H1 binding to chromatin in vivo. *J Biol Chem* *279*, 20028-20034.
- Hill, C.S., Rimmer, J.M., Green, B.N., Finch, J.T., and Thomas, J.O. (1991). Histone-DNA interactions and their modulation by phosphorylation of -Ser-Pro-X-Lys/Arg- motifs. *Embo J* *10*, 1939-1948.

- Hill, D.A., and Imbalzano, A.N. (2000). Human SWI/SNF nucleosome remodeling activity is partially inhibited by linker histone H1. *Biochemistry* *39*, 11649-11656.
- Holstege, F.C., Jennings, E.G., Wyrick, J.J., Lee, T.I., Hengartner, C.J., Green, M.R., Golub, T.R., Lander, E.S., and Young, R.A. (1998). Dissecting the regulatory circuitry of a eukaryotic genome. *Cell* *95*, 717-728.
- Horn, P.J., Carruthers, L.M., Logie, C., Hill, D.A., Solomon, M.J., Wade, P.A., Imbalzano, A.N., Hansen, J.C., and Peterson, C.L. (2002). Phosphorylation of linker histones regulates ATP-dependent chromatin remodeling enzymes. *Nat Struct Biol* *9*, 263-267.
- Horowitz, R.A., Agard, D.A., Sedat, J.W., and Woodcock, C.L. (1994). The three-dimensional architecture of chromatin in situ: electron tomography reveals fibers composed of a continuously variable zig-zag nucleosomal ribbon. *J Cell Biol* *125*, 1-10.
- Hu, M., Zhang, Y.B., Qian, L., Brinas, R.P., Kuznetsova, L., and Hainfeld, J.F. (2008). Three-dimensional structure of human chromatin accessibility complex hCHRAC by electron microscopy. *J Struct Biol* *164*, 263-269.
- Huynh, V.A., Robinson, P.J., and Rhodes, D. (2005). A method for the in vitro reconstitution of a defined "30 nm" chromatin fibre containing stoichiometric amounts of the linker histone. *J Mol Biol* *345*, 957-968.
- Ito, T., Bulger, M., Pazin, M.J., Kobayashi, R., and Kadonaga, J.T. (1997). ACF, an ISWI-containing and ATP-utilizing chromatin assembly and remodeling factor. *Cell* *90*, 145-155.
- Ito, T., Levenstein, M.E., Fyodorov, D.V., Kutach, A.K., Kobayashi, R., and Kadonaga, J.T. (1999). ACF consists of two subunits, Acf1 and ISWI, that function cooperatively in the ATP-dependent catalysis of chromatin assembly. *Genes Dev* *13*, 1529-1539.
- Ivanov, A.V., Peng, H., Yurchenko, V., Yap, K.L., Negorev, D.G., Schultz, D.C., Psulkowski, E., Fredericks, W.J., White, D.E., Maul, G.G., *et al.* (2007). PHD domain-mediated E3 ligase activity directs intramolecular sumoylation of an adjacent bromodomain required for gene silencing. *Mol Cell* *28*, 823-837.
- Izzo, A., Kamieniarz, K., and Schneider, R. (2008). The histone H1 family: specific members, specific functions? *Biol Chem* *389*, 333-343.
- Jaskelioff, M., Van Komen, S., Krebs, J.E., Sung, P., and Peterson, C.L. (2003). Rad54p is a chromatin remodeling enzyme required for heteroduplex DNA joint formation with chromatin. *J Biol Chem* *278*, 9212-9218.
- Jones, D.N., Searles, M.A., Shaw, G.L., Churchill, M.E., Ner, S.S., Keeler, J., Travers, A.A., and Neuhaus, D. (1994). The solution structure and dynamics of the DNA-binding domain of HMG-D from *Drosophila melanogaster*. *Structure* *2*, 609-627.
- Kagalwala, M.N., Glaus, B.J., Dang, W., Zofall, M., and Bartholomew, B. (2004). Topography of the ISW2-nucleosome complex: insights into nucleosome spacing and chromatin remodeling. *Embo J* *23*, 2092-2104.

- Karetsov, Z., Sandaltzopoulos, R., Frangou-Lazaridis, M., Lai, C.Y., Tsolas, O., Becker, P.B., and Papamarcaki, T. (1998). Prothymosin alpha modulates the interaction of histone H1 with chromatin. *Nucleic Acids Res* 26, 3111-3118.
- Kepert, J.F., Mazurkiewicz, J., Heuvelman, G.L., Toth, K.F., and Rippe, K. (2005). NAP1 modulates binding of linker histone H1 to chromatin and induces an extended chromatin fiber conformation. *J Biol Chem* 280, 34063-34072.
- Kikyo, N., Wade, P.A., Guschin, D., Ge, H., and Wolffe, A.P. (2000). Active remodeling of somatic nuclei in egg cytoplasm by the nucleosomal ATPase ISWI. *Science* 289, 2360-2362.
- Konev, A.Y., Tribus, M., Park, S.Y., Podhraski, V., Lim, C.Y., Emelyanov, A.V., Vershilova, E., Pirrotta, V., Kadonaga, J.T., Lusser, A., *et al.* (2007). CHD1 motor protein is required for deposition of histone variant H3.3 into chromatin in vivo. *Science* 317, 1087-1090.
- Langst, G., and Becker, P.B. (2004). Nucleosome remodeling: one mechanism, many phenomena? *Biochim Biophys Acta* 1677, 58-63.
- Li, B., Carey, M., and Workman, J.L. (2007). The role of chromatin during transcription. *Cell* 128, 707-719.
- Li, G., Levitus, M., Bustamante, C., and Widom, J. (2005). Rapid spontaneous accessibility of nucleosomal DNA. *Nat Struct Mol Biol* 12, 46-53.
- Lorch, Y., Maier-Davis, B., and Kornberg, R.D. (2006). Chromatin remodeling by nucleosome disassembly in vitro. *Proceedings of the National Academy of Sciences of the United States of America* 103, 3090-3093.
- Lowary, P.T., and Widom, J. (1998). New DNA sequence rules for high affinity binding to histone octamer and sequence-directed nucleosome positioning. *J Mol Biol* 276, 19-42.
- Loyola, A., and Almouzni, G. (2004). Histone chaperones, a supporting role in the limelight. *Biochim Biophys Acta* 1677, 3-11.
- Luger, K., Rechsteiner, T.J., Flaus, A.J., Waye, M.M., and Richmond, T.J. (1997). Characterization of nucleosome core particles containing histone proteins made in bacteria. *J Mol Biol* 272, 301-311.
- Lusser, A., and Kadonaga, J.T. (2003). Chromatin remodeling by ATP-dependent molecular machines. *Bioessays* 25, 1192-1200.
- Lusser, A., and Kadonaga, J.T. (2004). Strategies for the reconstitution of chromatin. *Nat Methods* 1, 19-26.
- Lusser, A., Urwin, D.L., and Kadonaga, J.T. (2005). Distinct activities of CHD1 and ACF in ATP-dependent chromatin assembly. *Nat Struct Mol Biol* 12, 160-166.
- Lyko, F., Ramsahoye, B.H., and Jaenisch, R. (2000). DNA methylation in *Drosophila melanogaster*. *Nature* 408, 538-540.

- Maier, V.K., Chioda, M., Rhodes, D., and Becker, P.B. (2008). ACF catalyses chromatosome movements in chromatin fibres. *Embo J* 27, 817-26
- Marmorstein, R., and Berger, S.L. (2001). Structure and function of bromodomains in chromatin-regulating complexes. *Gene* 272, 1-9.
- Martic, G., Karetsov, Z., Kefala, K., Politou, A.S., Clapier, C.R., Straub, T., and Papamarcaki, T. (2005). Parathymosin affects the binding of linker histone H1 to nucleosomes and remodels chromatin structure. *J Biol Chem* 280, 16143-16150.
- Mazurkiewicz, J., Kepert, J.F., and Rippe, K. (2006). On the mechanism of nucleosome assembly by histone chaperone NAP1. *J Biol Chem* 281, 16462-16472.
- Mellor, J., and Morillon, A. (2004). ISWI complexes in *Saccharomyces cerevisiae*. *Biochim Biophys Acta* 1677, 100-112.
- Misteli, T., Gunjan, A., Hock, R., Bustin, M., and Brown, D.T. (2000). Dynamic binding of histone H1 to chromatin in living cells. *Nature* 408, 877-881.
- Mizuguchi, G., Shen, X., Landry, J., Wu, W.H., Sen, S., and Wu, C. (2004). ATP-driven exchange of histone H2AZ variant catalyzed by SWR1 chromatin remodeling complex. *Science* 303, 343-348.
- Mizuguchi, G., Tsukiyama, T., Wisniewski, J., and Wu, C. (1997). Role of nucleosome remodeling factor NURF in transcriptional activation of chromatin. *Mol Cell* 1, 141-150.
- Mohrmann, L., and Verrijzer, C.P. (2005). Composition and functional specificity of SWI2/SNF2 class chromatin remodeling complexes. *Biochim Biophys Acta* 1681, 59-73.
- Morales, V., Straub, T., Neumann, M.F., Mengus, G., Akhtar, A., and Becker, P.B. (2004). Functional integration of the histone acetyltransferase MOF into the dosage compensation complex. *Embo J* 23, 2258-2268.
- Morrison, A.J., Highland, J., Krogan, N.J., Arbel-Eden, A., Greenblatt, J.F., Haber, J.E., and Shen, X. (2004). INO80 and gamma-H2AX interaction links ATP-dependent chromatin remodeling to DNA damage repair. *Cell* 119, 767-775.
- Nacheva, G.A., Guschin, D.Y., Preobrazhenskaya, O.V., Karpov, V.L., Ebralidse, K.K., and Mirzabekov, A.D. (1989). Change in the pattern of histone binding to DNA upon transcriptional activation. *Cell* 58, 27-36.
- Nagaich, A.K., Walker, D.A., Wolford, R., and Hager, G.L. (2004). Rapid periodic binding and displacement of the glucocorticoid receptor during chromatin remodeling. *Mol Cell* 14, 163-174.
- Nagl, N.G., Jr., Wang, X., Patsialou, A., Van Scoy, M., and Moran, E. (2007). Distinct mammalian SWI/SNF chromatin remodeling complexes with opposing roles in cell-cycle control. *Embo J* 26, 752-763.
- Ner, S.S., Blank, T., Perez-Paralle, M.L., Grigliatti, T.A., Becker, P.B., and Travers, A.A. (2001). HMG-D and histone H1 interplay during chromatin assembly and early embryogenesis. *J Biol Chem* 276, 37569-37576.

- Ner, S.S., and Travers, A.A. (1994). HMG-D, the *Drosophila melanogaster* homologue of HMG 1 protein, is associated with early embryonic chromatin in the absence of histone H1. *Embo J* *13*, 1817-1822.
- Nightingale, K., Dimitrov, S., Reeves, R., and Wolffe, A.P. (1996). Evidence for a shared structural role for HMG1 and linker histones B4 and H1 in organizing chromatin. *Embo J* *15*, 548-561.
- Orrego, M., Ponte, I., Roque, A., Buschati, N., Mora, X., and Suau, P. (2007). Differential affinity of mammalian histone H1 somatic subtypes for DNA and chromatin. *BMC Biol* *5*, 22.
- Patterson, H.G., Landel, C.C., Landsman, D., Peterson, C.L., and Simpson, R.T. (1998). The biochemical and phenotypic characterization of Hho1p, the putative linker histone H1 of *Saccharomyces cerevisiae*. *J Biol Chem* *273*, 7268-7276.
- Pennings, S., Meersseman, G., and Bradbury, E.M. (1994). Linker histones H1 and H5 prevent the mobility of positioned nucleosomes. *Proceedings of the National Academy of Sciences of the United States of America* *91*, 10275-10279.
- Peterson, C.L., and Herskowitz, I. (1992). Characterization of the yeast SWI1, SWI2, and SWI3 genes, which encode a global activator of transcription. *Cell* *68*, 573-583.
- Poirier, M.G., Bussiek, M., Langowski, J., and Widom, J. (2008). Spontaneous access to DNA target sites in folded chromatin fibers. *J Mol Biol* *379*, 772-786.
- Poot, R.A., Bozhenok, L., van den Berg, D.L., Steffensen, S., Ferreira, F., Grimaldi, M., Gilbert, N., Ferreira, J., and Varga-Weisz, P.D. (2004). The Williams syndrome transcription factor interacts with PCNA to target chromatin remodelling by ISWI to replication foci. *Nat Cell Biol* *6*, 1236-1244.
- Quivy, J.P., and Becker, P.B. (1997). Genomic footprinting of *Drosophila* embryo nuclei by linker tag selection LM-PCR. *Methods* *11*, 171-179.
- Ramachandran, A., Omar, M., Cheslock, P., and Schnitzler, G.R. (2003). Linker histone H1 modulates nucleosome remodeling by human SWI/SNF. *J Biol Chem* *278*, 48590-48601.
- Ramakrishnan, V., Finch, J.T., Graziano, V., Lee, P.L., and Sweet, R.M. (1993). Crystal structure of globular domain of histone H5 and its implications for nucleosome binding. *Nature* *362*, 219-223.
- Ramon, A., Muro-Pastor, M.I., Scazzocchio, C., and Gonzalez, R. (2000). Deletion of the unique gene encoding a typical histone H1 has no apparent phenotype in *Aspergillus nidulans*. *Mol Microbiol* *35*, 223-233.
- Redon, C., Pilch, D., Rogakou, E., Sedelnikova, O., Newrock, K., and Bonner, W. (2002). Histone H2A variants H2AX and H2AZ. *Curr Opin Genet Dev* *12*, 162-169.
- Richardson, R.T., Alekseev, O.M., Grossman, G., Widgren, E.E., Thresher, R., Wagner, E.J., Sullivan, K.D., Marzluff, W.F., and O'Rand, M.G. (2006). Nuclear autoantigenic sperm protein (NASP), a linker histone chaperone that is required for cell proliferation. *J Biol Chem* *281*, 21526-21534.

- Robinson, P.J., An, W., Routh, A., Martino, F., Chapman, L., Roeder, R.G., and Rhodes, D. (2008). 30 nm chromatin fibre decompaction requires both H4-K16 acetylation and linker histone eviction. *J Mol Biol* *381*, 816-825.
- Robinson, P.J., Fairall, L., Huynh, V.A., and Rhodes, D. (2006). EM measurements define the dimensions of the "30-nm" chromatin fiber: evidence for a compact, interdigitated structure. *Proceedings of the National Academy of Sciences of the United States of America* *103*, 6506-6511.
- Robinson, P.J., and Rhodes, D. (2006). Structure of the '30 nm' chromatin fibre: a key role for the linker histone. *Curr Opin Struct Biol* *16*, 336-343.
- Routh, A., Sandin, S., and Rhodes, D. (2008). Nucleosome repeat length and linker histone stoichiometry determine chromatin fiber structure. *Proceedings of the National Academy of Sciences of the United States of America* *105*, 8872-8877.
- Saeki, H., Ohsumi, K., Aihara, H., Ito, T., Hirose, S., Ura, K., and Kaneda, Y. (2005). Linker histone variants control chromatin dynamics during early embryogenesis. *PNAS* *102*, 5697-5702.
- Saha, A., Wittmeyer, J., and Cairns, B.R. (2006). Chromatin remodelling: the industrial revolution of DNA around histones. *Nat Rev Mol Cell Biol* *7*, 437-447.
- Sambrook, J., and Russell, D.W. (2001). *Molecular Cloning - A Laboratory Manual*, 3. edn (Cold Spring Harbor, Cold Spring Harbor Laboratory Press).
- Sarg, B., Helliger, W., Talasz, H., Forg, B., and Lindner, H.H. (2006). Histone H1 phosphorylation occurs site-specifically during interphase and mitosis: identification of a novel phosphorylation site on histone H1. *J Biol Chem* *281*, 6573-6580.
- Schalch, T., Duda, S., Sargent, D.F., and Richmond, T.J. (2005). X-ray structure of a tetranucleosome and its implications for the chromatin fibre. *Nature* *436*, 138-141.
- Schwarz, P.M., Felthauer, A., Fletcher, T.M., and Hansen, J.C. (1996). Reversible oligonucleosome self-association: dependence on divalent cations and core histone tail domains. *Biochemistry* *35*, 4009-4015.
- Shen, X., Mizuguchi, G., Hamiche, A., and Wu, C. (2000). A chromatin remodelling complex involved in transcription and DNA processing. *Nature* *406*, 541-544.
- Shen, X., Yu, L., Weir, J.W., and Gorovsky, M.A. (1995). Linker histones are not essential and affect chromatin condensation in vivo. *Cell* *82*, 47-56.
- Sheng, S., Czajkowsky, D.M., and Shao, Z. (2006). Localization of linker histone in chromatosomes by cryo-atomic force microscopy. *Biophys J* *91*, L35-37.
- Shogren-Knaak, M., Ishii, H., Sun, J.M., Pazin, M.J., Davie, J.R., and Peterson, C.L. (2006). Histone H4-K16 acetylation controls chromatin structure and protein interactions. *Science* *311*, 844-847.

- Simon, R.H., and Felsenfeld, G. (1979). A new procedure for purifying histone pairs H2A + H2B and H3 + H4 from chromatin using hydroxylapatite. *Nucleic Acids Res* 6, 689-696.
- Simpson, R.T. (1978). Structure of the chromatosome, a chromatin particle containing 160 base pairs of DNA and all the histones. *Biochemistry* 17, 5524-5531.
- Sprouse, R.O., Brenowitz, M., and Auble, D.T. (2006). Snf2/Swi2-related ATPase Mot1 drives displacement of TATA-binding protein by gripping DNA. *Embo J* 25, 1492-1504.
- Strahl, B.D., and Allis, C.D. (2000). The language of covalent histone modifications. *Nature* 403, 41-45.
- Strohner, R., Wachsmuth, M., Dachauer, K., Mazurkiewicz, J., Hochstatter, J., Rippe, K., and Langst, G. (2005). A 'loop recapture' mechanism for ACF-dependent nucleosome remodeling. *Nat Struct Mol Biol* 12, 683-690.
- Sudarsanam, P., and Winston, F. (2000). The Swi/Snf family nucleosome-remodeling complexes and transcriptional control. *Trends Genet* 16, 345-351.
- Sun, J.M., Ali, Z., Lurz, R., and Ruiz-Carrillo, A. (1990). Replacement of histone H1 by H5 in vivo does not change the nucleosome repeat length of chromatin but increases its stability. *Embo J* 9, 1651-1658.
- Swaminathan, J., Baxter, E.M., and Corces, V.G. (2005). The role of histone H2Av variant replacement and histone H4 acetylation in the establishment of *Drosophila* heterochromatin. *Genes Dev* 19, 65-76.
- Th'ng, J.P., Sung, R., Ye, M., and Hendzel, M.J. (2005). H1 family histones in the nucleus. Control of binding and localization by the C-terminal domain. *J Biol Chem* 280, 27809-27814.
- Thastrom, A., Lowary, P.T., Widlund, H.R., Cao, H., Kubista, M., and Widom, J. (1999). Sequence motifs and free energies of selected natural and non-natural nucleosome positioning DNA sequences. *J Mol Biol* 288, 213-229.
- Thatcher, T.H., and Gorovsky, M.A. (1994). Phylogenetic analysis of the core histones H2A, H2B, H3, and H4. *Nucleic Acids Res* 22, 174-179.
- Thomas, J.O. (2001). HMG1 and 2: architectural DNA-binding proteins. *Biochem Soc Trans* 29, 395-401.
- Thomas, J.O., and Rees, C. (1983). Exchange of histones H1 and H5 between chromatin fragments. A preference of H5 for higher-order structures. *Eur J Biochem* 134, 109-115.
- Tsukiyama, T., and Wu, C. (1995). Purification and properties of an ATP-dependent nucleosome remodeling factor. *Cell* 83, 1011-1020.
- Tsukiyama, T., and Wu, C. (1997). Chromatin remodeling and transcription. *Curr Opin Genet Dev* 7, 182-191.
- Tyler, J.K. (2002). Chromatin assembly. Cooperation between histone chaperones and ATP-dependent nucleosome remodeling machines. *Eur J Biochem* 269, 2268-2274.

- Tyler, J.K., and Kadonaga, J.T. (1999). The "dark side" of chromatin remodeling: repressive effects on transcription. *Cell* *99*, 443-446.
- Ura, K., Hayes, J.J., and Wolffe, A.P. (1995). A positive role for nucleosome mobility in the transcriptional activity of chromatin templates: restriction by linker histones. *Embo J* *14*, 3752-3765.
- van Attikum, H., Fritsch, O., Hohn, B., and Gasser, S.M. (2004). Recruitment of the INO80 complex by H2A phosphorylation links ATP-dependent chromatin remodeling with DNA double-strand break repair. *Cell* *119*, 777-788.
- van Holde, K.E. (1988). *Chromatin* (New York, Springer-Verlag).
- Vanolst, L., Fromental-Ramain, C., and Ramain, P. (2005). Toutatis, a TIP5-related protein, positively regulates Pannier function during *Drosophila* neural development. *Development* *132*, 4327-4338.
- Vaquero, A., Scher, M.B., Lee, D.H., Sutton, A., Cheng, H.L., Alt, F.W., Serrano, L., Sternglanz, R., and Reinberg, D. (2006). SirT2 is a histone deacetylase with preference for histone H4 Lys 16 during mitosis. *Genes Dev* *20*, 1256-1261.
- Varga-Weisz, P.D., Blank, T.A., and Becker, P.B. (1995). Energy-dependent chromatin accessibility and nucleosome mobility in a cell-free system. *Embo J* *14*, 2209-2216.
- Varga-Weisz, P.D., Wilm, M., Bonte, E., Dumas, K., Mann, M., and Becker, P.B. (1997). Chromatin-remodelling factor CHRAC contains the ATPases ISWI and topoisomerase II. *Nature* *388*, 598-602.
- Villar-Garea, A., and Imhof, A. (2008). Fine mapping of posttranslational modifications of the linker histone H1 from *Drosophila melanogaster*. *PLoS ONE* *3*, e1553.
- Wang, G.G., Allis, C.D., and Chi, P. (2007). Chromatin remodeling and cancer, Part II: ATP-dependent chromatin remodeling. *Trends Mol Med* *13*, 373-380.
- Wang, W. (2003). The SWI/SNF family of ATP-dependent chromatin remodelers: similar mechanisms for diverse functions. *Curr Top Microbiol Immunol* *274*, 143-169.
- Whitehouse, I., Stockdale, C., Flaus, A., Szczelkun, M.D., and Owen-Hughes, T. (2003). Evidence for DNA translocation by the ISWI chromatin-remodeling enzyme. *Molecular and cellular biology* *23*, 1935-1945.
- Wisniewski, J.R., Zougman, A., Kruger, S., and Mann, M. (2007). Mass spectrometric mapping of linker histone H1 variants reveals multiple acetylations, methylations, and phosphorylation as well as differences between cell culture and tissue. *Mol Cell Proteomics* *6*, 72-87.
- Wolffe, A. (1998). *Chromatin - Structure & Function*, 3. edn (London, Academic Press).
- Woodcock, C.L., Skoultschi, A.I., and Fan, Y. (2006). Role of linker histone in chromatin structure and function: H1 stoichiometry and nucleosome repeat length. *Chromosome Res* *14*, 17-25.

- Workman, J.L. (2006). Nucleosome displacement in transcription. *Genes Dev* 20, 2009-2017.
- Wysocka, J., Swigut, T., Xiao, H., Milne, T.A., Kwon, S.Y., Landry, J., Kauer, M., Tackett, A.J., Chait, B.T., Badenhorst, P., *et al.* (2006). A PHD finger of NURF couples histone H3 lysine 4 trimethylation with chromatin remodelling. *Nature* 442, 86-90.
- Yang, J.G., Madrid, T.S., Sevastopoulos, E., and Narlikar, G.J. (2006). The chromatin-remodeling enzyme ACF is an ATP-dependent DNA length sensor that regulates nucleosome spacing. *Nat Struct Mol Biol* 13, 1078-1083.
- Yellajoshyula, D., and Brown, D.T. (2006). Global modulation of chromatin dynamics mediated by dephosphorylation of linker histone H1 is necessary for erythroid differentiation. *Proceedings of the National Academy of Sciences of the United States of America* 103, 18568-18573.
- Zeng, L., and Zhou, M.M. (2002). Bromodomain: an acetyl-lysine binding domain. *FEBS Lett* 513, 124-128.
- Zhou, Y.B., Gerchman, S.E., Ramakrishnan, V., Travers, A., and Muyltermans, S. (1998). Position and orientation of the globular domain of linker histone H5 on the nucleosome. *Nature* 395, 402-405.
- Zhu, P., Zhou, W., Wang, J., Puc, J., Ohgi, K.A., Erdjument-Bromage, H., Tempst, P., Glass, C.K., and Rosenfeld, M.G. (2007). A histone H2A deubiquitinase complex coordinating histone acetylation and H1 dissociation in transcriptional regulation. *Mol Cell* 27, 609-621.
- Zlatanova, J., Caiafa, P., and Van Holde, K. (2000). Linker histone binding and displacement: versatile mechanism for transcriptional regulation. *Faseb J* 14, 1697-1704.
- Zofall, M., Persinger, J., and Bartholomew, B. (2004). Functional role of extranucleosomal DNA and the entry site of the nucleosome in chromatin remodeling by ISW2. *Molecular and cellular biology* 24, 10047-10057.

6. Abbreviations

α	Anti
A	Adenine
ACF	ATP-utilizing chromatin assembly and remodelling factor
ADP	Adenosindiphosphate
AEL	After egg laying
ATP	Adenosintriphosphate
BAF	BRG1-associated factors
BAP	Brahma-associated proteins
bp	Basepairs
BPTF	Bromodomain PHD finger transcription factor
BRM	Brahma
BRG1	Brahma-related gene 1
BSA	Bovine serum albumin
C	Cytosine
CENP-A	Centromere protein A
CHD	Chromodomain-helicase-DNA-binding
crDNA	Competitor DNA
CHRAC	Chromatin accessibility complex
dATP	Desoxyadenosintriphosphate
DB	Dialysis buffer
dCTP	Desoxycytosintriphosphate
dGTP	Desoxyguadintriphosphate
Dls1	Dpb3-like subunit
DMSO	Dimethylsulfoxide
DNA	Desoxyribonucleic acid
DNMT	DNA methyltransferase
dNTP	Desoxyribonucleotidetriphosphate
Dpb3/Dpb4	DNA polymerase B (DNA Pol ϵ) subunit 3/4
DREX	<i>Drosophila</i> embryonic extract
<i>Drosophila</i>	<i>Drosophila melanogaster</i>
DTT	Dithiothreitol
dTTP	Desoxythymidintriphosphate
<i>E. coli</i>	<i>Escherichia coli</i>
EDTA	Ethylendiamintetraacetate
EGTA	Ethylenglycol-bis(2-aminoethyl)-N,N,N',N'-tetraacetic acid
EM	Electron microscopy
EMSA	Electrophoretic mobility shift assay
EtBr	Ethidiumbromide
EW	Embryo wash
EX	Extraction buffer
FRAP	Fluorescence recovery after photobleaching
fw	Forward
G	Guanine
Gcn5	General control non-derepressible
H2Av	H2A variant
HAT	Histone acetyltransferase
HDAC	Histone deacetylase
HEPES	(N-(2-Hydroxyethyl)piperazine-H ⁺)-(2-ethanesulfonic acid)
HDM	Histone demethylase

HMG	High mobility group
HMT	Histone methyltransferase
HP1	Heterochromatin protein 1
HRP	Horseradish peroxidase
Ig	Immunoglobulin
INO80	Inositol requiring
IPTG	1-isopropyl- β -D-1-thiogalacto-pyranoside
IR	Infrared
ISW1/ISW2	Imitation switch (<i>Sacharomyces cerevisiae</i>)
ISWI	Imitation switch (<i>Drosophila</i> , <i>Xenopus</i>)
Ite1	ISW2 ('ISW two') complex subunit
K	Lysine
kb	Kilobase
MBD3	Methyl-CpG-binding protein 3
MEL	Murine erythroleukemia
MNase	Micrococcal nuclease
MW	Molecular weight
NAP-1	Nucleosome assembly protein 1
NASP	Nuclear autoantigenic sperm protein
NB	Nuclei buffer
NoRC	Nucleolar remodelling complex
NURD	Nucleosome remodelling and deacetylation
NURF	Nucleosome remodelling factor
OD	Optical density
PAF	Paraformaldehyde
PAGE	Polyacrylamide gel electrophoresis
PBAF	Polybromo-associated BAF
PBAP	Polybromo-associated BAP
PBS	Phosphate buffered saline
PCNA	Proliferating cell nuclear antigen
PCR	Polymerase chain reaction
PHD	Plant homeo domain
PMSF	Phenylmethanesulfonyl fluoride
PNK	Polynucleotide kinase
psi	Pounds per square inch
PTM	Posttranslational monification
PVDF	Polyvinylidene Fluoride
Rad54	Radiation sensitive
RB	Remodelling buffer
RNA	Ribonucleic acid
RNAi	RNA interference
RPD3	Reduced potassium dependency 3
rpm	Revolutions per minute
RSC	Remodels the structure of chromatin
RSF	Remodelling and spacing factor
RT	Room temperature
Rv	Reverse
SANT	SWI3, ADA2, N-CoR and TFIIB B''
SDS	Sodiumdodecylsulfate
SHL	Superhelical location
SLIDE	SANT-like ISWI domain
SirT1	Sirtuin (silent mating type information regulation 2 homolog) 1
S/MAR	Scaffold/matrix attachment region
SNF2	Sucrose non-fermenting protein 2 homolog
SNF2H	Sucrose non-fermenting protein 2 homolog
SNF2L	Sucrose non-fermenting protein 2-like

Sth1	Snf two homologous 1
SUMO	Small ubiquitin-related modifier
SWI/SNF	Switch/sucrose non-fermenting
SWR1	Swi2/Snf2-related 1
T	Thymine
Temed	N,N,N',N'-Tetramethylethylenediamine
TLC	Thin layer chromatography
Tris	Tris(hydroxymethyl)aminomethane
TSA	Trichostatin A
UV	Ultraviolet
v/v	Volume per volume
WICH	WSTF-ISWI chromatin remodelling complex
WSTF	Williams syndrome transcription factor
WT	Wild-type
w/v	Weight per volume
<i>Xenopus</i>	<i>Xenopus laevis</i>

CURRICULUM VITAE

Verena K. Maier

Date of birth February 24th 1981
Place of birth Munich

Education

- 10/2005 - present **PhD thesis at the Ludwigs-Maximilians-University of Munich, Adolf-Butenandt-Institute, Prof. Peter Becker**
 Member of the International Max Planck Research School for Molecular and Cellular Life Sciences
 Project: ATP-dependent remodelling of Linker Histone-Containing Nucleosomal Fibres
- 10/2004 - 09/2005 **Diploma thesis at the Ludwigs-Maximilians-University of Munich, Adolf-Butenandt-Institute, Prof. Peter Becker**
 Project: Establishment of an *in vitro* chromatin remodelling assay on short nucleosomal arrays for *Drosophila* ACF
- 10/2002 - 09/2005 **Studies of Biochemistry at the University of Witten/Herdecke**
 Diploma
- 10/2000 - 09/2002 **Studies of Chemistry at the Technical University of Munich**
 Preliminary Diploma
- 09/1991 - 06/2000 **Gymnasium München/Moosach**
 Abitur
- 09/1987 - 07/1991 **Elementary school**

Publications

- Maier, V.K.**, Chioda, M., and Becker, P.B. (2008). ATP-dependent chromatosome remodelling. *Biological Chemistry* 389(4), 345-52, review
- Maier, V.K.**, Chioda, M., Rhodes, D., and Becker, P.B. (2008). ACF catalyses chromatosome movements in chromatin fibres. *The EMBO journal* 27, 817-26
- Straub, T., Gilfillan, G. D., **Maier, V. K.**, and Becker, P. B. (2005). The *Drosophila* MSL complex activates the transcription of target genes. *Genes & Development* 19, 2284-2288